Mechanical and Physical Risk Prevention

Studies and Research Projects

REPORT **R-923**

A laboratory study of a low-cost system for measuring coupling forces

Subhash Rakheja
Pierre Marcotte
Mayank Kalra
Surajudeen Adewusi
Krishna Dewangan

irsst

The Institut de recherche Robert-Sauvé en santé et en sécurité du travail (IRSST), established in Québec since 1980, is a scientific research organization well-known for the quality of its work and the expertise of its personnel.

OUR RESEARCH is *working* for you !

Mission

To contribute, through research, to the prevention of industrial accidents and occupational diseases and to the rehabilitation of affected workers;

To disseminate knowledge and serve as a scientific reference centre and expert;

To provide the laboratory services and expertise required to support the public occupational health and safety network.

Funded by the Commission de la santé et de la sécurité du travail, the IRSST has a board of directors made up of an equal number of employer and worker representatives.

To find out more

Visit our Web site for complete up-to-date information about the IRSST. All our publications can be downloaded at no charge.
www.irsst.qc.ca

To obtain the latest information on the research carried out or funded by the IRSST, subscribe to *Prévention au travail,* the free magazine published jointly by the IRSST and the CSST.
Subscription: *https://abonnement.lacsst.com/prevention*

Legal Deposit
Bibliothèque et Archives nationales du Québec
2016
ISBN: 978-2-89631-872-8 (PDF)
ISSN: 0820-8395

IRSST – Communications and Knowledge Transfer Division
505 De Maisonneuve Blvd. West
Montréal, Québec
H3A 3C2
Phone: 514 288-1551
publications@irsst.qc.ca
www.irsst.qc.ca

Mechanical and Physical Risk Prevention

Studies and Research Projects

REPORT **R-923**

A laboratory study of a low-cost system for measuring coupling forces

Subhash Rakheja[1], Pierre Marcotte[2]
Mayank Kalra[1], Surajudeen Adewusi[1],
Krishna Dewangan[1]

[1]Université Concordia
[2]IRSST

Clic Research
www.irsst.qc.ca

A PDF version of this publication is available on the IRSST Web site.

This study was funded by the IRSST. The conclusions and recommendations are solely those of the authors.

PEER REVIEW

In compliance with IRSST policy, the research results published in this document have been peer-reviewed.

SUMMARY

The assessment of hand-transmitted vibration exposure and of potential injuries to the hand-arm system when using hand-held power tools is currently based on the ISO 5349-1 guidelines. The recommended guidelines, however, do not account for the effects of the coupling forces exerted at the hand-handle interface, although many studies have shown the importance of these forces in the transmission of vibration to the hand-arm system. This is partly attributed to the lack of practical methods for measuring hand-tool interface forces in field applications and in-part to the lack of sufficient data relating injury risks to the applied forces. This study explored a low-cost system for measuring hand-handle interface forces and its feasibility when applied to a hand-held power tool handle.

The study was conducted in three sequential phases. In the first phase, a measurement system based upon low-cost thin-film and flexible resistive sensors (*FlexiForce*®) was developed and the properties of the sensors were explored through systematic laboratory measurements. The sensors could also be trimmed to be adapted to different handles. The properties included the hysteresis, linearity and repeatability of the sensor applied to flat as well as curved surfaces. From repeated measurements, it was observed that the sensors exhibit negligible hysteresis and very good linearity with the applied force. The measurements, however, revealed strong dependence on the loading area, position of the load on the sensor, length of the sensor and flexibility of the loading media (elastomer). Furthermore, considerable differences were observed in the outputs of different sensors, and the sensors showed degradation of the output signal with time and usage. Subsequent measurements performed with 5 different instrumented cylindrical and elliptical handles also showed very good linearity of the sensors but strong dependence on the hand size and the handle size. It was concluded that the sensors could provide reasonably good estimates of the hand forces provided that each sensor was calibrated for the specific handle and hand size.

Optimal locations of the 40 mm wide sensors on the handle surface were determined through the measurement of hand positions on different handle sizes, and from the hand-handle interface force distributions acquired in an earlier study for different sizes of cylindrical handles. It was concluded that two sensors located symmetrically on opposite sides of the handle, in the forearm axis, could provide very good estimates of the palm- and finger-side contact forces. The hand grip and push forces were subsequently derived from the measured palm and finger forces. The validity of the low-cost measurement system was investigated through repeated measurements with 7 subjects and 5 different handles, including three cylindrical handles (32, 38 and 43 mm diameter) and two elliptical handles (32 mm x 38 mm and 38 mm x 44 mm). A LabView program was developed to acquire the *FlexiForce*® palm and grip forces, and reference grip and push forces from the instrumented handles, which were displayed to the subject. The experiments were conducted with each subject grasping the stationary instrumented handle with 12 different combinations of hand grip (10, 30 and 50 N) and push (25, 50 and 75 N) forces. The measurements were also repeated under two different levels of broad band vibration in the 4 to 1000 Hz frequency range (frequency-weighted rms acceleration of 1.5 and 3 m/s^2). The results showed good linearity and repeatability of the sensors for all the subjects and handles under static as well vibration conditions, but the sensor outputs differed for each handle and subject. This further confirmed the need for calibrating the sensors for each subject and handle.

In the second phase, the feasibility of the sensors for the measurement of the biodynamic response of the hand-arm system was explored. The study was conducted with 6 subjects grasping the 38 mm instrumented handle with nine different combinations of grip and push forces, and two levels of broadband vibration. The handle was also equipped with two *FlexiForce*® sensors for the measurements of the palm-handle and finger-handle interface dynamic forces. The data acquired from the instrumented handle were analyzed to determine the palm- and finger-side driving point mechanical impedance responses, which served as the reference values. The driving-point palm- and finger-impedance responses were also obtained from the *FlexiForce*® sensors and compared with the reference values to evaluate the feasibility of the measurement system. The comparisons revealed very similar trends, while the impedance magnitude responses of the *FlexiForce*® sensors were substantially lower in the entire frequency range, except at very low frequencies. This was attributed to poor frequency response of the *FlexiForce*® measurement system. The frequency response characteristics of the sensors were subsequently obtained from the measured responses, which revealed strong dependence on the hand-handle interface forces, handle size and vibration level. The application of a compensation function based upon the measured frequency response characteristics resulted in impedance responses of the *FlexiForce*® sensors comparable to the reference values for all the experimental conditions considered in the study. It was concluded that the proposed low-cost measurement system could be applied for measurements of the biodynamic responses and hand forces on real tool handles in the field. The determination of the frequency response functions of the sensors, however, would be quite challenging considering its nonlinear dependence on the hand size, hand forces and handle size. Furthermore, the proposed system eliminates the need for inertial compensation of the measured biodynamic responses, which is known to be a source of error in the reported biodynamic responses of the human hand-arm system exposed to handle vibration.

Finally, in the third phase, the validity of the measurement system was examined with hand grasping a static as well as a vibrating tool handle under different combinations of hand grip and push forces. The experiments were conducted with a chisel hammer operating in an energy dissipator in the laboratory. Two *FlexiForce*® sensors were applied to the primary handle of the tool to measure the palm- and finger-side forces. A methodology was developed to calibrate both sensors. The validity of the measurement system was evaluated with three subjects grasping the static as well as the vibrating tool handle under different combinations of hand grip, push and coupling forces. Measurements revealed very good correlations between the hand forces estimated from the *FlexiForce*® sensors and reference values for the static as well as for the vibrating tool. The ratio of the palm force obtained from the *FlexiForce*® measurement system to the coupling force ranged from 0.96 to 1.05, when the subjects grasped the vibrating tool handle. This ratio varied from 0.96 to 1.06 for the stationary tool handle.

TABLE OF CONTENTS

LIST OF TABLES

LIST OF FIGURES

1 HAND-HANDLE INTERFACE FORCES - BACKGROUND

Occupational exposure to hand-transmitted vibration (HTV) arising from operations of hand-held power tools has been associated with an array of adverse health effects including vascular, neurological and musculoskeletal disorders, collectively termed as hand-arm vibration syndrome (HAVS) [1-3]. Raynaud's phenomenon of occupational origin has been related to impaired blood circulation in the fingers and palm of the exposed hands, and exposure to cold. The HTV exposure is measured in terms of frequency-weighted acceleration of the vibrating tool handle using the method described in ISO 5349-1 [4]. Health effects of HTV are influenced by many extrinsic and intrinsic variables such as vibration magnitude and frequency, push and grip forces, grip type and grip-force distribution, dynamic torque, handle geometry, and other inter-individual factors. The HTV exposure assessment guidelines defined in ISO 5349-1 [4] only address the contribution of the vibration magnitude and frequency, and neglect the effects of other contributing factors. In addition, the standard has been widely criticized with regards to the frequency weighting and lack of consideration of the hand-handle coupling forces and the working posture. Moreover, a few recent studies have presented contradictory findings on the basis of the injury risks obtained from the ISO 5349-1 guidelines and epidemiological studies [5,6].

The hand-handle interface coupling forces, often considered as a combination of grip and push/feed forces, permit the flow of vibration energy from the tool into the hand. The coupling forces thus directly affect the severity of the vibration transmitted to the operator's hand and arm [7,8]. The coupling forces associated with the operation of vibrating tools generally consist of two components: (i) the static hand forces applied to achieve essential control and guidance of the tool and to achieve desired productivity, which has been the primary focus of ISO 15230 [9]; and (ii) the dynamic force arising from the biodynamic response of the hand-arm system. It has been shown that the HTV and the hand-arm biodynamic responses increase with grip force [10-12]. Furthermore, an increase in grip force tends to compress the soft tissues of the hand and fingers leading to reduced blood flow in the fingers and thus produce a greater risk of developing Raynaud's syndrome [13]. A few studies have proposed additional weighting functions to account for the strong effects of hand-handle interface forces on the exposure assessment [14-16].

Although the importance of considering the coupling forces on the quantification of the hand-arm vibration exposure has been widely recognized, the measurements of hand forces on vibrating tools have met only limited success. This is primarily attributed to the lack of definite relations between the static coupling forces and the HTV, and lack of reliable measurement systems, particularly for field applications. The VIBTOOL study by the European Community (EC) is perhaps the most comprehensive effort towards the development of a capacitive polymer sensing grid for the acquisition of the hand-handle interface forces [17]. Lemerle et al. [18] investigated the feasibility of the capacitive sensors (Novel *emed*® system) to measure the hand-handle coupling forces. Such a measurement system, however, would pose challenges with regard to applications in the field, specifically in view of its high cost, and strenuous demands on data acquisition and analysis. Moreover, such sensors are fragile and may incur damages during field applications.

This study is aimed at the development of a low-cost measurement system for acquiring hand forces when coupled with a vibrating handle, particularly the grip and push forces. The

feasibility of the measurement system, based on low-cost resistive sensors, is explored for applications on simulated instrumented handles and a power tool handle. It needs to be noted that the mechanical impedance responses of the hand-arm system have been widely measured in the laboratory using instrumented handles [12,13,19-24,28], which involve inertial corrections to account for contribution of the handle inertia to the measured biodynamic force. These have also shown strong dependence of the static forces generated by the hand on the posture of the hand-arm system [25-27]. Owing to the very low apparent mass of the hand at higher frequencies, the inertial corrections could lead to substantial errors [29,30]. The proposed low-cost measurement system, being applied to the handle surface, would not require an inertial correction and may thus provide a more accurate measurement of the biodynamic responses. The feasibility of the measurement system is thus also explored for measurement of the mechanical impedance of the hand-arm system under broadband vibration along the forearm (z_h-) axis.

1.1 Significance of hand forces

A number of studies have also shown important effects of coupling forces exerted at the hand-handle interface on the hand-arm biodynamic responses and vibration power absorption [11,19,21,31]. Riedel [15] suggested the use of a hand force coupling factor to account for the effect of the coupling force on the vibration dose value of the hand-arm system. The study showed insignificant differences between the acute effects of the hand grip and push forces, and thus recommended the sum of the two to derive the coupling force. The proposed correction factor ranged from 0.6 to 1.2 for coupling forces ranging from 20 to 200 N. The addition of a correction factor to the frequency-weighting defined in ISO 5349-1 [4] has been considered by the ISO/TC 108/SC 4 working group, which recognized the lack of sufficient data relating coupling force to the transmitted vibration [32].

The International Standard, ISO 15230 [9], defines the push, grip, contact and coupling forces in the context of the hand forces applied to a handle. The standard defines the contact force by the summation of distributed elemental forces F_{ci}, as shown in Figure 1.1. The push force imposed by the hand is defined as the sum of axial components of F_{ci} caused by the distributed pressure p_i over the contact area S_i, such that (Figure 1.1):

$$\boldsymbol{F_{pu} = \sum_i F_{ci} \cos\alpha_i = \sum_i p_i S_i \cos\alpha_i} \tag{1.1}$$

where F_{pu} is the push force and α_i is the angle of the elemental force $F_{ci,}$ with respect to the handle axis, as seen in Figure 1.1. The grip force, a clamp-like force exerted by the hand when grasping the handle, is compensated within the hand by the opposing gripping actions towards a dividing plane, as shown in Figure 1.2. The standard also defines the coupling force as the sum of hand push and grip forces:

$$\boldsymbol{F_{coup} = F_{gr} + F_{pu}} \tag{1.2}$$

where, F_{gr} and F_{coup} are the grip and coupling forces, respectively.

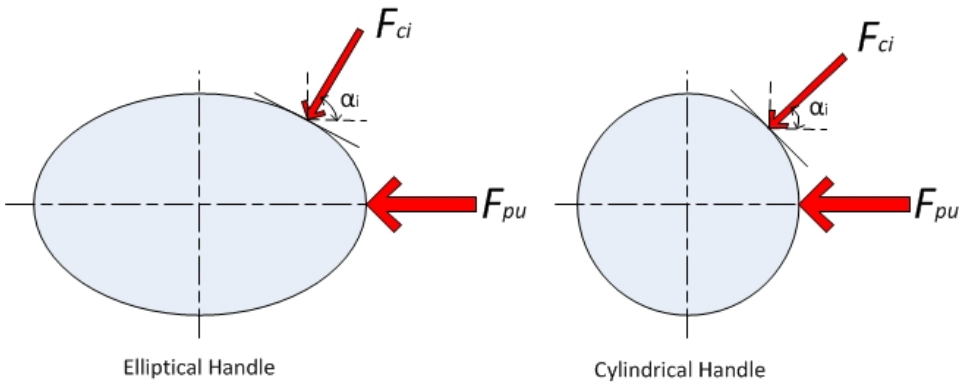

Figure 1.1 Elemental contact force (F_{ci}) and pus h force (F_{pu}), as defined in ISO 15230 [9].

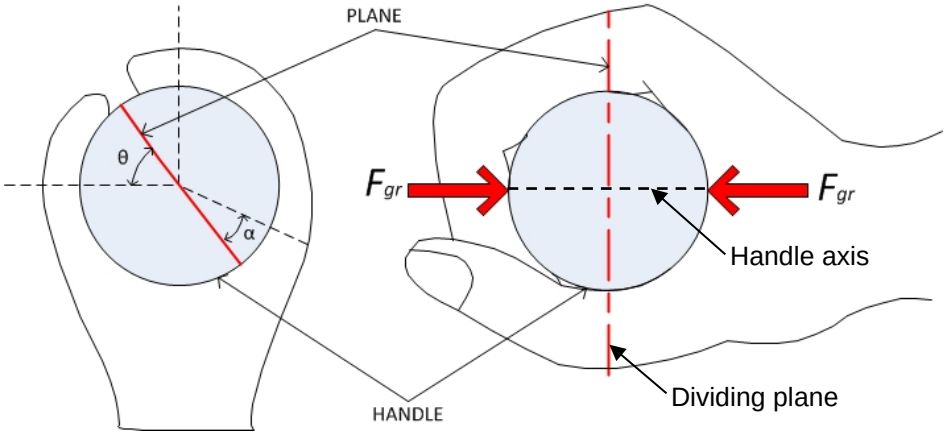

Figure 1.2 Illustration of the gripping force (F_{gr}) as a clamping force [9].

Owing to substantial effects of hand grip and push forces on the musculoskeletal loading, hand-transmitted vibration and biodynamic responses [11,12,15,19,31], quantifying hand forces is vital for the understanding of the human hand arm system responses to vibration. The current frequency weighting defined in ISO 5349-1 [4] has been subjected to many criticisms for lack of considerations of various contributory factors, such as coupling forces [5,21]. Owing to the complexities associated with the measurements of hand forces at the hand-handle interface, reported studies have widely explored different measurement systems, which are briefly described in the following sub-section.

1.2 Methods of measuring hand forces

1.2.1 Instrumented handles

Different designs of instrumented handles have been developed for measuring the hand forces with static as well as vibrating handles. The earlier designs of instrumented handles employed

strain gauges for measurements of the hand grip force [13,23,33-36]. These were used to study the effects of hand-handle coupling forces on HTV and biodynamic responses of the human hand-arm system. Such handles generally revealed resonances at frequencies below 1000 Hz and thus could not provide reliable measurements of biodynamic responses of the hand-arm system in the broad frequency ranges of typical tool vibration [29,30]. Chadwick et al. [34] proposed an instrumented handle comprising of 6 segments of cantilevers with strain gauges attached at the fixed end (Figure 1.3). In recent years, Wimer et al. [35] explored the designs of 6, 8 and 10 segment instrumented handles similar to the design presented by Chadwick et al. [34]. These studies concluded that a six segment instrumented handle provided more accurate measurements of coupling forces under various gripping tasks. A similar handle design was proposed by McGorry [33] for the measurement of grip force and moment in hand-held tools, as shown in Figure 1.3.

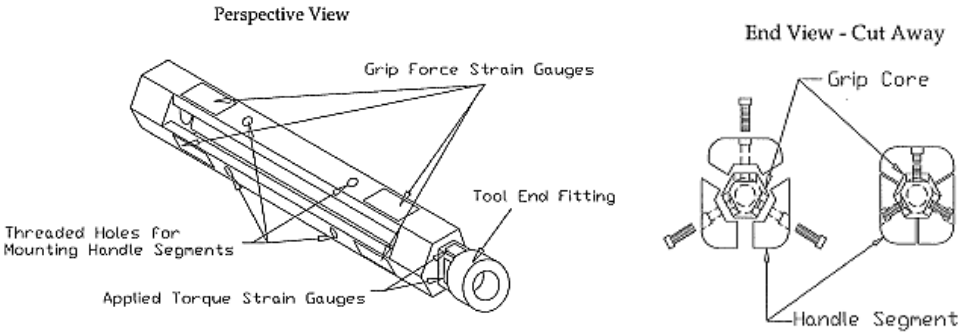

Figure 1.3 An instrumented handle for deployment in tool handles [33].

The instrumented handles employing piezoelectric load cells have been designed for the measurement of hand grip, push and dynamic forces for studies on human hand-arm biodynamic responses to vibration as well as for the assessment of anti-vibration gloves [12,20,22,37]. Such handles consist of two load cells sandwiched between a split handle to measure hand grip force, while two additional load cells are employed between the handle and a base fixture to measure the push and dynamic forces. These handles generally exhibit high stiffness and thus higher resonance frequencies above 1000 Hz. Figure 1.4 illustrates the schematic of a split instrumented handle designed for the measurement of static as well as dynamic hand forces and biodynamic responses of the hand-arm system in the laboratory. The pictorial view of the handle is shown in Figure 1.5. The two force sensors (Kistler 9212) are installed within the handle, and two additional load cells (Kistler 9317b) are located between the handle and its support. This handle design has been recommended in ISO 10819 [38] for evaluations of vibration transmissibility characteristics of anti-vibration gloves.

The aforementioned instrumented handles have been widely used in the laboratory for the measurement of hand forces with static as well as vibrating handles. These, however, are not suited for field applications due to extreme complexities associated with their implementations to the power tools. Furthermore, it has been reported that split instrumented handle designs affect the rigidity of the handle in an adverse manner. The dynamic response of the handle to vibration may introduce significant errors in the laboratory-measured mechanical impedance, particularly in the high frequency range [29,30]. A number of studies have shown that instrumented handles

employing either strain gages or load cells cannot always be used in the field with hand-held power tools as they require special fixtures [33,34,39,40].

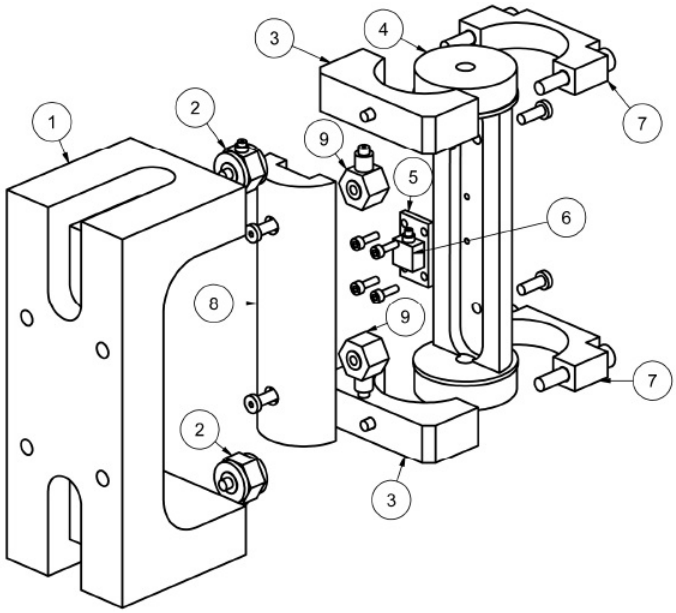

Parts List	
ITEM	DESCRIPTION
1	base
2	force sensor X 2
3	rear bracket X 2
4	handle 40mm
5	accelerometer base
6	accelerometer
7	front bracket X 2
8	front handle 40mm
9	small force sensor X 2

Figure 1.4 Schematic diagram of the instrumented handle with load cells [12].

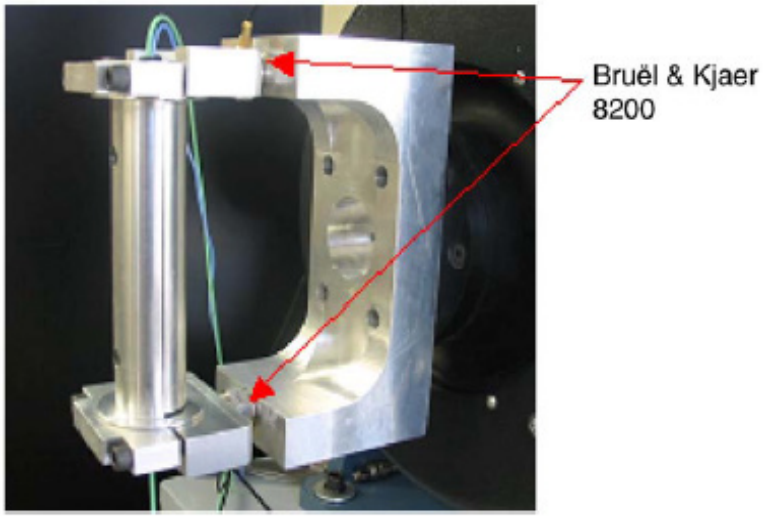

Figure 1.5 Pictorial view of the instrumented handle and the support fixture for the measurement of hand grip and push forces [12].

1.2.2 Hand-handle interface pressure measurement methods

In recent years, a few studies have explored the feasibility of thin-film pressure sensing systems for the measurement of hand-handle coupling forces. Such sensors exhibit adequate flexibility for their use on handles with different cross-sections and curved surfaces. Semiconducting, capacitive and resistive thin film sensors have been used to measure hand-handle coupling forces under static conditions. The capacitive sensors consist of dielectric material between elastomeric layers and thus provide adequate flexibility and capacitance variations with the applied normal load. Resistive sensors, on the other hand, are designed with pressure-sensitive resistors encased between two thin Mylar layers. The pressure sensing mats with matrix arrangements of capacitive or resistive sensors have been commercially developed for applications to power tool handles. Gurram et al. [13] employed a 6x6 matrix of capacitive sensors on cantilevered split handles for the measurement of grip pressure distribution in static as well as in dynamic conditions. Subsequently, Welcome et al. [41] and Aldien et al. [42] used the capacitive sensing matrices for acquisition of hand-handle contact and coupling forces under static conditions alone. The studies employed instrumented handles with load cells for verifications of the capacitive sensors, and proposed empirical expressions relating hand grip, push, coupling and contact forces as a function of the handle size. These studies have shown that the capacitive sensing matrix could provide accurate measurements of hand-handle grip, push and contact forces in a static laboratory setting under a controlled hand-arm posture. The proposed relation between the grip, push and the contact forces has been documented in ISO 15230 [9]. Young et al. [43] used the capacitive sensing matrix to map distributed hand-handle interface forces under different gripping and pulling tasks. Deboli et al. [41] used the similar sensing matrix for the determination of the hand grip force imparted on a hand-held olive harvester.

Lemerle et al. [18] further explored a capacitive pressure sensing matrix, developed by Novel GmbH (based in Munich, Germany), to measure the push and grip forces on power tools. The study was a part of the comprehensive VIBTOOL project, sponsored by the European Union in collaboration with Novel GmbH. A new design of a capacitive pressure sensing hand matrix was subsequently developed for the assessment of hand forces imposed on power tool handles [17,18]. The sensing system could provide the hand-handle interface pressure distribution either by wrapping the sensing matrix around the handle or by using the sensor integrated to a glove, as seen in Figure 1.6. The study conducted a thorough static and dynamic analysis of the pressure sensing system through direct measurements of hand-handle interface pressure distribution and indirect measurements of push and grip forces considering handles of different diameters.

Although the VIBTOOL project clearly demonstrated sound reliability of the capacitive pressure sensing matrix for the measurement of hand-handle interface pressure distribution and coupling forces, the measurement system is not considered to be well-suited for field applications due to its very high cost. The capacitive sensors are also known to be relatively fragile, and may incur damage or failure during field applications. Moreover, the validity of such sensors in capturing the dynamic hand-handle forces in frequency ranges of power tools has not yet been demonstrated.

Alternatively, a few studies have explored low cost force sensing resistors (FSR) for the measurement of hand-handle interface forces. Similar to the capacitive measurement system, the FSR have also been applied in different matrix arrangements for acquisition of interface force distribution. Komi et al. [45] evaluated three different thin and flexible sensors for measuring

grip force imposed on a golf club. These included a resistive force sensing grid (Tekscan 9811, Tekscan Inc., USA), an arrangement of small-size *FlexiForce*® sensors, also developed by Tekscan Inc. (USA), and flexible Quantum tunneling composite (*QTC*™) sensors (Peratech Ltd, United Kingdom). The study evaluated the relative performance of the sensors under controlled laboratory conditions in terms of static accuracy, hysteresis, repeatability, drift errors, dynamic accuracy, as well as shear load and surface curvature effects. The results showed a better performance of the resistive force sensing grid and of the *FlexiForce*® sensors compared to the QTC sensors, although all the sensors revealed high drift errors. The results of the study further showed a reduced measurement sensitivity of both resistive sensors developed by Tekscan Inc., as compared to the static sensitivity of the QTC sensors. Furthermore, the sensitivity of all three sensors decreased with use. In a recent study, Rossi et al. [46] applied resistive pressure sensors (Tekscan 3200, Tekscan Inc., USA) to study the influence of handle diameter on hand forces.

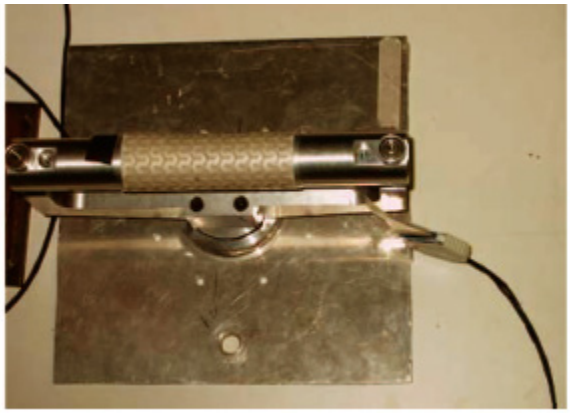

(a)

(b)

Figure 1.6 The Novel *emed*® capacitive pressure sensing matrices: (a) wrapped around a cylindrical handle; and (b) used as an instrumented glove [17,18].

Despite the aforementioned drawbacks, the resistive pressure sensing systems, owing to their substantially lower cost and flexibility, offer attractive potential for effective measurement of

hand-handle coupling forces in the field during typical work conditions. Such sensing matrices have been commercially developed with high-speed scanning hardware and software, which could permit acquisition of the coupling forces in both static as well as dynamic environments [51]. The primary advantage of such sensors lies with their very low cost compared to the capacitive sensors. The effectiveness of such sensors in providing reliable measurements of hand forces under different static and dynamic conditions, however, have not yet been thoroughly explored.

1.3 Measurements of hand-arm biodynamic responses

The biodynamic response characteristics of the human hand-arm system to hand-transmitted vibration have been widely characterized to obtain mechanical-equivalent properties of the hand and arm, define alternate frequency-weightings and to develop a better understanding of the vibration power absorption. The biodynamic responses have been described in terms of through-the-hand-arm and to-the-hand response functions [48]. The through-the-hand-arm response function describes the transmission of vibration to different segments of the hand-arm system, expressed as the ratio of the vibration magnitude measured at a specific segment on the hand-arm system to that at the hand-handle interface [11]. The to-the-hand biodynamic response relates the vibration in the vicinity of the hand to the force at the driving point, expressed in terms of the driving-point mechanical impedance (DPMI), or apparent mass (APMS) or the absorbed power, given by:

$$\boldsymbol{Z(j\omega)} = \frac{\boldsymbol{F(j\omega)}}{\boldsymbol{v(j\omega)}} \qquad \boldsymbol{M(j\omega)} = \frac{\boldsymbol{F(j\omega)}}{\boldsymbol{a(j\omega)}} \qquad \boldsymbol{P(j\omega)} = \boldsymbol{Re}[\boldsymbol{Z(j\omega)}]\boldsymbol{v^2} \tag{1.3}$$

where *Z*, *M* and *P* are the complex DPMI, APMS and the absorbed power frequency response functions, respectively, *v* and a are the velocity and acceleration, respectively, measured at the driving point, *F* is the force measured at the driving-point along the axis of the motion, ω is the circular frequency of vibration, and $j = \sqrt{-1}$. In the above equation, *Re* denotes the real component of the DPMI.

The biodynamic responses of the hand-arm system have been widely characterized in the laboratory using instrumented handles under different experimental conditions, namely, the magnitude and frequency of handle vibration, hand-arm posture, hand-grip and push forces, and handle geometry and sizes [12,19-23,28-31,36,37]. These have generally presented the response in terms of the DPMI as a frequency response function relating the dynamic force and the velocity at or close to the hand-handle interface, such that:

$$\boldsymbol{Z(j\omega)} = \frac{\boldsymbol{S_{Fv}(j\omega)}}{\boldsymbol{S_{vv}(j\omega)}} \tag{1.4}$$

where S_{Fv} is the cross spectral density of the force F and the velocity v, and S_{vv} is the auto spectral density of the velocity.

The driving-point mechanical impedance characteristics describing the “to-the hand” biodynamic response of the hand-arm system have been extensively investigated under a wide range of vibration excitations and test conditions. These have shown that the biodynamic responses of the hand-arm system strongly depend upon the hand forces. The DPMI magnitude increases with increasing hand grip force [21,23,37,50,51]. On the basis of a synthesis of the reported mechanical impedance data reported in ISO 10068 [24], it has been concluded that the biodynamic response of the human hand-arm is relatively less sensitive to variations in the push/pull forces, although only a few data sets reported the effect of the push force [52]. The effect of the grip force alone has thus been emphasized in the current standard [24]. Mann and Griffin [49] investigated the influence of various physical factors on the point mechanical impedance measured at the palmar surface of the finger. The results showed that the transmission of vibration to the fingers is highly dependent on the magnitude of the contact force.

The biodynamic measurements performed using instrumented handles may exhibit considerable errors, partly attributed to handle dynamics and inertia effects [29,30]. An inertial correction is invariably applied to account for the inertia of the instrumented handle by subtracting the DPMI of the handle alone from the DPMI of the combined handle and the hand-arm system, such that:

$$\boldsymbol{Z_{hand-arm}(j\omega) = Z_{coupled}(j\omega) - Z_{handle}(j\omega)} \tag{1.5}$$

where $Z_{hand\text{-}arm}$ is the DPMI of the hand-arm system, $Z_{coupled}$ is the directly measured DPMI of the coupled handle-hand-arm system and Z_{handle} is DPMI of the handle alone.

The magnitude of the DPMI of the handle alone could be substantially higher than that of the hand at higher frequencies, particularly when the handle mass supported by the force sensors is relatively large. It has been shown that the contributions due to handle inertia at higher frequencies cannot be entirely eliminated through mass cancellation [29]. A few studies have shown that the apparent mass of the hand-arm system tends to be very low at frequencies above 500 Hz and approaches about 25 grams near 1000 Hz, which is significantly lower than that of the instrumented handle [19,53]. The discrepancies among the reported impedance responses above 500 Hz were in-part attributed to the inertial effects of the instrumented handles [29]. The magnitude of error due to inertial effects could be minimized by reducing the effective handle mass supported by the force sensors. Reducing the mass, however, tends to increase flexibility of the handle structure and thus lowers the resonant frequency.

Thin-film pressure sensing matrices of negligible mass can be applied directly to the handle surface and thereby preserve its rigidity. Apart from the hand grip and push forces, such sensors could also be used to measure the dynamic force so as to obtain the DPMI responses without any inertial correction. The accuracy of the dynamic measurements, however, would greatly depend upon the bandwidth and frequency response characteristics of the pressure sensing systems, which has not yet been explored.

2 OBJECTIVES OF THE STUDY

The overall objective of this study is to contribute towards the development of a low cost device for the measurement of hand-handle coupling forces with hand-held power tools. The primary goal is to explore the feasibility of a low cost resistive force sensor system for the measurement of hand-handle forces under static and dynamic conditions. The specific objectives of the study include:

1) Developing a two-channel hand-handle interface force measurement system using the *FlexiForce*® sensors, including a signal conditioning circuit;

2) Exploring the validity of the *FlexiForce*® sensors and the conditioning circuit through systematic static and dynamic calibration tests;

3) Developing a data analysis software to derive the hand push and grip forces with sensors wrapped around cylindrical and elliptical handles of different sizes, and identifying optimal location of sensors through the analysis of hand-handle interface pressure distribution;

4) Examining the validity of the sensors for capturing hand push and grip forces under static and dynamic environments;

5) Exploring the feasibility of the sensors for the measurement of the biodynamic response of the human hand-arm system exposed to broadband random vibration along the forearm axis;

6) Exploring the feasibility of the measurement system for assessing the grip and push forces while grasping a percussion tool handle under static as well as vibrating conditions.

The study was conducted in three systematic phases. In the initial phase, the *FlexiForce*® sensors were used to measure the contact force through the development of a two-channel variable gain signal conditioning circuit. Static calibration of the sensors was performed under a wide range of loads, while the sensors were placed on flat as well as curved surfaces (Chapter 3). The sensors were subsequently applied to cylindrical and elliptical cross-section handles for estimating the hand grip and push forces from the measured palm and finger forces. Hand-handle interface pressure distribution data were thoroughly reviewed to identify the optimal position of the sensors on different handle sizes. The feasibility of the measurement system for determining the hand grip and push forces with vibrating handles was further evaluated under broadband random vibration applied to the handle (Chapter 4). The feasibility of the sensors for the measurement of the biodynamic response of the hand-arm system was explored in the subsequent phase (Chapter 5). The applicability of the measurement system to a real tool handle was examined in the final phase of the study using a chisel hammer operating in an energy dissipator. The validity of the sensors was examined with the hand grasping the static as well as the vibrating tool handle under a wide range of hand forces (Chapter 6).

3 DEVELOPMENT OF THE MEASUREMENT SYSTEM AND CHARACTERIZATION OF THE SENSORS ON FLAT AND CURVED SURFACES

3.1 Development of the force measurement system

As the primary goal of this project was to develop a low cost reliable hand-handle interface force measurement system for the determination of hand grip and push forces imparted on tool handles. Different low cost force sensing resistive sensors were thus explored for use under both static and vibrating conditions. After reviewing different sensor specifications, the *FlexiForce*® sensors (model 1230), manufactured by Tekscan Inc. (USA), were selected for the study, due to the following features:

- Very low cost compared to capacitive sensors;
- Thin and flexible, and could be easily applied to tool handles;
- Minimal mass and rapid response time;
- Sensor size well suited for power tool handles, with the possibility of trimming each sensor to the desired length and width to adapt to different handle sizes;
- Unlike the sensing matrix, the sensors are used as a single unit to measure the total force imposed on the entire sensor, and thereby can provide acquisition at very high sampling rates;
- Simple signal conditioning requirements.

The selected *FlexiForce*® sensor is shown in Figure 3.1. Each sensor is 149 mm long, 40 mm wide and 0.21 mm thick. The sensor employs the principle of force sensing resistors (FSR), which exhibit a change in resistance when a force is applied to the active sensor surface. A FSR consists of two polymer layers. One of the layers contains a pair of intertwined conductors forming the active sensing area. The second layer is an adhesive layer coated with carbon-based FSR ink. In the absence of a force, the resistance between the two layers may be as high as 10 MΩ and the sensor behaves similar to an open circuit. Based upon the general principle of FSR, an applied force on the sensor causes the ink to contact the conductive strips and create a short circuit, which decreases the resistance. Therefore, the conductance of the sensors varies linearly with the applied force. A signal conditioning circuitry is needed to measure the change in resistance in terms of a conveniently measurable voltage change, which can be directly related to the applied force. It is essential to note that the sensors will only yield an output when a force is applied at a location where conductive strips intersect, also denoted as a ‘sensel’. The selected *FlexiForce*® sensor (model 1230) comprised a total of 102 sensels. For a surface load, this characteristic is irrelevant since the applied load would span over several sensels but yield a single output corresponding to the total load applied to all the sensels (as they are interconnected).

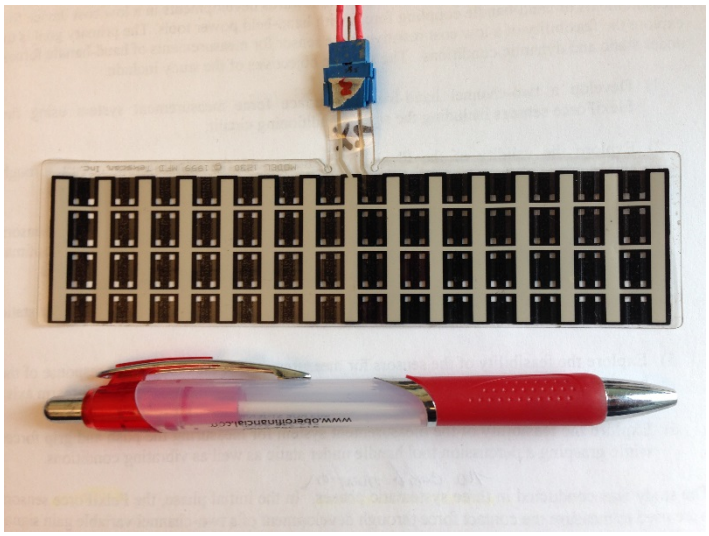

Figure 3.1 *FlexiForce*® sensor (Model 1230) selected for the measurement of hand-handle interface force.

In this study, a signal conditioner was developed to measure the change in sensor resistance in terms of change in the circuit voltage. The conditioning circuit was initially developed on the basis of that recommended by Tekscan. The recommended circuit consisted of an inverting operational amplifier arrangement to produce an analog output based on the sensor resistance and a fixed reference resistance. The sensitivity of the sensor could be varied by changing the reference resistance and/or the driving voltage. Preliminary measurements conducted with the recommended conditioning circuit design revealed a substantial drift in the output as well as an output saturation under a low level force. The circuit was subsequently modified to increase its measurement range so as to eliminate the output saturation under loads up to 200 N, and to perform simultaneous acquisition of two sensors to be located on the handle. A zeroing circuit was integrated to offset a possible bias due to preload of the sensor and to control the drift. A variable gain circuit was also incorporated to ensure adequate level of the voltage output in the desired force range (0 to 200 N). Figure 3.2 illustrates the conditioning circuit designed for simultaneous acquisitions of two sensor outputs. The packaged two-channel signal conditioner is pictorially shown in Figure 3.3.

3.2 Methods - Static characterisation of *FlexiForce*® sensors on flat and curved surfaces

Static calibration of a number of *FlexiForce*® sensors coupled with the two-channel signal conditioner was performed to establish the relationships between the applied force and the sensor outputs, the consistency across the sensors, the linearity and hysteresis, and the influence of sensor length, load position and loading area. The measurements were performed under a wide range of static loads by placing the sensors on a flat surface and on a curved surface to simulate a tool handle geometry. The measured data were used to evaluate the static sensitivity of a set of *FlexiForce*® sensors. The sensor loading was applied through a relatively stiff elastomer to ensure more uniform contact of the sensor layers. It should be noted that the stiffness of the

elastomer was not quantified. Further, repeated measurements on the same sensors were performed on different days to evaluate the deterioration of the sensor output over time.

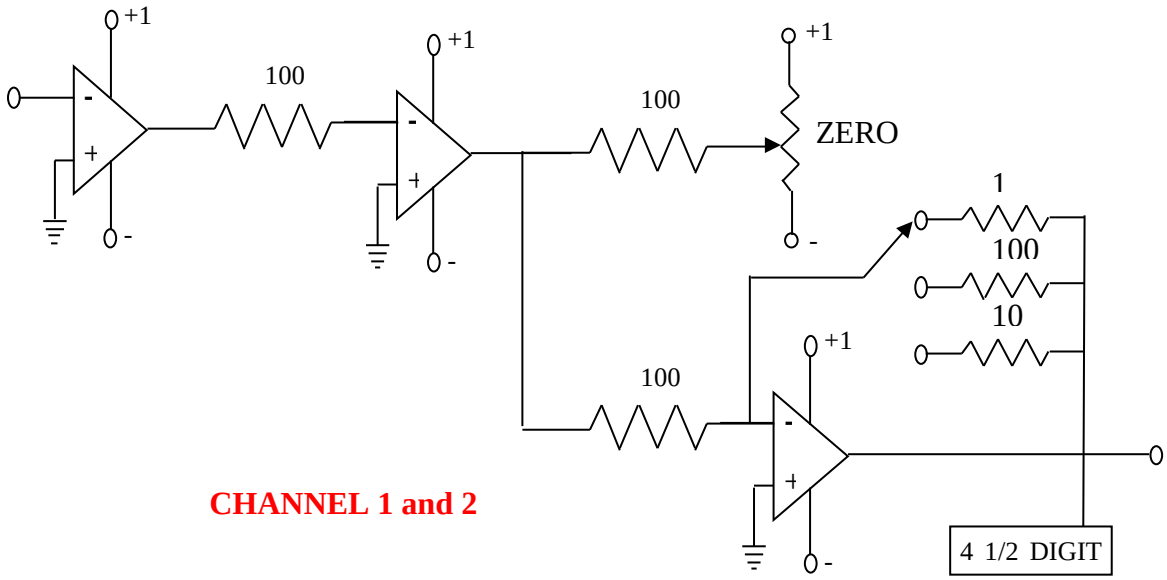

Figure 3.2 A two-channel conditioning circuit with zeroing and variable gain circuits (only one channel shown).

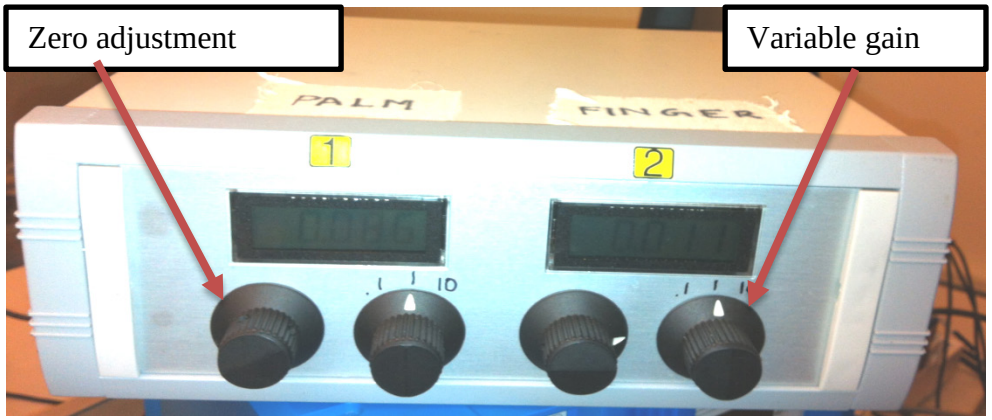

Figure 3.3 A two-channel signal conditioner developed for simultaneous acquisition of finger- and palm-side *FlexiForce*® sensors.

Loading of the sensor was done using a force indenter (Dillon Model GL 500) with a digital force display. The range of the indenter was 0 - 500 N with a resolution of 0.2 N. Force was applied to each sensor through an elastomer and a 18 mm thick metal strip attached to the indenter, as shown in Figure 3.4(a). The static calibration setup with the force indenter is shown in Figure 3.4(b). Initial measurements were conducted by gradually increasing the force applied

to the sensors from 0 to 100 N in increments of about 10 N. The applied force was then gradually decreased to 0 N in order to evaluate the hysteresis of the sensors. Measurements were repeated for three loading and unloading cycles to evaluate their repeatability. Measurements were also performed considering different loading areas by varying the size of the elastomeric pad, and through variations in the indenter position on the sensor. Measurements of the same sensor were repeated on several different days. The data were analyzed to study the sensitivity of the sensor output to variations in the contact area and loading position, and possible degradation of the sensor output over time. Static calibration tests were subsequently performed by placing the sensor on a curved surface, as shown in Figure 3.5.

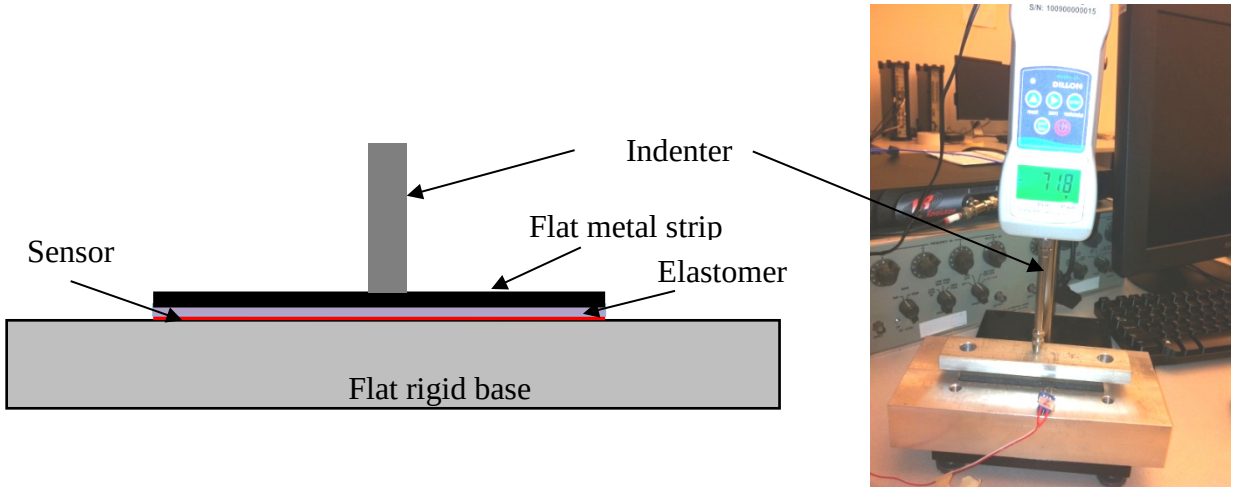

Figure 3.4 Experimental setup for static calibration of the sensors on a flat surface: (a) sensor loading arrangement; and (b) a pictorial view of the force indenter.

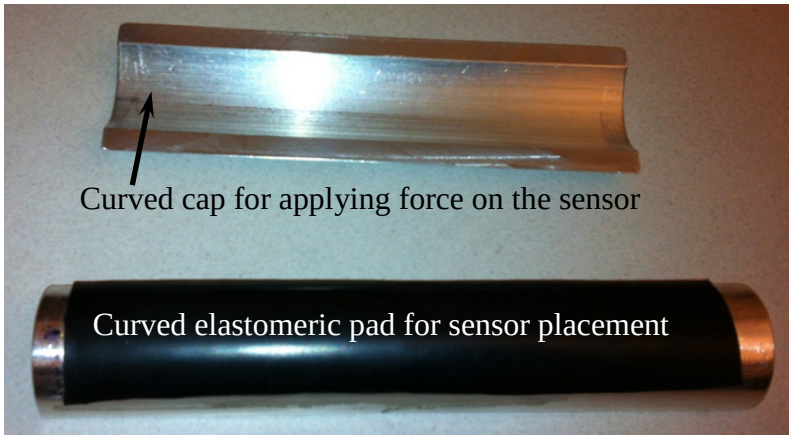

Figure 3.5 Experimental setup designed for static calibration of the sensors on a curved surface.

3.3 Properties of the *FlexiForce*® sensor

Initial measurements were performed to characterize the sensor outputs under different static loads up to 120 N. These measurements involved a total of 12 different sensors, which were numbered sequentially from 1 to 12. Each sensor was placed on a flat surface and the load was applied through an elastomeric interface using the loading indenter shown in Figure 3.4. The data acquired were analyzed to determine the sensor characteristics in terms of linearity, hysteresis, and dependence on the location of applied force, on elastomer stiffness and on sensor length.

3.3.1 Hysteresis of the sensors

The hysteresis properties of the different sensors were characterized by gradually loading the sensor up to 120 N in increments of 10 N, followed by a gradual unloading. These measurements revealed considerable drift in the output signal following each load change, which was attributed to the relaxation properties of the elastomer that was also evident from the drift in the applied force signal. The elastomer was thus permitted to relax for nearly 1 minute after each load change until a steady force value was attained. The measurements obtained with different sensors generally revealed linear voltage output with an increase in the applied load, although some sensors revealed a rapid saturation of the output. As an example, Figure 3.6 illustrates the input-output characteristics of two different sensors during loading and unloading. The results show very low hysteresis of the sensors. Reasonably good linearity of measurement is evident in the entire force range for sensor #4 ($r^2 > 0.99$), while sensor #1 exhibits high linearity only up to 40 N ($r^2 > 0.93$). The results further show considerable differences in the output voltage, although they were both subjected to identical loads. Through discussions with the manufacturer, it was found that these sensors were designed only for qualitative tactile sensing and thus, would likely show poor repeatability of objective measurements from one sensor to another. It is however feasible to fabricate sensors with an enhanced consistency for repeatable objective measurements, but at a more substantial setup cost. The vast majority of the sensors that were tested (10 out of 12) showed similar linear output voltage for the entire range of the applied force. It was thus concluded that these sensors can be used for measuring static force, provided that each sensor is individually calibrated.

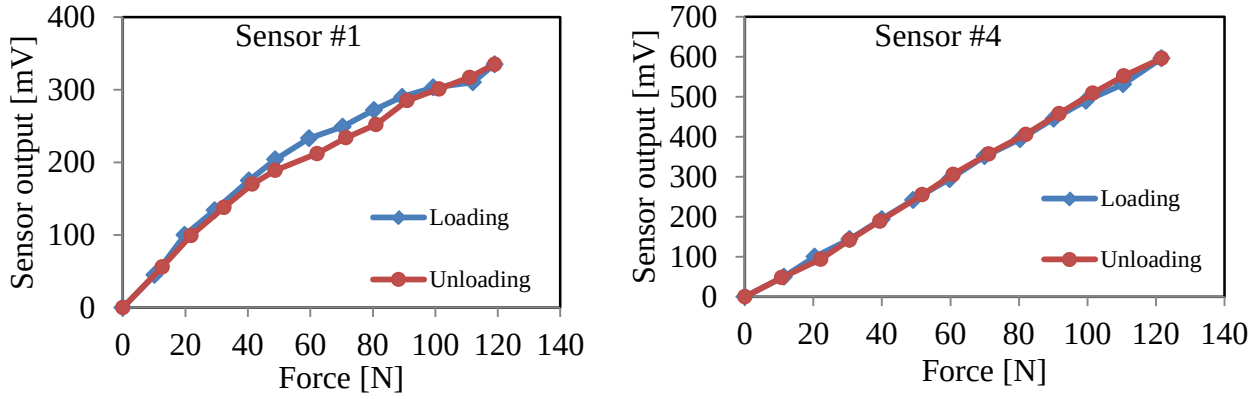

Figure 3.6 Input-output properties of two sensors subjected to gradual loading and unloading.

3.3.2 Effect of sensor length

The *FlexiForce*® sensors (model 1230) are available in a standard length of 149 mm. The sensor, however, could be trimmed to the desired length to adapt to different tool handles. A number of sensors were cut to 117 mm when applied to standardized instrumented handles. The effect of sensor trimming on its linearity and output characteristics was studied by comparing the properties of trimmed and untrimmed sensors. Considering the different sensitivity of the sensors, the measurements were performed with the same sensors so as to evaluate the effect of trimming alone. The measurements with the trimmed sensors used a smaller loading elastomer. Figure 3.7 illustrates the measured input-output properties of the untrimmed and trimmed sensor, for three trials. The results show reasonably good linearity ($r^2 > 0.99$) and good repeatability of the measurements during the three trials. The sensor, however, showed higher sensitivity after trimming, which was attributed to a reduced contact area and thereby a higher contact pressure under similar loads. The mean sensitivity of the untrimmed sensor was 4.28 mV/N (SD = 0.06 mV/N), while the sensitivity of the trimmed sensor increased to 5.71 mV/N (SD = 0.07 mV/N). The results suggest that the output of the *FlexiForce*® sensor depends on both the applied force and the effective area. Trimming the sensor, however, does not affect its linearity.

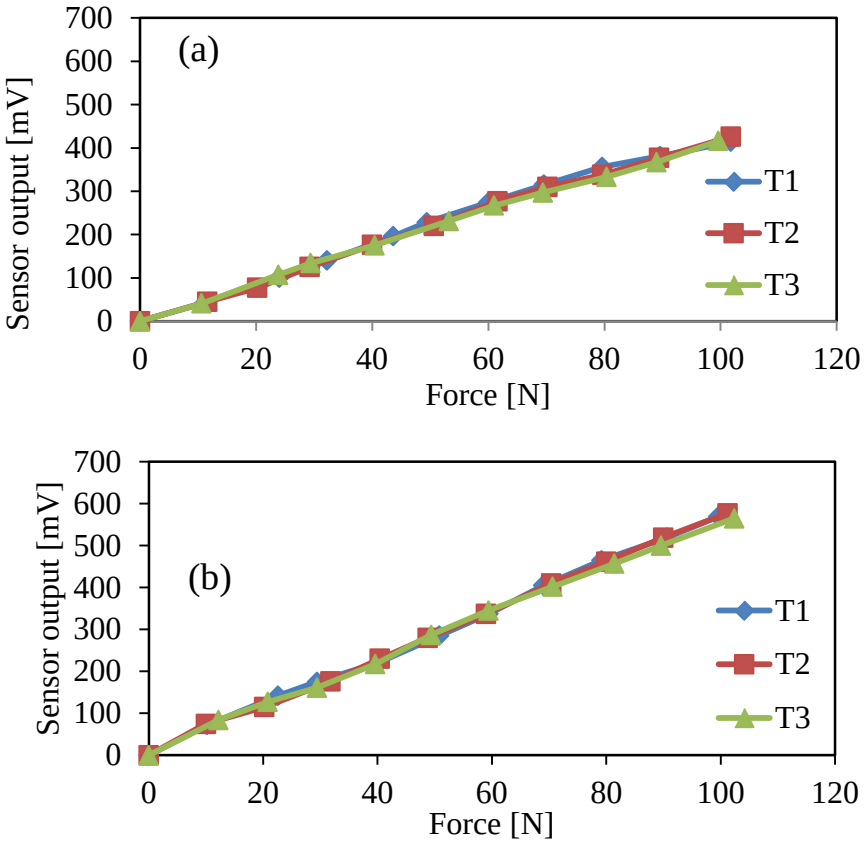

Figure 3.7 Input-output characteristics of an untrimmed and trimmed sensor for three trials: (a) untrimmed sensor, length = 149 mm; (b) trimmed sensor, length = 117 mm.

3.3.3 Effect of elastomer size and rigidity

Static properties of the sensors were measured to study the effects of the loading elastomer size and rigidity. Three rectangular shaped elastomeric pads of different dimensions were used, denoted as long (141.7 mm x 33.3 mm), medium (115.6 mm x 32.7 mm) and short (60.7 mm x 30.0 mm). Each pad was positioned at the center of a full-length sensor and was subjected to a static load of approximately 100 N. The results suggest important effects of the pad dimensions (Figure 3.8). The short and long pads exhibit comparable sensor output for forces up to 60 N, while the long pad yields lower output compared to the short pad under higher forces. This is most likely due to a higher contact pressure imposed by the short pad on the sensor. The medium pad, however, resulted in considerably lower sensor output for the entire force range. The lower output of the medium pad was likely caused by a slight misalignment of the pad with respect to the sensor, which may result in loading of relatively fewer sensels.

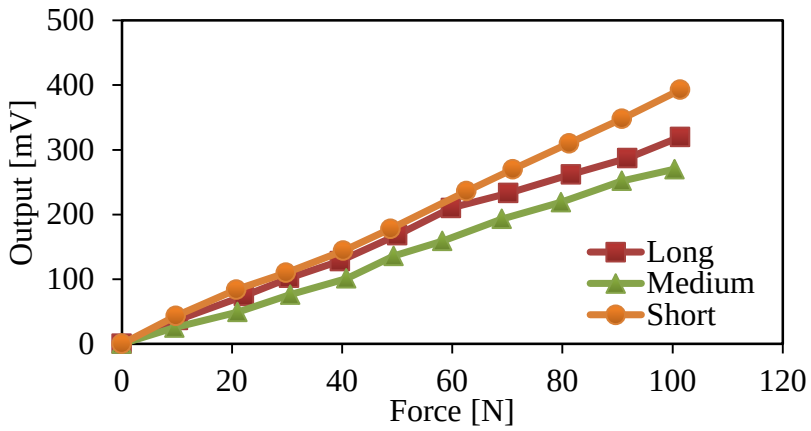

Figure 3.8 Effect of the length of the loading elastomer pad on the sensor output.

Figure 3.9 illustrates the effect of the loading pad rigidity on the sensor output. Two-trial measurements performed with a relatively stiff pad, denoted as ‘stiff’ and a relatively soft pad, denoted as ‘soft’, show substantial effects of the pad rigidity. The sensor loading with the stiff pad resulted in a substantially higher sensor output compared to the soft pad. This was partly attributed to a large deformation of the soft elastomer, causing a nonuniform pressure distribution on the contact surface, and to its longer relaxation time. From these results, it can be concluded that the sensor output is strongly dependent upon the flexibility of the loading medium and its effective contact area. Sensor outputs would thus be expected to vary with different hand sizes when applied to power tool handles. A calibration of the sensors may thus be required for each individual subject.

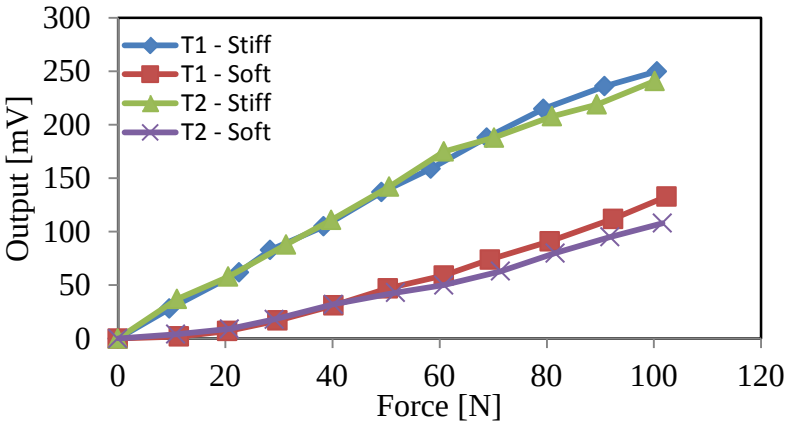

Figure 3.9 Influence of the elastomer rigidity on the sensor output for two trials.

3.3.4 Effect of load position on sensor output

The effect of the load position on the sensor was further investigated through repeated measures taken with the short loading pad (60.7 mm x 30.0 mm) placed at four different positions on the untrimmed sensor. Figure 3.10 shows this effect for the 0 to 100 N force range. The loading pad positioned in the center of the sensor is referred to as 'position 1', while 'position 2' refers to the pad located at one end of the sensor area. 'Position 3' and 'position 4' correspond to the pad located at 60 mm and 85 mm, respectively, from one end of the sensor. The results clearly show a substantial effect of the load position on the sensor sensitivity, which was 4.22, 3.68, 2.45, and 1.93 mV/N for the four positions, respectively. The sensor exhibits the highest output when the applied force is symmetric about the center of the sensor. The sensor yields nonlinear input-output relationships when the loading pad is located asymmetrically about the center of the sensor.

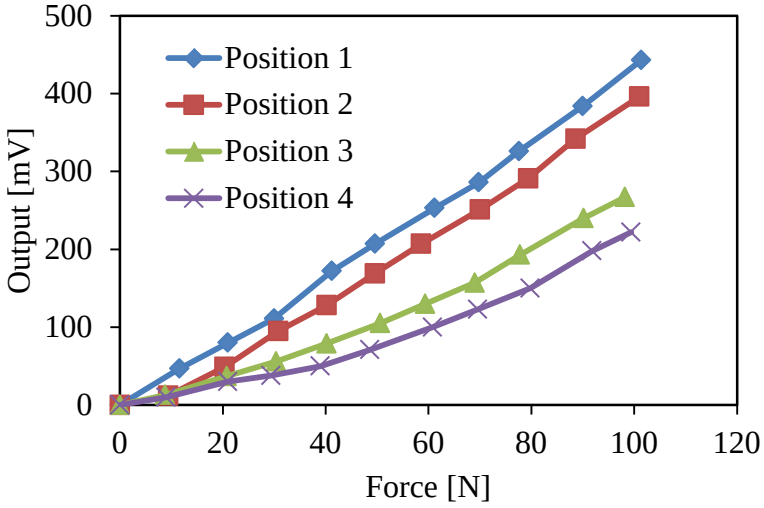

Figure 3.10 Effect of load position on the sensor output.

3.3.5 Temporal degradation of the sensor output

Komi et al. [45] suggested that the output of a *FlexiForce*® sensor decreases with its usage. An experiment was designed to measure the outputs of three different sensors over a period of about three weeks. The same sensors were used for other measurements during the same period. The repeated measures revealed a gradual deterioration of the sensor output over that period. Figure 4.3 shows the change in sensitivity of the three sensors with time. The results show that the sensor sensitivity decreased by 22%, 29% and 40%, for sensor 1, 4 and 7 respectively, within the 24-day period. This is likely caused by wear of the sensor conductors, and suggests the need for sensor calibration prior to its usage.

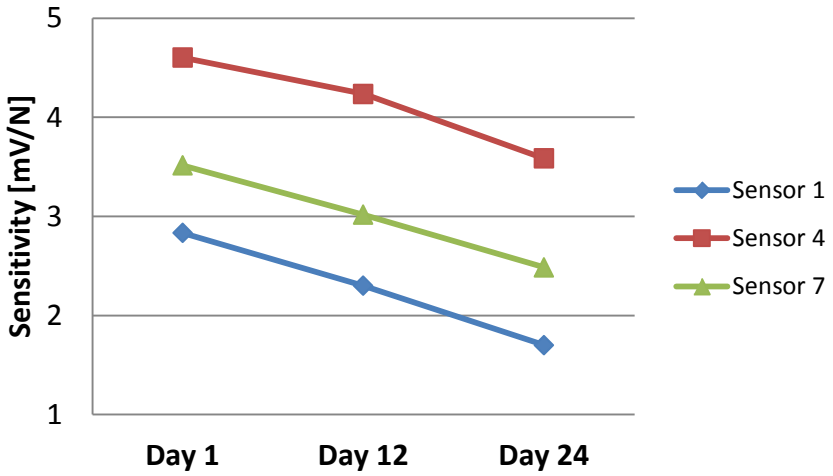

Figure 3.11 Degradation of the sensor sensitivity with time.

3.3.6 Properties of the sensor applied to a curved surface

The input-output properties of the sensor were evaluated when placed on the curved surface (shown in Figure 3.5) to assess their applicability to tool handles. A light-weight curved loading cap (141 mm long) was used to apply the load on the sensor positioned on the 38 mm diameter curved surface through a 2 mm thick elastomer pad. A preload of 7 N was applied to the cap prior to measurement to ensure uniform contact between the sensor and the loading cap. Figure 3.12 illustrates the input-output properties of two sensors acquired during three trials in the 0 to 100 N force range. Nearly linear input-output properties and good repeatability of the measurements were obtained, as observed in the measurements taken with the sensor placed on the flat surface. The sensor output amplitude, however, differ from those obtained with the sensor placed on a flat surface. The static sensitivities of the sensors obtained during the three trials together with the r^2 are summarized in Table 3.1.

Table 3.1 Sensitivity and r^2 values of two sensors calibrated on a curved surface.

Trial	T1	T2	T3
Sensor #4			
Sensitivity [mV/N]	7.41	7.36	7.30
r^2	0.999	0.998	0.999
Sensor #7			
Sensitivity [mV/N]	6.54	6.96	6.91
r^2	0.998	0.997	0.997

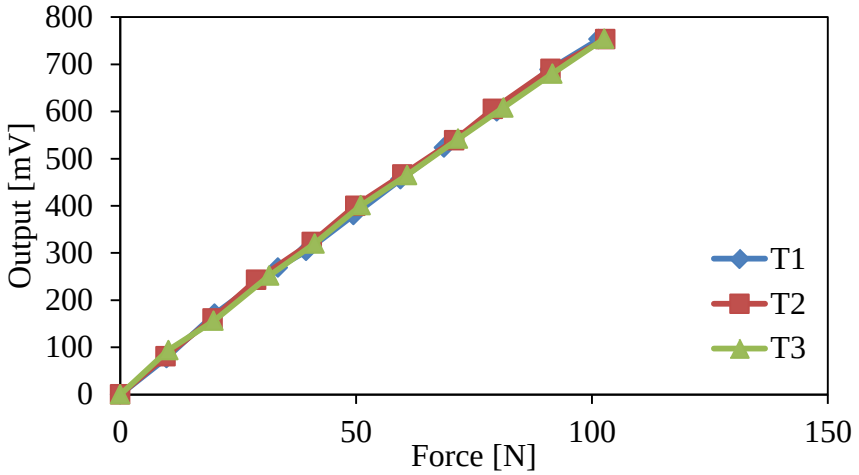

(a)

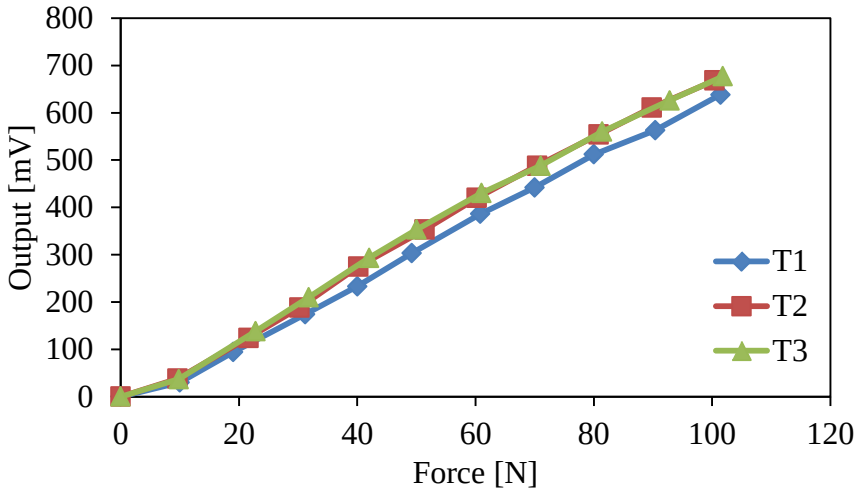

(b)

Figure 3.12 Static input-output characteristics of two sensors subjected to loading on the curved surface: (a) sensor #4; and (b) sensor #7.

4 DESIGN AND APPLICATION OF *FLEXIFORCE*® SENSORS TO CYLINDRICAL AND ELLIPTICAL HANDLES

4.1 Hand-handle pressure and contact force distribution

The hand-handle interface pressure distribution, acquired in an earlier study [41, 42], was analyzed to identify adequate positions of the sensor to achieve reliable estimates of hand grip and push forces. The distributed hand-handle interface force was acquired using 30, 40 and 48 mm diameter instrumented cylindrical handles, similar to those used in the current study. In the previous study, each handle was installed on an electrodynamic shaker in a horizontal plane to permit gripping of the handle along the z_h-axis, as shown in Figure 4.1. A 16 x 11 (16 rows and 11 columns) capacitive interface pressure sensing matrix was used together with the *pliance*® data acquisition system (Novel GmbH, Munich, Germany) to measure the hand-handle interface contact pressure distributed over the contact area. The 2 mm thick sensing mat was wrapped around the selected handle, as shown in Figure 4.2. Each sensor covered an area of 0.766 cm^2, including the spacing between adjacent sensors. Overlapping of active sensors encountered with smaller handles was eliminated by masking selected rows of sensors.

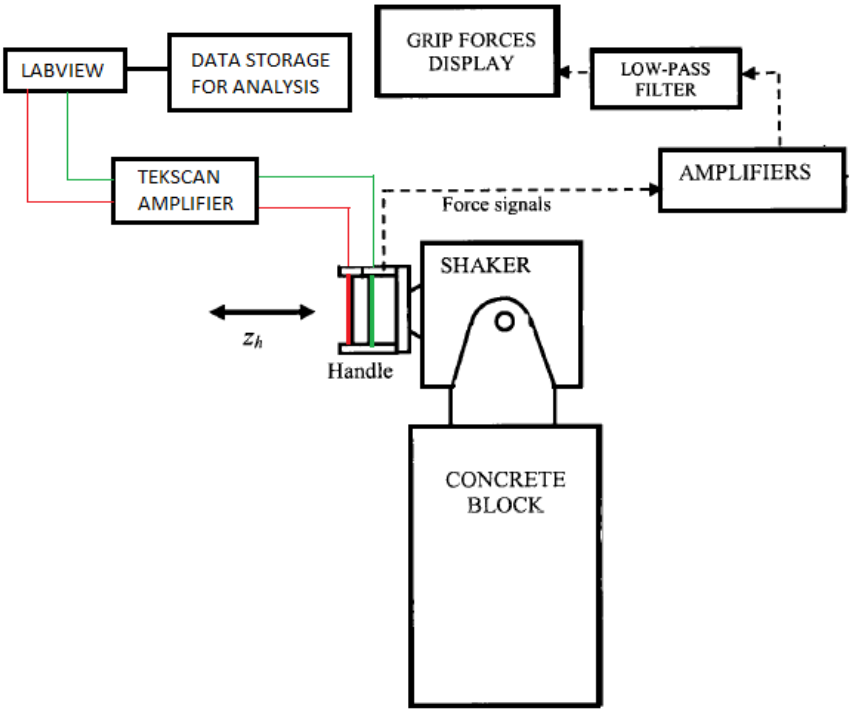

Figure 4.1 Experimental setup for calibration of *FlexiForce*® sensors mounted on instrumented handles [41,42].

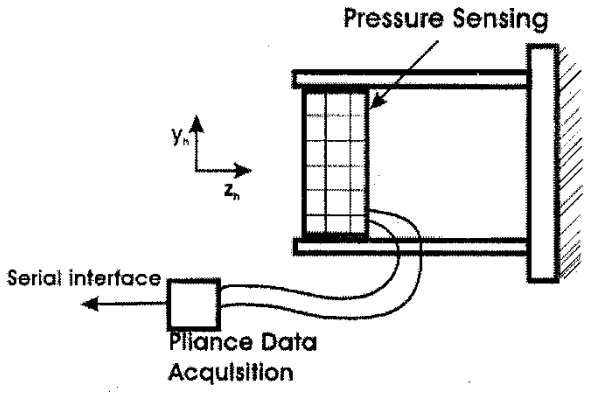

Figure 4.2 Capacitive pressure mat wrapped around the instrumented handle for measuring hand-handle interface contact pressure.

A total of 10 male adult subjects participated in the study. Each subject was advised to stand on a force platform and grasp the instrumented handle with his dominant right hand with a specified arm posture (elbow angle ≈ 90°). The platform height was adjusted to ensure a nearly horizontal forearm and 0° shoulder abduction. The subjects were advised to maintain specified grip and push forces using the feedback from the visual display of the force signals as acquired from the instrumented handle. The measurements were performed under different magnitudes of grip and push forces in the 0-75 N range, to study the effect of force variations on the magnitude and location of peak pressures. For each subject, the experimental design consisted of three handles (diameter = 30, 40 and 48 mm), and combinations of five levels of grip force (F_{gr} = 0, 15, 30, 50 and 75 N) and four levels of push force (F_{pu} = 0, 25, 50 and 75 N). Each measurement was done twice and the data obtained in terms of contact force were examined for the consistency of the measurement.

The hand surface was divided into five different contact zones, as shown in Figure 4.3, to study the localized peak pressure and contact force developed within each zone. Zone 1 contains the fingertips of the second, third and fourth digits for the range of hand sizes considered, while zone 2 envelops the tip and middle phalange of the first digit (little finger) and the middle phalanges of digits II, III and IV. Zone 3 consists of the proximal phalanges of the four digits and the adjacent upper extremity of the palm. Zone 4 encompasses the upper lateral side of the palm, while Zone 5 envelops the upper medial side of the palm. The zone comprising the lower palm and the carpals was excluded, as the contact between this zone and the handles was not observed to be relevant. The measurement system also provides the effective contact area, defined as the area enclosed by active sensors with pressure values exceeding a threshold value of 0.143 N/cm^2.

The force developed over the entire contact surface and within individual zones could be derived through integration of the local pressure over the effective contact area. Because each sensor area is constant, by assuming that the pressure is uniformed over the small sensor area, the contact force F_c (overall and within a zone) is estimated from:

$$F_c = \Delta A \sum_{i=1}^{n} p_{\mathrm{i}} \tag{4.6}$$

where $\Delta A = 0.766\ cm^2$ is the sensor area, p_i is the pressure measured by sensor i and n is the number of active sensors within a zone.

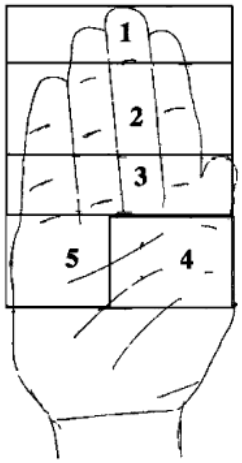

Figure 4.3 Illustration of the five hand-handle contact zones defined to study the contact force distribution [41,42].

The subject hand position with respect to the sensing matrix on each handle was marked during the first test and the subject was advised to use the same position in subsequent tests. The data acquired for 10 subjects and two trials were analyzed to derive the mean and standard deviation (SD) of the overall and the local pressure peaks, and of the contact force corresponding to each test condition. The data from the two trials revealed good repeatability in terms of the contact force, but larger variations in peak pressure were observed, which were attributed to variations in the hand position with respect to a particular sensor location within the grid, as well as the hysteresis effect of the pressure sensors.

The distribution of the contact force at the hand-handle interface was analyzed for different handle sizes and combinations of grip/push forces in terms of the contact force ratio (CFR), defined as the ratio of the contact force developed within a zone to the total hand-handle contact force. The measured hand-handle interface pressure and contact force distribution generally showed high contact pressure peak and contact force in zone 4 (the upper lateral side of the palm), particularly for the 40 and 48 mm diameter handles, and for a push force of 25 N or greater. The peak contact pressure and force, however, shifted towards the finger distal side (zones 1 and 2) in the absence of a push force. These results were then used to identify suitable positions of the *FlexiForce*® sensors for capturing the palm- and finger-side forces in a reliable manner for the handles considered in the current study.

4.2 Identification of the *FlexiForce*® sensor positions

In the current study, the location of these same individual zones on cylindrical and elliptical handles were further determined considering the hand dimensions of four subjects. The hand sizes of the selected subjects ranged from 9 to 10, as per EN 420 [48]. The dominant hand for each subject was mapped on a tracing paper that was wrapped around the handle. The trace was divided into five zones, as shown in Figure 4.3. As an example, Figure 4.4 illustrates the location of the zones mapped around the handle circumference. It should be noted that zones 4 and 5 overlap, when mapped around the handle circumference. The distributed contact force data acquired for the three cylindrical handles are subsequently used to reflect the contact force ratios corresponding to different zones. It should be noted that the diameters of the handles considered in the reported study differed only slightly from those employed in the current study. The effect of this small variation was assumed negligible. As an example, Figure 4.5 illustrates the distribution of the mean CFR over each zone for a combination of a 30 N grip and a 50 N push forces. The CFRs are indicated at the center of each zone, assuming a uniform pressure over each zone, as the center of pressure data were not available. From the illustration, it is evident that zones 4 and 5 contribute substantially to the total hand-handle force, which are mostly located about the handle axis (Figure 4.4), irrespective of the handle size. It is further seen that zone 2 also lies about the handle axis of most of the handles, opposite to zones 4 and 5, with the exception of the smallest handle (32 mm diameter).

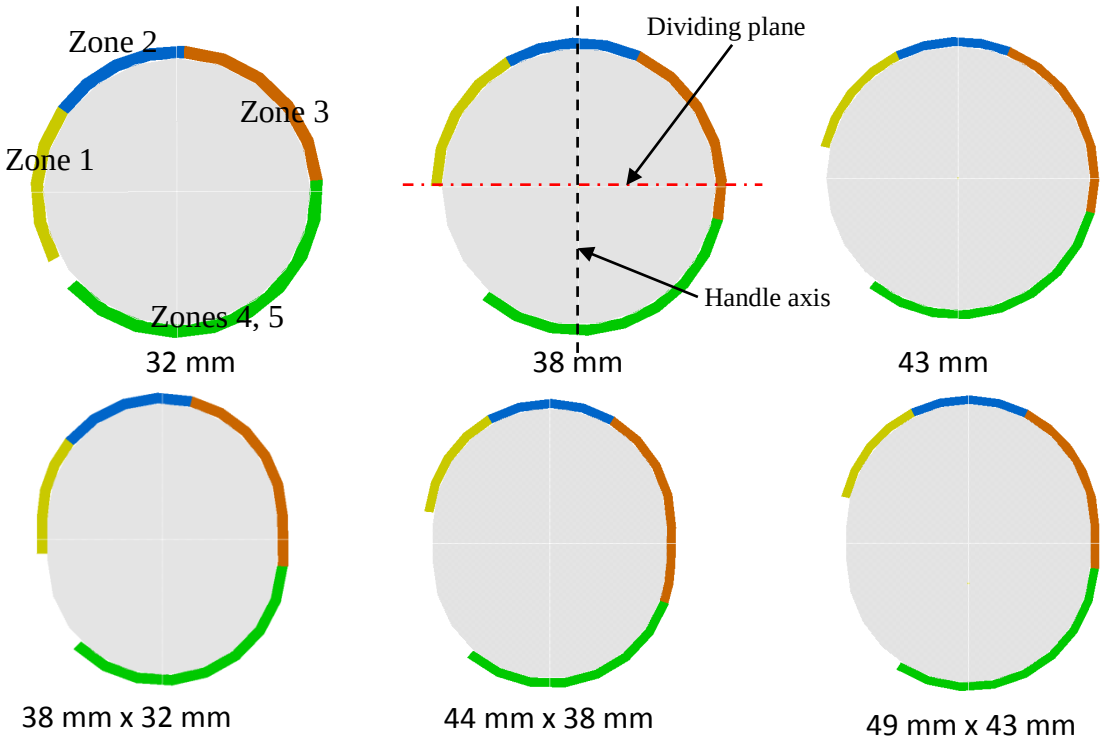

Figure 4.4 Location of different contact zones on cylindrical and elliptical handles considered in the current study (hand size = 9).

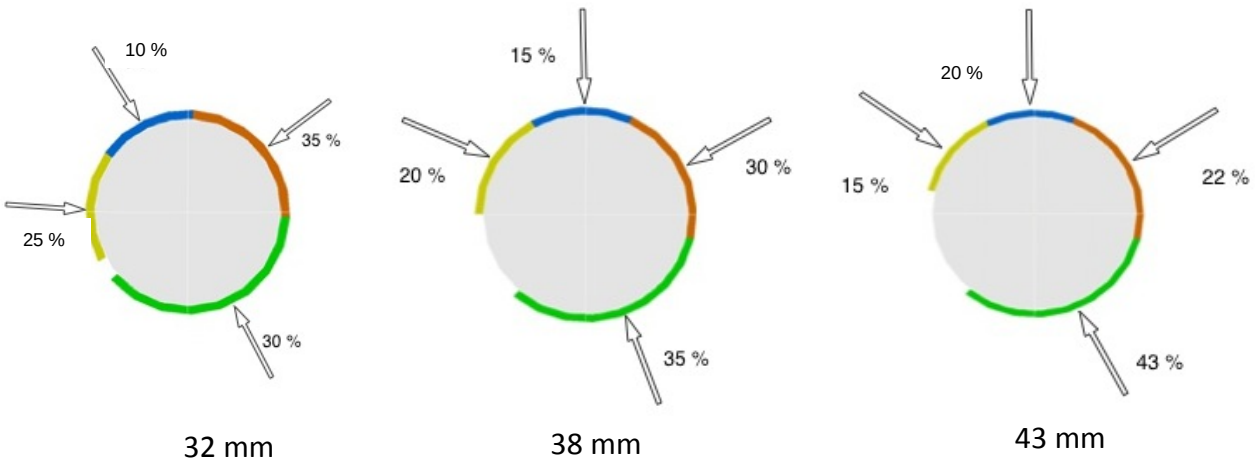

Figure 4.5 Distribution of the contact force ratio (CFR) over different contact zones.

Figure 4.6 illustrates the positions of the resultant forces for all six handles. Considering the *FlexiForce*® sensor width of 40 mm, each sensor covers a span of ±36°, ±30°, and ±27° from the handle axis for the 32, 38 and 43 mm handles, respectively. From the zone maps, it is further deduced that the two sensors shifted by 5 mm counter-clockwise from the handle axis may yield better estimates of the palm- and finger-side forces. Static and dynamic calibrations of the sensors were thus performed by locating two sensors symmetrically on the handle circumference (with the center of the sensor aligned with the handle axis), and by shifting them by 5 mm.

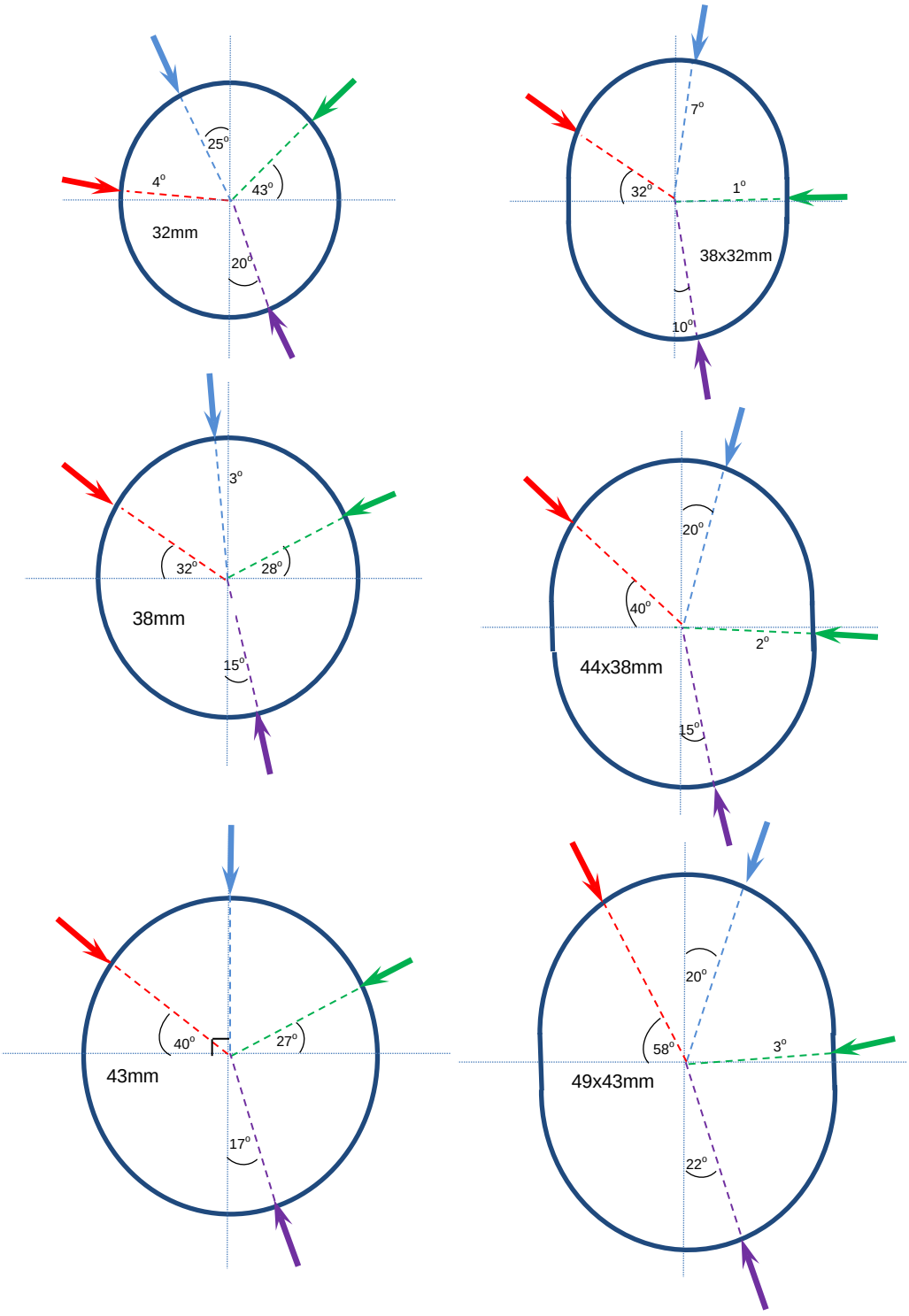

Figure 4.6 Location of the estimated resultant forces over different contact zones with cylindrical and elliptical handles (red – zone 1; blue – zone 2; green – zone 3; and purple – zones 4 and 5).

4.3 Methods - Calibration of *FlexiForce*® sensors mounted on instrumented handles

4.3.1 Experimental device for measuring grip and push forces

The international standard ISO 15230 [9] defines the push force as the sum of the axial components (along the forearm axis) of the hand-handle contact force. The grip force, on the other hand, is the resultant compensated force within the hand due to the opposing gripping action of the palm and fingers of the hand, as shown in Figure 1.2. While the push force may be directly related to the net force applied on the handle through the palm of the hand, the grip force may be expressed by the compensating force exerted by the fingers. The relationships between the palm- and finger-side forces and the grip and push forces can thus be expressed as [47]:

$$F_{gr} = \frac{1}{2}\left(F_{palm} + F_{finger} - \left|F_{palm} - F_{finger}\right|\right) \quad (4.1)$$

$$F_{pu} = F_{palm} - F_{finger} \quad (4.2)$$

where F_{palm} and F_{finger} denote the axial components of the contact force on the palm- and finger-side, respectively. The above relationships suggest that the determination of the hand push and grip forces require the measurements of the axial component on the palm- and finger-side forces of the hand. The *FlexiForce*® sensors applied on the palm- and finger-contact regions can provide good estimates of these force components, as shown in

Figure 4.7. The figure illustrates the arrangement of two *FlexiForce*® sensors (indicated in red color) in the palm- and finger-side contact regions. The validity of this sensor layout was evaluated by mounting the sensors, with this layout on three circular and two elliptical cross-section handles. These included 32, 38 and 43 mm diameter cylindrical handles, as well as and 32 mm x 38 mm and as 38 mm x 44 mm elliptical handles. The evaluation was also attempted with a larger elliptical handle (43 mm x 49 mm), but it was then excluded from the study as most subjects found it to be too large. Each handle was fabricated following a design presented in an earlier study [12], as recommended in ISO 10819 [38] (see Figures 1.4 and 1.5).

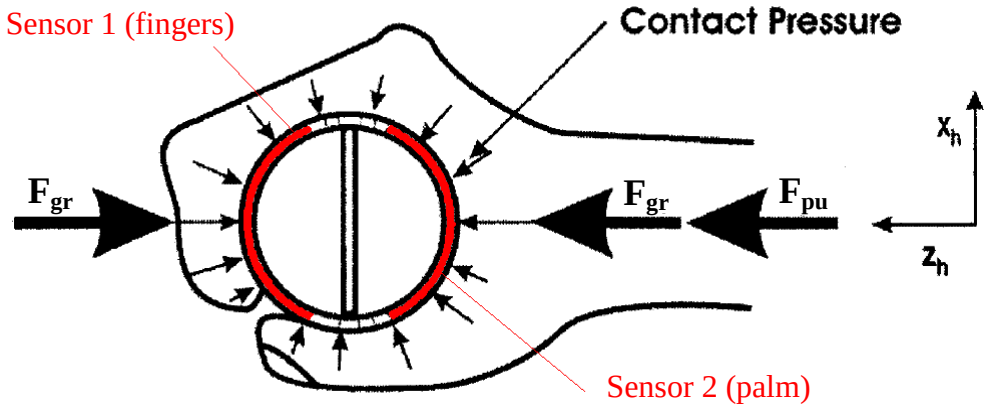

Figure 4.7 Layout of two *FlexiForce*® sensors placed around a cylindrical handle to obtain estimates of the axial component of the palm and finger contact forces.

Each handle was also instrumented to measure the hand grip and push forces, as these forces served as reference values for the calibration of the *FlexiForce*® sensors. For this purpose, two Kistler force sensors (model 9212) were installed between the split handle and the cap for measuring the grip force (Figure 4.8a). Two additional force sensors (Kistler model 9317b) were installed between the handle base and the support fixture to measure the push force (Figure 4.8b). A tri-axial PCB accelerometer was also mounted within the handle to measure handle vibration. This device, comprising the instrumented handle and the *FlexiForce*® sensors, was thus used to perform static and dynamic calibrations of the *FlexiForce*® sensors.

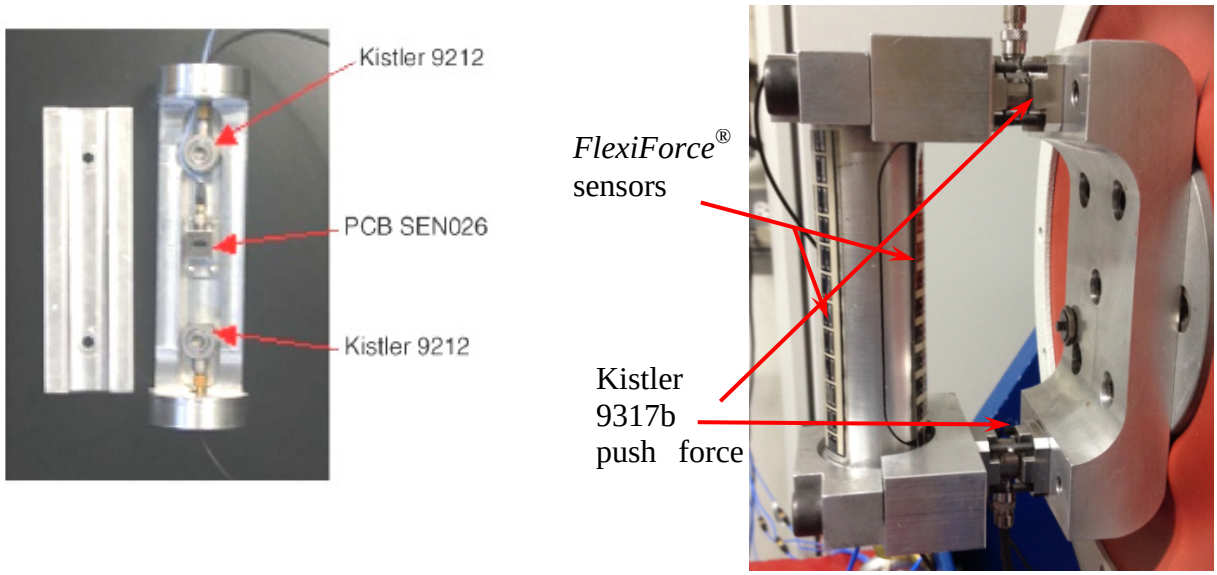

Figure 4.8 (a) Split handle design with grip force sensors and an accelerometer; and (b) handle with *FlexiForce*® sensors supported on push force sensors.

4.3.2 Subjects and test matrix for calibration of FlexiForce® sensors

Nine adults male subjects were recruited for the static and dynamic calibrations of the sensors applied to the instrumented handles. Eight subjects were chosen for the static calibration of the sensors, while seven subjects participated in the dynamic calibration tests. Table 4.1 shows the hand dimensions together with the standing mass and height of the subjects. The table also lists the hand size, as determined in accordance with EN 420 [48].

Both static and dynamic calibrations were performed using the setup shown in Figure 4.1. Static calibrations were done with the subject grasping three cylindrical and two elliptical handles mentioned above (section 4.3.1), while dynamic calibrations were performed with the participant grasping only two different cylindrical handles (38 and 43 mm).

Each subject received a brief training session about gripping and pushing the handle while monitoring the hand grip and push forces, and was permitted a number of practice runs prior to the measurements. The subjects were advised to grip and push the handle, while maintaining the

desired grip and push forces by monitoring the displayed forces, and maintaining a hand-arm posture with an elbow angle of about 90 degrees.

Table 4.1 Anthropometric parameters of the participants.

Subject#	Height (cm)	Body mass (kg)	Hand length (cm)	Width at Metacarpophalangeal joint (cm)	Width at thumb (cm)	Length of distal phalange (cm)	Length of middle phalange (cm)	Length of proximal phalange (cm)	Palm length (cm)	Hand thickness at thumb (cm)	Hand size (EN 420 [48])
1	182.0	95	19.0	8.6	9.9	1.6	2.5	2.5	11.8	4.2	**9**
2	164.5	75	18.2	8.2	10.0	2.3	2.4	2.4	10.2	4.9	**8-9**
3	178.0	65	18.5	8.4	10.1	2.7	2.4	2.5	10.8	3.1	**9**
4	176.5	91	20.5	9.5	10.9	2.9	3	3.1	12.0	5.1	**10**
5	164.0	62	20.0	8.0	9.6	2.9	2.6	3.1	11.2	4.6	**10**
6	175.3	77	18.2	7.7	9.6	2.3	2.1	2.9	11.0	3.8	**8-9**
7	173.2	70	17.0	8.5	9.9	2.5	2.7	2.5	10.1	4.0	**8-9**
8	188.0	74	19.7	8.6	10.4	2.7	2.5	2.9	11.7	4.2	**10**
9	180.0	77	21.2	8.7	10.4	3.1	2.7	3.1	12.8	4.5	**10-11**
Mean	175.7	76.2	19.1	8.5	10.1	2.6	2.5	2.8	11.3	4.3	
SD[1]	7.78	10.9	1.32	0.50	0.42	0.45	0.25	0.30	0.88	0.60	

[1]SD – standard deviation

The sensors were calibrated under static as well as dynamic conditions. For the dynamic measurements, the shaker was operated to generate two different levels of broadband random vibration (1.5 and 3.0 m/s^2 frequency weighted rms acceleration in accordance with the weighting defined in ISO 5349-1 [4]), with nearly flat acceleration power spectral density (PSD) in the 4-1000 Hz frequency range. The desired vibration spectrum was synthesized using a vibration controller, where the handle accelerometer (PCB SEN026) served as the feedback accelerometer.

For both static and dynamic conditions, 12 different combinations of grip and push forces, ranging from 10 to 30 N and 0 to 75 N, respectively, were used. For each condition, the order of the forces was randomized and each measurement was repeated three times. The static and dynamic measurements were conducted in a sequential manner (static first) to evaluate the usability of the measurement system in the presence of handle vibration. Table 4.2 summarizes the test matrix used for the two types of calibration.

Table 4.2 Test conditions for calibration of *FlexiForce*® sensors applied to handles.

Static calibration **Cylindrical handles:** 32 mm, 38 mm, 43 mm **Elliptical handles:** 32 mm x 38 mm, 38 mm x 44 mm **Sensor position**: 0 mm and 5 mm **Number of subjects:** 8 **Posture**: Standing upright with a 90^{o} elbow angle
Dynamic calibration **Excitation:** Broadband random vibration in 4-1000 Hz frequency range; 1.5 and 3.0 m/s^{2} weighted rms acceleration **Cylindrical handles:** 38 mm, 43 mm **Sensor position**: 0 mm **Number of subjects:** 7 **Posture**: Standing upright with a 90^{o} elbow angle

4.3.3 Data acquisition and analysis

The conditioned signals from the instrumented handle sensors, and the signals arising from the *FlexiForce*® sensors were acquired through a multi-channel National Instrument (NI) data acquisition System (model cDAQ-9172; National Instrument Corporation, Austin, TX, USA). A LabView program was developed to derive, from the palm and finger *FlexiForce*® signals, the grip and push forces using Eqs. 4.1 and 4.2. These estimated grip and push forces were recorded and displayed (in mV) on a computer monitor, together with the grip and push forces obtained from the instrumented handle Kistler sensors (displayed in N). These displays were refreshed at a rate of 4 samples/s. The display monitor was installed at the subject's eye level at a distance of about 1 m.

The subjects were asked to maintain the desired grip and push forces by monitoring the display of forces obtained from the instrumented handle. The measurements of the reference force and the *FlexiForce*® sensors signals were recorded for 5 s after a subject achieved steady levels of hand forces. The measured data was subsequently exported to Excel spreadsheets and a macro was developed to derive the push and grip forces from the palm and finger *FlexiForce*® sensor signals using Eqs. (4.1) and (4.2). The macro program also provided the static sensitivity of each *FlexiForce*® sensor together with the correlation of the *FlexiForce*® sensor output with the reference signals.

The sensitivity of the palm *FlexiForce*® sensor was obtained from the reference palm force $F_{r,palm}$ and the sensor output V_{palm}, such that:

$$\boldsymbol{S_{palm} = \frac{V_{palm}}{F_{r,palm}}} \tag{4.3}$$

where S_{palm} is the sensitivity of the palm *FlexiForce*® sensor. The reference palm force, $F_{r,palm}$, is computed from the push and grip forces measured by the reference force sensors integrated within the handle and its support fixture, such that:

$$F_{r,palm} = F_{kis,gr} + F_{kis,pu} \tag{4.4}$$

where $F_{kis,gr}$ and $F_{kis,pu}$ are the grip and push forces, respectively, obtained from the instrumented handle (Kistler sensors). Similarly the sensivity of the finger *FlexiForce*® sensor, S_{finger}, was computed from the reference finger force $F_{r,finger}$ and the sensor output V_{finger}, such that:

$$S_{finger} = \frac{V_{,finger}}{F_{r,finger}} \tag{4.5}$$

where the reference finger force is identical to the reference grip force $F_{kis,gr}$:

$$F_{r,finger} = F_{kis,gr} \tag{4.6}$$

4.4 Static properties of the sensors applied to handles

4.4.1 Repeatability of measurements and intra- and inter-subject variability

Static properties of the sensors were evaluated when applied to handles. The sensors were initially positioned on the handle axis of each handle, as described in section 4.3. The measurements were performed with 8 subjects grasping the handle with different combinations of grip and push forces. The subjects applied the desired forces by monitoring the instrumented handle force signals. Each measurement was repeated three times, and the data was analyzed to determine the repeatability of the measurements and variations in the static sensitivity of the sensors across the subjects. The static calibration of the palm-side sensor was obtained with reference to the palm force applied by the subject, which was determined from the sum of the grip and push forces measured by the force sensors integrated within the instrumented handle fixture. In a similar manner, the finger-side *FlexiForce*® sensor was calibrated with reference to the grip force measured by the instrumented handle sensors.

Results revealed linear relationships between the forces as measured by the *FlexiForce*® sensors and the reference forces derived from the instrumented handle (see equations 4.4 and 4.6), for all handles. Figure 4.9 illustrates the data obtained with one subject while grasping the 38 mm handle. The results show reasonably good repeatability and linearity of the measurements. The mean sensitivity of the palm sensor was 4.37 mV/N (SD = 0.06), while that of the finger sensor was 4.82 mV/N (SD = 0.36). The correlation coefficients of the mean palm and finger force measurements were above 0.98 and 0.94, respectively. The relatively higher variations in the

measured finger forces were attributed to differences in positioning the fingers on the handle between different trials.

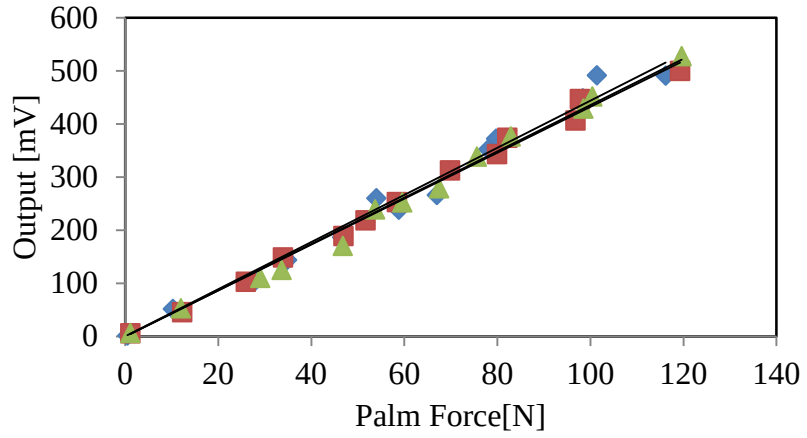

(a)

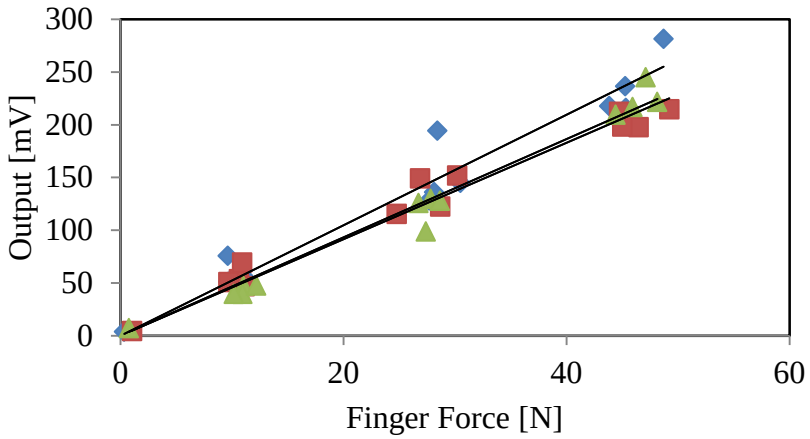

(b)

Figure 4.9 Static input-output characteristics of the palm- and finger-side *FlexiForce*® sensors obtained during three trials with one subject (#5): (a) palm sensor (r^2 >0.98); and (b) finger sensor (r^2 >0.94).

Sensitivity of both palm and finger sensors differed across subjects when gripping a cylindrical handle (38 mm; Table 4.3) as well as an elliptical handle (38 mm x 44 mm; Table 4.4). This variation was attributed to differences in hand sizes and grasping styles of the subjects, which resulted in differences in contact pressure distribution on the sensors. It should also be noted that a different set of *FlexiForce*® sensors was employed for the measurements with the different handles. The tables also present the palm and finger lengths of the subjects. A linear correlation between hand dimensions and sensor outputs, however, could not be established. The coefficients of variations (COV) of the measurements obtained during the three trials for the cylindrical and elliptical handles ranged from 0.8 to 7.8 % for the cylindrical handle, and 0.9 to 11.8 % for the elliptical handle, as shown in the tables.

Table 4.3 Inter- and intra-subject variability in static sensitivity of the palm and finger *FlexiForce*® sensors (38 mm cylindrical handle).

Subject	Palm Length [cm]	Palm sensor sensitivity [mV/N]					
		T1	T2	T3	Mean	SD	COV [%]
1	11.8	4.70	4.48	4.19	4.45	0.26	5.8
2	10.2	4.29	4.12	4.22	4.21	0.09	2.1
3	10.8	4.22	4.08	4.13	4.14	0.07	1.8
4	12.0	4.10	4.12	4.06	4.09	0.03	0.8
5	11.2	4.44	4.32	4.35	4.37	0.06	1.3
6	11.0	4.48	4.71	4.41	4.53	0.16	3.5
7	10.1	4.69	4.66	4.52	4.63	0.09	1.9
8	11.7	4.49	4.29	4.17	4.32	0.16	3.7
Subject	Finger Length [cm]	Finger sensor sensitivity [mV/N]					
		T1	T2	T3	Mean	SD	COV [%]
1	7.2	4.43	4.69	4.54	4.55	0.13	2.8
2	8.0	4.00	3.71	4.33	4.01	0.31	7.8
3	7.7	4.67	4.72	4.57	4.65	0.08	1.7
4	8.5	4.61	4.93	4.92	4.82	0.18	3.8
5	8.8	5.24	4.57	4.66	4.82	0.36	7.5
6	7.2	5.12	4.97	4.91	5.00	0.11	2.2
7	7.2	5.53	5.04	4.96	5.18	0.31	6.0
8	8.0	4.61	4.86	4.63	4.70	0.14	3.0

Table 4.4 Inter- and intra-subject variability in the static sensitivity of the palm and finger *FlexiForce*® sensors (38 mm x 44 mm elliptical handle).

Subject	Palm Length [cm]	Palm sensor sensitivity [mV/N]					
		T1	T2	T3	Mean	SD	COV [%]
1	11.8	1.18	1.05	1.09	1.11	0.07	6.1
2	10.2	1.93	1.85	1.66	1.81	0.14	7.5
3	10.8	2.54	2.18	2.02	2.25	0.26	11.7
4	12.0	1.78	1.65	1.66	1.70	0.07	4.1
5	11.2	2.06	1.90	2.19	2.05	0.15	7.1
6	11.0	1.92	1.83	1.75	1.83	0.08	4.6
7	10.1	2.16	1.92	1.98	2.02	0.13	6.2
8	11.7	1.74	1.73	1.77	1.75	0.02	0.9
Subject	Finger Length [cm]	Finger sensor sensitivity [mV/N]					
		T1	T2	T3	Mean	SD	COV [%]
1	7.2	1.66	2.00	2.09	1.92	0.23	11.8
2	8.0	2.36	2.32	2.21	2.30	0.08	3.6
3	7.7	2.82	2.70	2.55	2.69	0.13	5.0
4	8.5	2.53	2.44	2.61	2.53	0.08	3.3
5	8.8	2.61	2.72	2.86	2.73	0.12	4.6
6	7.2	2.76	2.75	2.62	2.71	0.08	2.9
7	7.2	2.29	2.20	2.24	2.24	0.04	2.0
8	8.0	1.49	1.45	1.48	1.47	0.02	1.5

Figures 4.10 and 4.11 illustrate the variations in the mean static sensitivity of the palm and finger sensors across the 8 subjects for the 38 mm cylindrical and 38 mm x 44 mm elliptical handles, respectively. The results are presented for two positions of the *FlexiForce*® sensors: (i) located symmetrically on each side of the dividing plane of the handle (centered with the handle axis), denoted as ‘0 mm’; and (ii) shifted 5 mm counter-clockwise from the handle axis, denoted as ‘5 mm’ (see Figure 1.2). The results show substantial inter-subject variation in the mean sensitivities of the sensors, as noted above. In addition, the elliptical handle exhibits relatively higher inter-subject variability compared to the cylindrical handle.

The mean sensitivity of all the sensors used with the handles, together with the SD and COV are summarized in Table 4.5. The results are presented for both positions of the *FlexiForce*® sensors, 0 mm and 5 mm. The results clearly show a greater variability in the measurements for both elliptical handles compared to the cylindrical handles. Furthermore, the results show a relatively small effect of the sensor position on the finger force measurements. This suggests that the finger sensor in both positions could effectively capture the force which developed in the contact zones 2 and 3 of the hand (as seen in Figures 4.4 to 4.6). Shifting the palm sensor by 5 mm, however,

generally resulted in lower sensitivity of the palm sensor. The COV of the mean sensitivity attained with the cylindrical handles with centrally positioned sensors (0 mm) ranged from 4.4 to 8.2 % for the palm sensors, and from 7.3 to 11.4 % for the finger sensors. The corresponding values for the sensors shifted by 5 mm were 8.2 to 9.4 % and 11.0 to 15.9 % for the palm and finger sensors, respectively. The COV of the sensitivity obtained with the elliptical handles ranged from 10.9 to 20.0 % for both sensor positions. From the results, it is deduced that the sensors located at the center of the handle axis could yield relatively lower inter-subject variability of the measurements and relatively higher static sensitivity of the palm sensor.

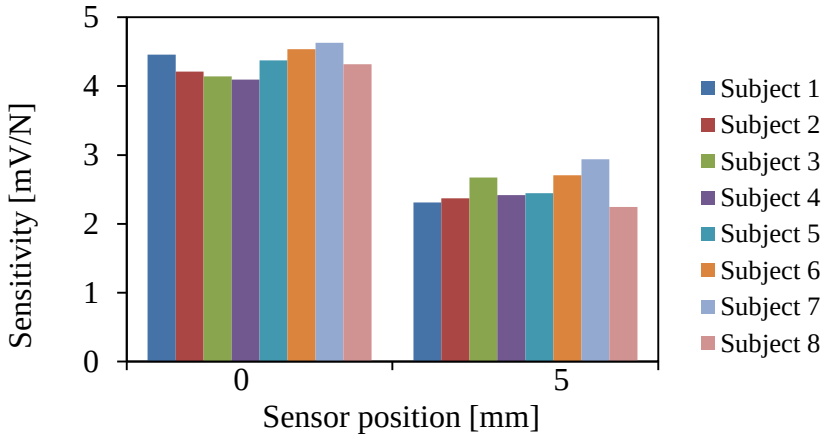

(a)

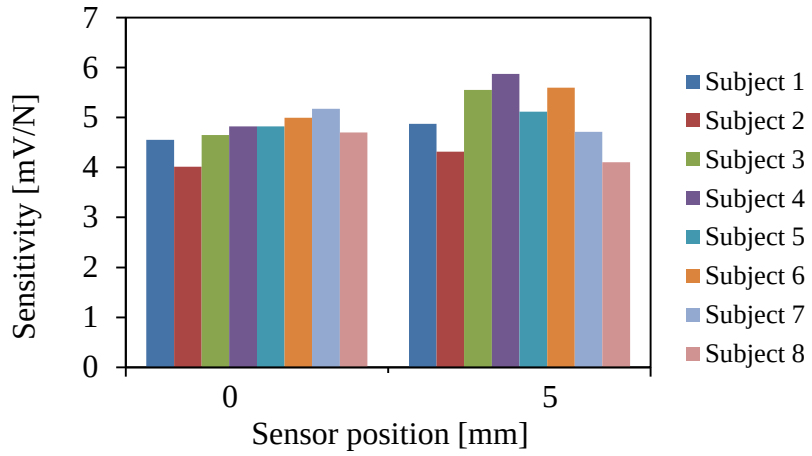

(b)

Figure 4.10 Inter-subject variation in the mean static sensitivity of the *FlexiForce*® sensors when applied in line with the handle axis or shifted by 5 mm, for a 38 mm cylindrical handle: (a) palm sensor; and (b) finger sensor.

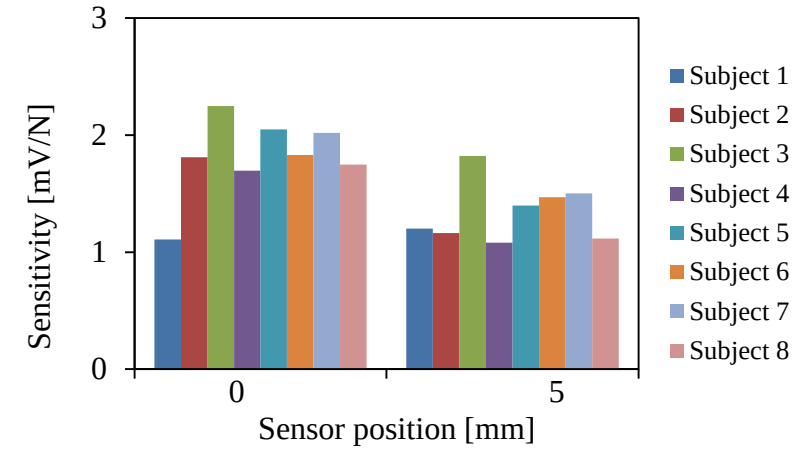

(a)

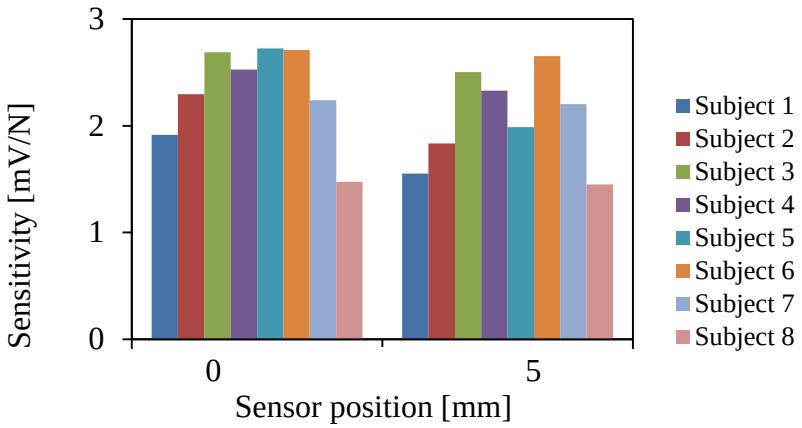

(b)

Figure 4.11 Inter-subject variation in mean static sensitivity of the *FlexiForce*® sensors when applied in line with the handle axis or shifted by 5 mm, for a 38 mm x 44 mm elliptical handle: (a) palm sensor; and (b) finger sensor.

Table 4.5 Inter-subject variability in the static sensitivity of the palm and finger *FlexiForce*® sensors applied to different handles.

Handle size	Sensor #	Mean [mV/N]	SD [mV/N]	COV [%]	Sensor #	Mean [mV/N]	SD [mV/N]	COV [%]
		Palm - 0 mm				**Finger – 0 mm**		
32 mm	**4**	4.67	0.33	7.06	**11**	5.07	0.50	9.95
38 mm	**12**	4.34	0.19	4.36	**10**	4.72	0.35	7.34
43 mm	**4**	2.16	0.18	8.20	**11**	2.32	0.26	11.39
32 mm x 38 mm	**16**	2.55	0.38	14.86	**17**	2.83	0.36	12.63
38 mm x 44 mm	**13**	1.81	0.20	10.87	**18**	2.32	0.45	19.20
		Palm - 5 mm				**Finger – 5 mm**		
32 mm	**4**	4.15	0.34	8.22	**11**	4.34	0.48	11.02
38 mm	**12**	2.51	0.24	9.39	**10**	5.02	0.63	12.61
43 mm	**4**	1.66	0.15	9.21	**11**	2.27	0.36	15.88
32 mm x 38 mm	**16**	2.75	0.54	19.73	**17**	3.04	0.46	15.26
38 mm x 44 mm	**13**	1.34	0.27	19.74	**18**	2.06	0.41	20.04

It needs to be emphasized that the above-reported measurements were attained with the same set of sensors applied to the individual handles, as shown by the sensor identifiers in Table 4.5. The measurements with a given handle were thus performed during a single session of 4 hours, so as to reduce the sensor degradation effect.

The reduction in the sensor sensitivity was clearly observed when a set of sensors was re-applied to another handle, as it had been done for sensors #4 and #11. This is evident from the change in the mean sensitivity with the number of re-applications shown in Figure 4.12. The results are presented for the set of sensors (#4 - palm and #11 - finger) re-applied to the 43 mm handle following the measurements with the 32 mm cylindrical handle. The measurements were repeated 4 times during different sessions, where the sensors were removed and re-applied after each trial. The results clearly show a substantial reduction in the sensor sensitivity with an increasing number of re-applications.

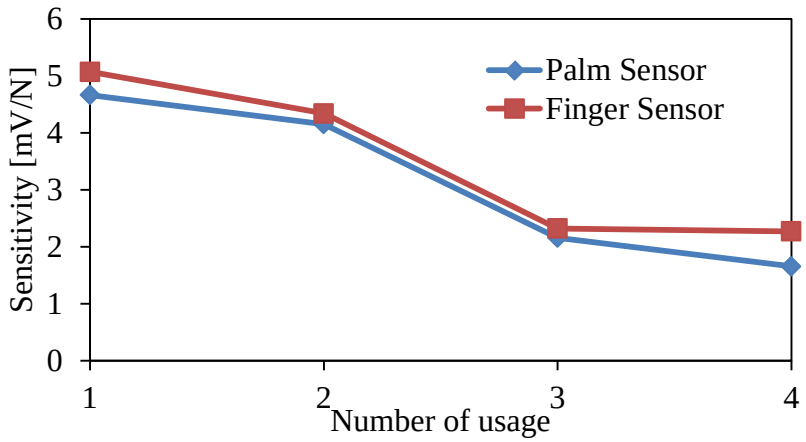

Figure 4.12 Variation in the palm sensor (#4) and finger sensor (#11) sensitivity with increasing re-applications on the 43 mm cylindrical handle.

4.4.2 Effect of finger- and palm-side sensor position

Sensor outputs, presented above, show strong effects of hand dimension, handle diameter and cross-section, and sensor re-usage. The effects of hand size or handle cross-section alone could not be identified due to the degradation of the sensors with usage and large inter-subject variability. Owing to the complex contribution of various factors, the data acquired for the 38 mm cylindrical handle, which showed the least inter-subject variability (Table 4.5), was further analyzed to identify a suitable position for the palm and finger sensors. Figure 4.13(a) shows the effect of sensor position on the mean sensitivity obtained for all subjects. The results clearly show a higher sensitivity of the palm sensor, when positioned in line with the handle axis, compared to that shifted by 5 mm. The mean sensitivity of the palm sensor decreases nearly by 42.1 % when it is shifted by 5 mm from the handle axis (Table 4.6). The finger sensor sensitivity, however, increased slightly (6.4 %) when it is shifted by 5 mm from the handle axis. The data obtained for the 38 mm x 44 mm handle, however, showed an opposite trend for the finger sensor as it resulted in a decrease in its sensitivity by 11 % when shifted by 5 mm from the handle axis, as seen in Figure 4.13(b) and in Table 4.6. It is seen that the zones 2 and 3 of the hand lie either close to the handle axis or towards the right side of it (Figure 4.4). Shifting of the finger sensor in the counterclockwise direction thus yields beneficial effect for the cylindrical handle, while the sensor output is adversely affected for the elliptical handle. From these results, it is deduced that sensors located symmetrically on each side of the dividing plane of the handle would yield a relatively higher sensor output for the 38 mm cylindrical and the 38 mm x 44 mm elliptical handles, in agreement with the results obtained from the contact force distribution presented in section 4.2.

Figure 4.14 compares the overall mean static sensitivity obtained with the two positions of the palm and finger sensors for all handles considered in the study. The results clearly show a dependence of the sensor position on the handle dimensions. The 32 and 43 mm cylindrical handles and the 32 mm x 38 mm elliptical handle show relatively smaller reductions in the mean palm force sensitivity when shifted by 5 mm, compared to the 38 mm cylindrical handle and

38 mm x 44 mm elliptical handle. The 43 mm handle, on the other hand, exhibits very little effect of the finger sensor position on its mean sensitivity.

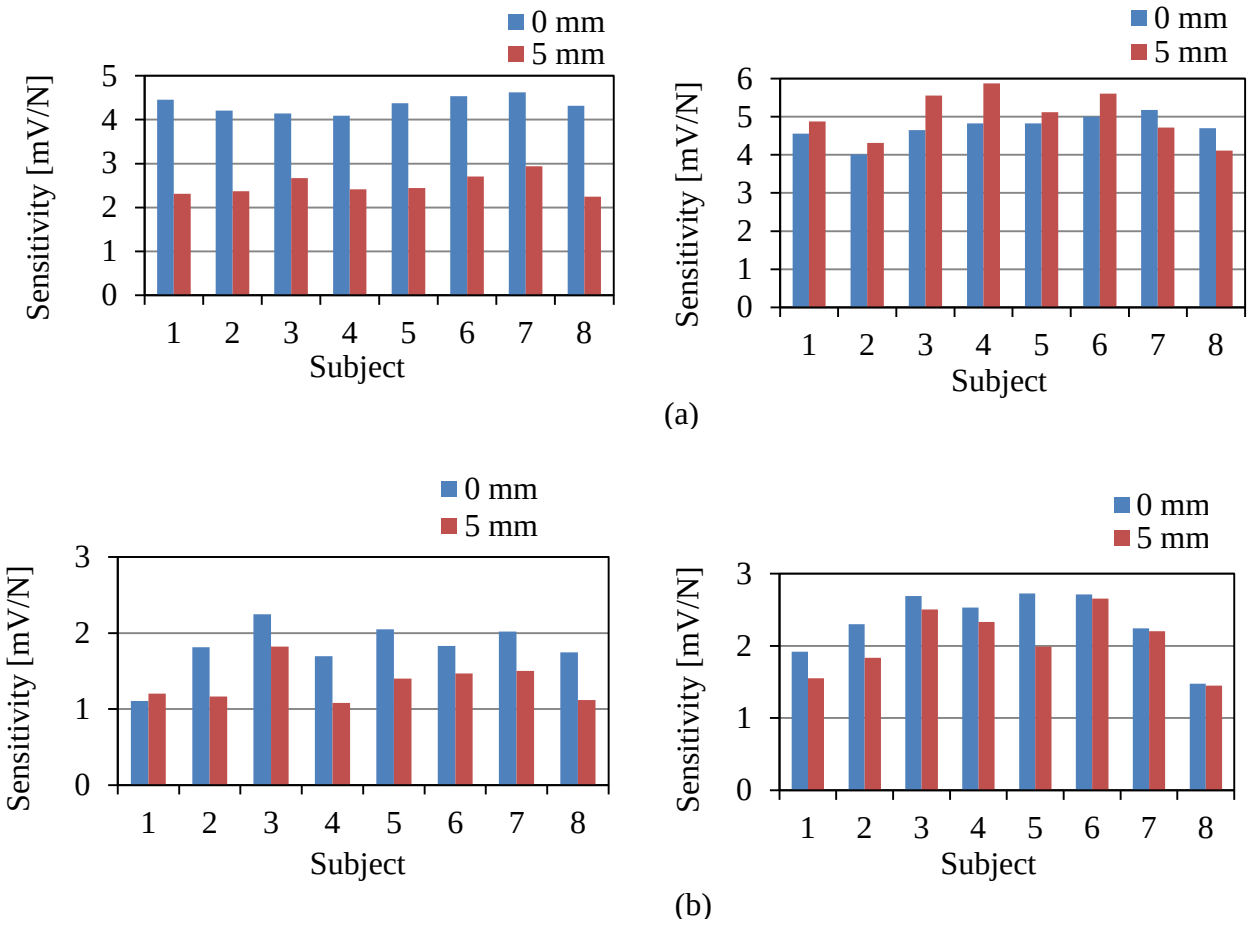

Figure 4.13 Effect of sensor position on the mean static sensitivity of the palm force sensors (left) and finger force sensors (right): (a) 38 mm cylindrical handle; (b) 38 mm x 44 mm elliptical handle.

Table 4.6 Percent change in the mean palm and finger sensor sensitivity caused by a 5 mm shift of the sensors from the handle axis.

	Palm		Finger	
Handle size	Sensor #	% change	Sensor #	% change
32 mm	4	-11.0	11	-14.4
38 mm	12	-42.1	10	+6.4
43 mm	4	-23.2	11	-2.2
32 mm x 38 mm	16	+7.5	17	+7.4
38 mm x 44 mm	13	-25.9	18	-11.1

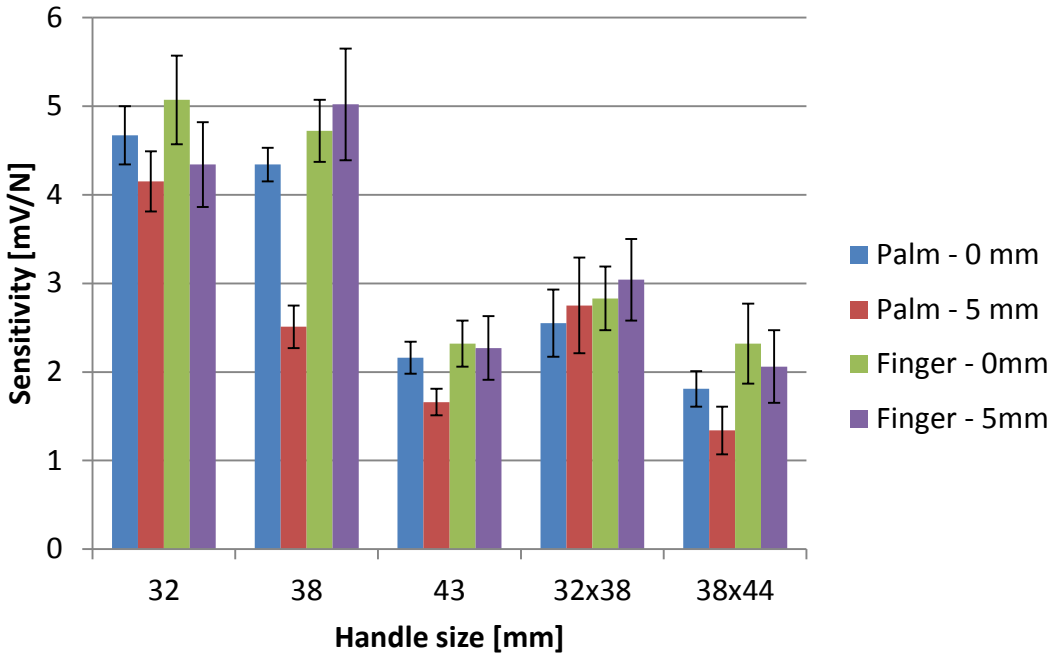

Figure 4.14 Effect of sensor position on the mean palm and finger sensor sensitivity for different cylindrical and elliptical handles.

4.5 Properties of the *FlexiForce*® sensor under handle vibration

4.5.1 Repeatability, inter- and intra-subject variability

The dynamic properties of the sensors are evaluated using the method described in section 4.3, so as to evaluate their usability for measurements of hand forces on vibrating tool handles. Measurements were performed under two magnitudes of broadband handle vibration (1.5 and 3 m/s^2 frequency-weighted rms acceleration) in the 4 to 1000 Hz frequency range. The palm and finger sensors were located symmetrically on each side of the dividing plane, centered with the handle axis. Owing to the changes in sensor sensitivity over time, a static calibration of the sensors was conducted with each subject prior to applying the vibration. The measured *FlexiForce*® signals were low pass filtered to obtain the mean palm and finger forces. The measurements were performed with a total of 7 subjects and two cylindrical handles (38 and 43 mm). As an example, Figure 4.15 illustrates the correlation of the palm and finger forces obtained from the *FlexiForce*® sensors with the corresponding reference values measured with subject #5 grasping the 38 mm handle under the higher level of vibration (3 m/s^2 frequency-weighted rms acceleration). The results, shown for two trials, illustrate good repeatability and linearity of the measurements with the vibrating handles.

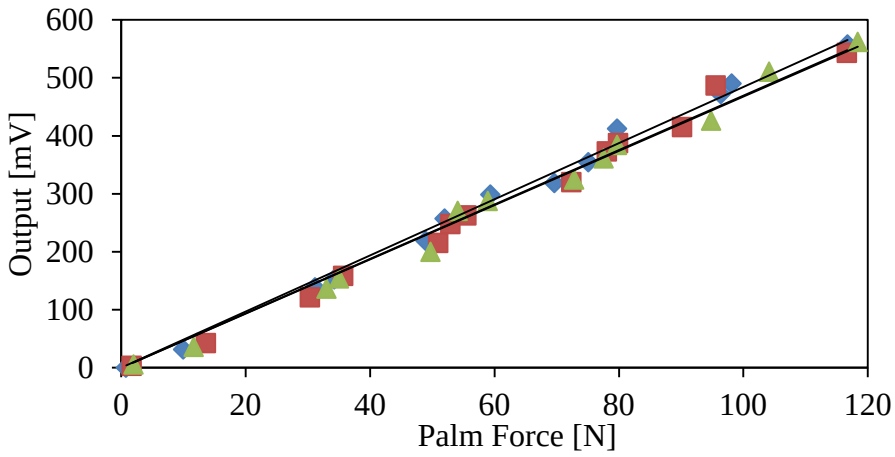

(a)

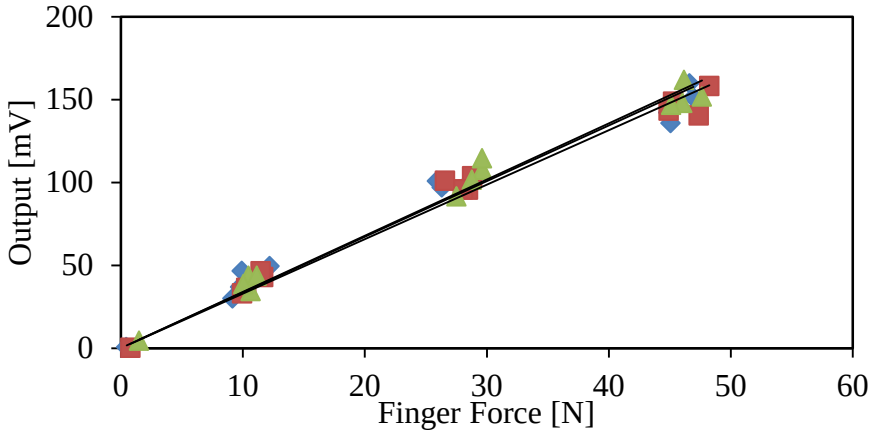

(b)

Figure 4.15 Input-output properties of *FlexiForce*® sensors under a broadband handle vibration at 3 m/s^2 frequency-weighted rms acceleration in the 4 - 1000 Hz frequency range: (a) palm sensor - r^2 >0.98; and (b) finger sensor - r^2 >0.96 (38 mm handle, subject #5).

The mean sensitivity of the palm and finger sensors was 4.74 mV/N (SD = 0.09, COV = 1.91 %) and 3.34 mV/N (SD = 0.05, COV = 1.57 %), respectively, with r^2 > 0.96. Similar degree of repeatability and linearity was observed for the measurements with all subjects, although the sensor sensitivity differed as it was observed under static tests. Tables 4.7 and 4.8 summarize the sensor sensitivity obtained with seven subjects grasping the 38 and 43 mm handles under a 3 m/s^2 vibration excitation, respectively. The tables also present the intra-subject variability expressed as SD and COV, which was considerably smaller than the variability observed for the static measurements. The measurements under vibration generally show reasonably good repeatability. The COV for the two handles and the 7 subjects ranged from 0.9 to 3.7 % for the palm sensor and from 1.6 to 7.1 % for the finger sensor.

Table 4.7 Intra-subject variability in the mean sensitivity of the palm and finger sensors (38 mm cylindrical handle; 3 m/s^2 frequency-weighted rms acceleration excitation).

Subject	Palm Length [cm]	Palm sensor sensitivity [mV/N]					
		T1	T2	T3	Mean	SD	COV [%]
1	11.8	3.93	3.78	3.71	3.81	0.12	3.1
2	10.2	4.02	3.92	3.85	3.93	0.08	2.1
3	10.8	4.77	4.84	4.91	4.84	0.07	1.4
4	12.0	4.49	4.59	4.59	4.56	0.06	1.3
5	11.2	4.84	4.69	4.68	4.74	0.09	1.9
6	11.0	4.39	4.33	4.26	4.33	0.06	1.5
9	12.8	4.86	4.87	4.75	4.83	0.07	1.4
Subject	Finger Length [cm]	Finger sensor sensitivity [mV/N]					
		T1	T2	T3	Mean	SD	COV [%]
1	7.2	2.52	2.28	2.27	2.36	0.14	6.0
2	8.0	2.96	2.81	2.69	2.82	0.14	4.8
3	7.7	3.46	3.28	3.37	3.37	0.09	2.7
4	8.5	2.56	2.45	2.50	2.50	0.05	2.2
5	8.8	3.36	3.29	3.39	3.34	0.05	1.6
6	7.2	2.98	3.06	3.09	3.04	0.06	1.9
9	8.4	2.71	2.39	2.56	2.55	0.16	6.3

Table 4.8 Intra-subject variability in the mean sensitivities of the palm and finger sensors (43 mm cylindrical handle; 3 m/s^2 frequency-weighted rms acceleration excitation).

Subject	Palm Length [cm]	Palm sensor sensitivity [mV/N]					
		T1	T2	T3	Mean	SD	COV [%]
1	11.8	5.50	5.15	5.31	5.32	0.17	3.2
2	10.2	4.31	4.34	4.21	4.29	0.07	1.6
3	10.8	4.19	4.27	4.43	4.30	0.12	2.9
4	12.0	4.72	4.47	4.40	4.53	0.17	3.7
5	11.2	4.27	4.35	4.46	4.36	0.09	2.1
6	11.0	5.77	5.84	5.88	5.83	0.05	0.9
9	12.8	4.74	4.57	4.41	4.57	0.16	3.6
Subject	Finger Length [cm]	Finger sensor sensitivity [mV/N]					
		T1	T2	T3	Mean	SD	COV [%]
1	7.2	3.65	3.60	3.71	3.65	0.06	1.6
2	8.0	2.95	2.79	2.88	2.87	0.08	2.8
3	7.7	2.50	2.78	2.69	2.66	0.14	5.3
4	8.5	3.30	3.13	3.11	3.18	0.10	3.2
5	8.8	3.17	3.05	2.98	3.07	0.10	3.1
6	7.2	4.02	3.95	3.67	3.88	0.19	4.9
9	8.4	3.24	2.91	2.84	3.00	0.21	7.1

The mean sensitivity of the palm and finger sensors obtained with the 7 subjects and the two levels of vibration are further compared in Figure 4.16 and Figure 4.17 for the 38 and 43 mm handles, respectively. These figures also illustrate the static sensitivity of the sensors measured prior to the application of vibration. Although a considerable difference in the mean sensitivity of the sensors is evident across the subjects, these data suggest very a small effect of handle vibration. Analyses of the data for the 3 m/s^2 frequency-weighted rms acceleration excitation revealed peak inter-subject variability of 20.1 and 17.4 %, respectively, for the 43 and 38 mm handles. Relatively higher variability with the 43 mm handle was caused by substantially higher palm sensor outputs for subjects # 1 and #6 compared to the other subjects.

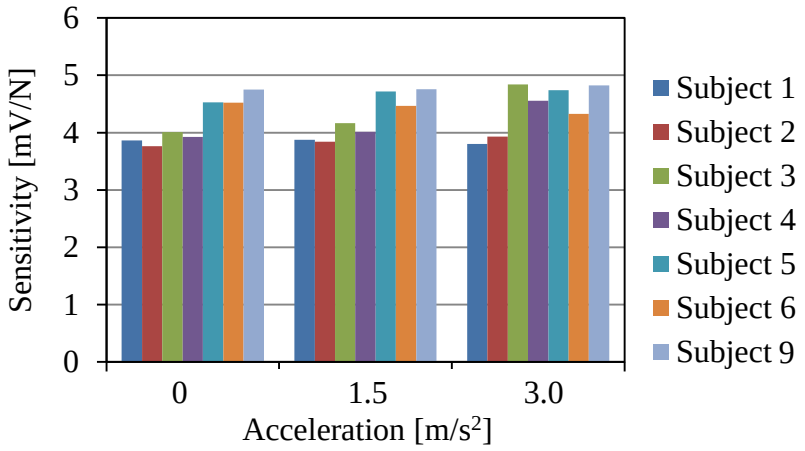

(a)

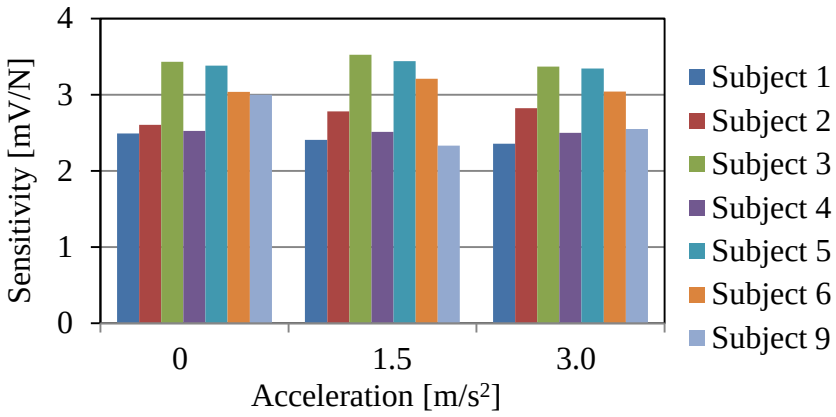

(b)

Figure 4.16 Inter-subject variation in the mean sensitivity of the *FlexiForce*® sensors under static and dynamic conditions: (a) palm sensor; and (b) finger sensor (38 mm handle).

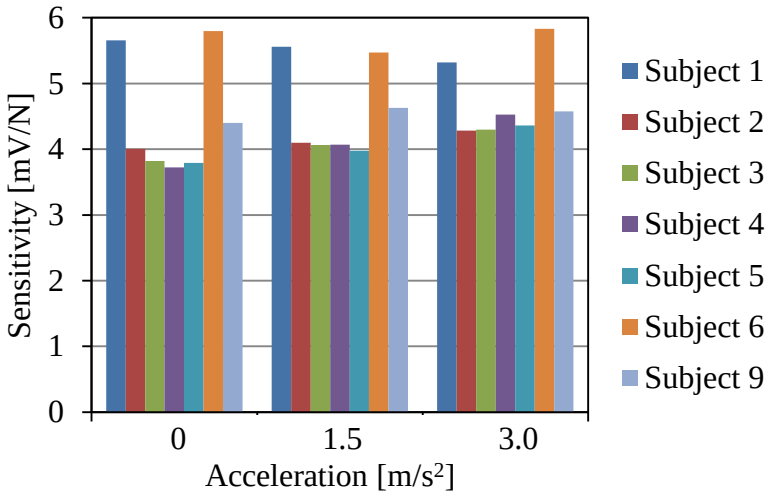

(a)

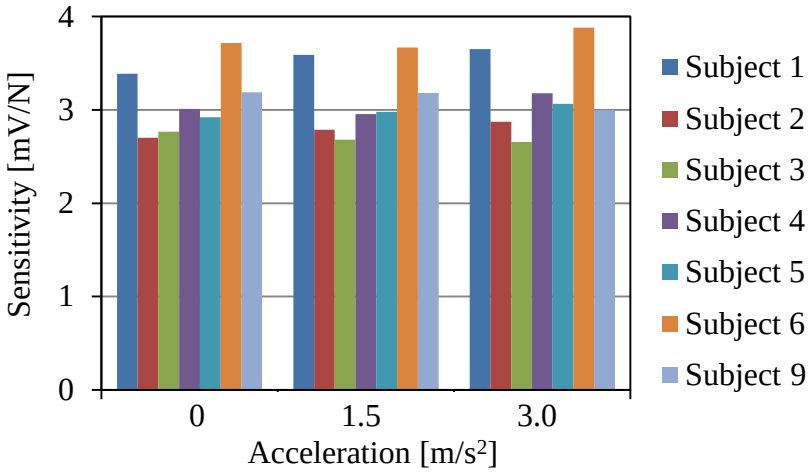

(b)

Figure 4.17 Inter-subject variation in the mean sensitivity of the *FlexiForce*® sensors under static and dynamic conditions: (a) palm sensor; and (b) finger sensor (43 mm handle).

4.5.2 Comparison of FlexiForce® sensor output under static and dynamic conditions

The overall mean sensitivity under static and dynamic conditions are further compared in Figure 4.18. The results generally show a slightly higher palm sensor sensitivity in the presence of vibration for both handles compared to the respective static sensitivity. This may be due to a higher contact pressure on the sensors, as the subjects tend to grasp the handle more firmly in the presence of vibration. The finger sensor sensitivity, however, decreased with vibration for the

38 mm handle. This may be caused by larger variations in the finger-handle contact pressure and possible intermittent loss of finger-handle contact. Measurements done with the 43 mm handle showed a slight increase in the finger sensor sensitivity with vibration, which may be partly caused by the sensor mostly enveloping the contact zones 2 and 3, as seen in Figure 4.5. From the results obtained with both handles, it is evident that these sensors can be used for measuring palm and finger forces on vibrating tool handles as their outputs in the presence of vibration are similar to those attained under static condition.

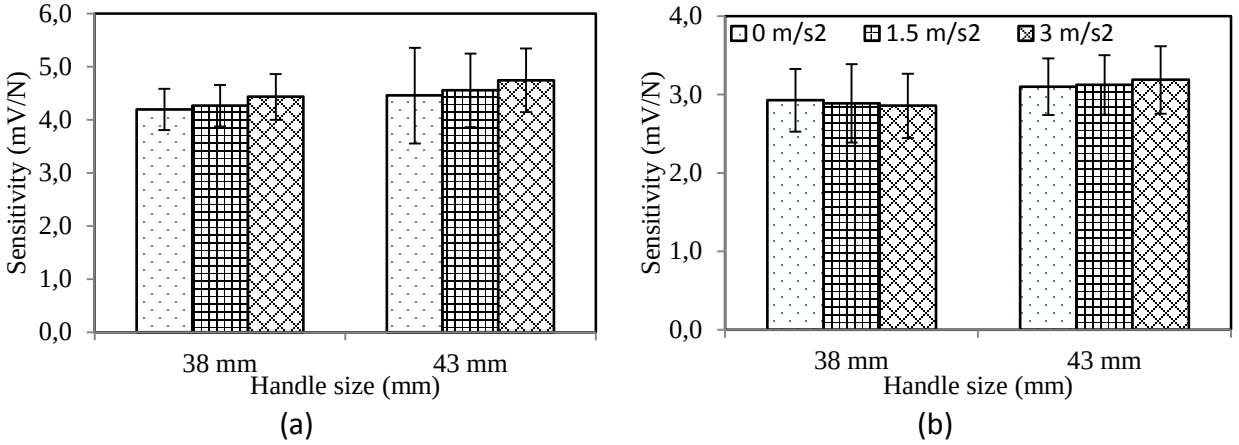

Figure 4.18 Influence of vibration magnitude on the overall mean sensitivities of the *FlexiForce*® sensors: (a) palm sensor; and (b) finger sensor.

Table 4.9 summarizes the percent change in the sensitivity of four different sensors measured under vibration in relation to the static sensitivity. These include the sensors #2, 12, 14 and 19, which were applied for the measurements of the palm and finger forces under vibration. The measurements revealed changes in the sensitivity of 1.6, 2.2, 1.3 and 0.7 %, respectively, which are not statistically significant.

Table 4.9 Overall mean sensitivity of four sensors and change in their sensitivity under vibration relative to the static sensitivity.

Handle	Sensor #	Static [mV/N]	Dyn-1.5 [mV/N]	Dyn-3 [mV/N]	SD	COV
				Palm		
38 mm	14	4.19	4.26	4.43	0.12	2.8%
% change			**1.63**	**4.03**		
43 mm	12	4.46	4.55	4.74	0.15	3.2%
% change			**2.17**	**4.26**		
				Finger		
38 mm	19	2.92	2.89	2.86	0.03	1.2%
% change			**-1.29**	**-1.07**		
43 mm	2	3.10	3.12	3.19	0.05	1.4%
% change			**0.70**	**2.11**		

5 MEASUREMENT OF HUMAN HAND-ARM BIODYNAMIC RESPONSES

The biodynamics of the hand–arm system is one of the important foundations for understanding the mechanisms of vibration-induced disorders and for developing frequency-weightings for assessing risk of vibration exposure. The biodynamic responses of the hand-arm system exposed to vibration are also required for design and assessments of vibration isolation methods, and for developing hand–arm simulators for assessing powered hand tools [12,49]. The biodynamic responses of the hand-arm system have been invariably measured in the laboratory using instrumented handles. Wide differences, however, have been observed among the reported impedance responses of the hand-arm system, particularly at higher frequencies. The observed differences have been attributed to variations in intrinsic and extrinsic variables, test conditions, and the methodologies employed in the various studies [50]. A few studies have shown that the dynamic characteristics of the instrumented handle could contribute to considerable errors in the biodynamic response, particularly those associated with the handle inertia force [29,30]. Adewusi et al. [29] showed that the contributions due to handle inertia at higher frequencies (above 500 Hz) cannot be entirely eliminated through mass cancellation. Dong et al. [30] observed uneven vibration distribution along the instrumented handle (above 500 Hz) that may cause measurement errors and changes in the coupling force at the hand handle interface. These studies suggested the use of handles with very small effective mass and high stiffness, which forms a complex design challenge considering high frequencies of the tools' vibrations.

In this study, the applicability of the *FlexiForce*® sensors is explored for the measurements of the biodynamic responses of the human hand-arm system exposed to vibration. Owing to their negligible mass, these sensors could eliminate the errors attributed to the effective handle inertia. Moreover, these sensors could be applied to the tool handles to directly enable the measurements of biodynamic responses such as driving-point mechanical impedance and the vibration power absorbed into the hand-arm system under realistic field conditions, in addition to the static hand grip and push forces.

5.1 Experimental setup and methods

The feasibility of the *FlexiForce*® sensors for measuring biodynamic responses was investigated through experiments with 6 subjects and the 38 mm diameter cylindrical handle. Figure 5.1 illustrates the experimental setup used for the measurement of the biodynamic responses of the hand-arm system in terms of the driving-point mechanical impedance. Two *FlexiForce*® sensors were installed on the instrumented handle symmetrically on each side of the dividing plane, centered around the handle axis, a prolongation of the forearm axis of the subjects.

Each subject was advised to grasp the handle with the specified push and grip forces, while standing upright with the forearm horizontally aligned with the handle and the elbow flexed at an angle of 90º. An adjustable standing platform was provided for each subject to achieve the desired hand-arm posture. The experiments involved nine different grip/push force combinations with three levels of the push force (25, 50 and 75 N) and three levels of the grip force (10, 30 and 50 N) presented in randomized order, and two levels of broadband vibration in the 4-1000 Hz range (frequency-weighted rms acceleration of 1.5 and 3 m/s^2). Table 5.1 summarizes the test

conditions considered in the study. The subject maintained the desired forces by using a display of the grip and push forces, as measured by the instrumented handle. The handle acceleration and push force signals, together with the palm- and finger-side *FlexiForce*® signals were acquired in a multi-channel data acquisition and analysis system (Brüel & Kjær Pulse system). The data corresponding to each measurement were acquired over a period of approximately 20 seconds, while the subjects were asked to maintain the push and grip forces near the required values. The impedance was evaluated using a frequency resolution of 0.125 Hz, 30 spectral averages and 75% overlap. Measurements corresponding to each test condition were repeated two times.

Table 5.1 Test conditions for impedance measurements.

Instrumented handle: 38 mm cylindrical
***FlexiForce*® sensor position**: 0 mm
Number of subjects: 6
Subject posture: Standing upright with the elbow flexed at 90^o
Excitation: Broadband random vibration in the 4 -1000 Hz range (1.5 and 3.0 m/s^2 frequency-weighted rms acceleration)

The mechanical impedance of the hand-arm system corresponding to each force combination and vibration level was measured in two stages involving the mechanical impedance at the palm (Z_{palm}) and the fingers (Z_{finger}). The handle was initially oriented so as to align the handle axis with the palm of the hand (see Figure 5.1). The *FlexiForce*® sensor was installed on the measuring cap (as shown in Figure 5.1) so as to capture the palm force. Signals from the grip force sensors integrated within the instrumented handle, from the *FlexiForce*® palm sensor and from the accelerometer were acquired and analyzed in order to derive the mechanical impedance at the palm. The impedance evaluated from the grip force sensors was inertia corrected to account for the inertia force due to the measuring cap mass. For this purpose, a Pulse program was written to apply the compensation automatically. The inertia-compensated palm impedance obtained from the instrumented handle sensors ($Z_{r,palm}$) was obtained from:

$$Z_{r,palm}(j\omega) = \frac{S_{Fk,v}(j\omega)}{S_{vv}(j\omega)} \tag{5.1}$$

where $S_{Fk,v}(j\omega)$ is the cross-spectral density of the interface force F_k and the handle velocity v. This impedance response served as the reference value. The palm impedance, measured from the *FlexiForce*® sensor, was evaluated in a similar manner:

$$Z_{palm}(j\omega) = \frac{S_{Fpf,v}(j\omega)}{S_{vv}(j\omega)} \tag{5.2}$$

where $S_{Fpf,v}(j\omega)$ is the cross-spectral density of the interface force F_{pf} measured by the *FlexiForce*® sensor and the handle velocity.

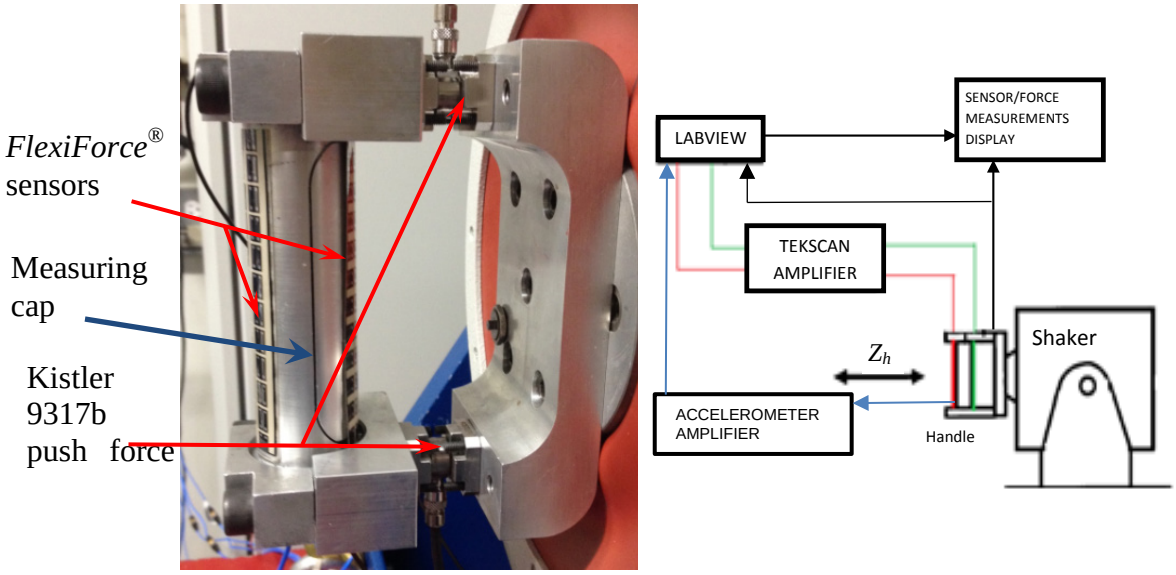

Figure 5.1 Experimental setup for the hand-arm impedance measurement using both the *FlexiForce*® sensors and the instrumented handle.

The handle was subsequently rotated by 180° to align the finger-side contact with the measuring cap, which provided the measurement of the finger force. The finger impedance was evaluated from both the *FlexiForce*® finger sensor and the instrumented handle force signals, using:

$$Z_{r,finger}(j\omega) = \frac{S_{Fk,v}(j\omega)}{S_{vv}(j\omega)}; \quad \text{and} \quad Z_{finger}(j\omega) = \frac{S_{Fff,v}(j\omega)}{S_{vv}(j\omega)} \tag{5.3}$$

where $Z_{r,finger}$ is the reference value of the finger-side impedance obtained from the driving-point force measured by the instrumented handle force sensors, Z_{finger} refers to the impedance derived from the force measured by the *FlexiForce*® finger sensor, and $S_{Fff,v}(j\omega)$ is the cross-spectral density of the finger force F_{ff} and the handle velocity. The total impedance of the hand-arm system Z was obtained through the summation of the palm and finger impedances [49]:

$$Z(j\omega) = Z_{palm}(j\omega) + Z_{finger}(j\omega) \tag{5.4}$$

In the above formulations, the palm force is the sum of the grip and push forces measured by the instrumented handle, as seen in Eq. 3.2. The LabView program was then revised to display the palm and finger forces instead of the grip and push forces. For instance, a 50 N push and a 30 N grip force combination would be displayed as a 80 N palm force and a 30 N finger force. All grip and push force combinations were thus revised in terms of the corresponding palm and finger

forces. Furthermore, owing to the strong dependence of the *FlexiForce*® sensor outputs on the subjects' hand dimensions and effective contact area, calibrations were performed with each subject to determine the sensitivity of the palm- and finger-side sensors prior to the biodynamic response measurements.

5.2 Biodynamic responses measured at the palm- and finger-handle interfaces

5.2.1 Inter-subject variability

Figure 5.2 presents the mean palm-handle interface impedance magnitude and phase response of six subjects obtained from the instrumented handle. The results are shown for the 30 N grip and 50 N push force combination (palm force = 80 N; finger force = 30 N), and 1.5 m/s^2 excitation. The graphs also show the mean palm impedance responses. The palm impedance response measured by the *FlexiForce*® sensor under the same experimental conditions is presented in Figure 5.3. The results obtained from the two measurement systems exhibit comparable trends, while the magnitude differ substantially. The measured data also show considerable variations in the responses attained with the six subjects. The responses measured with one of them (subject #2 in Table 4.1), in particular, show large differences around the primary resonance peak. The impedance response of this subject, obtained from the instrumented handle, exhibits a nearly flat magnitude in the 26-78 Hz frequency range, while the data for other subjects show a resonance peak in this frequency range.

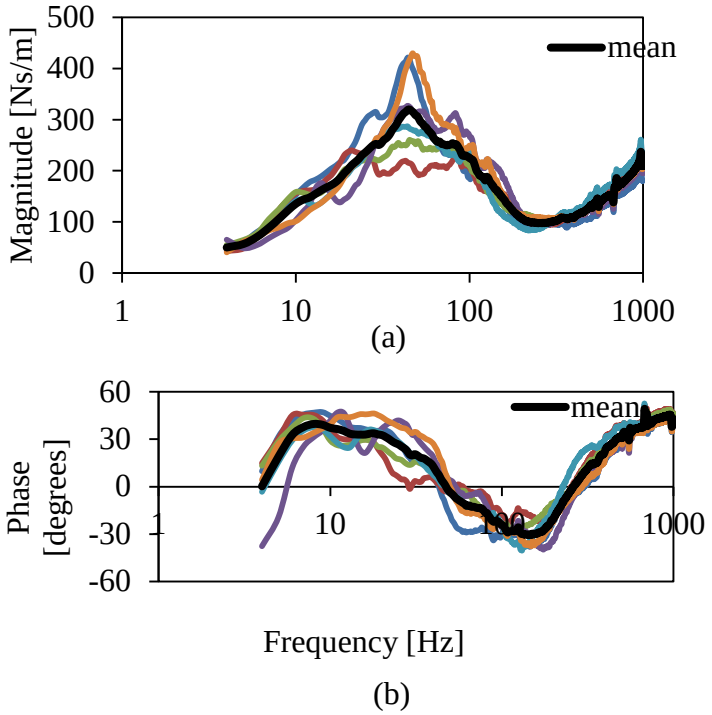

Figure 5.2 Comparison of the palm impedance of 6 subjects as measured with the instrumented handle for a 30 N grip force, a 50 N push force and a 1.5 m/s^2 excitation: (a) magnitude and (b) phase.

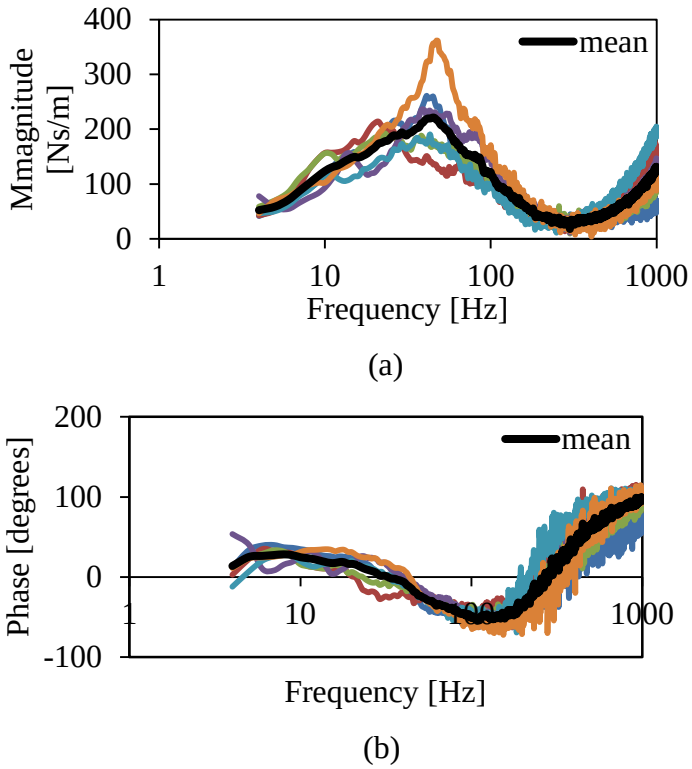

Figure 5.3 Comparison of the palm impedance of 6 subjects as measured with the *FlexiForce*® sensor for a 30 N grip force, a 50 N push force and a 1.5 m/s^2 excitation: (a) magnitude and (b) phase.

Figures 5.4 and 5.5 present the impedance magnitude and phase responses of the subjects measured at the finger-handle interface using the instrumented handle and the *FlexiForce*® sensor, respectively. The results are presented for the 1.5 m/s^2 excitation, and a 30 N grip and a 50 N push force combination. The variability in the *FlexiForce*® measurements was particularly large, which was partly attributed to a considerably lower magnitude of the finger force when compared to the palm force, particularly at low frequencies. Large inter-subject variability was observed in the finger impedance phase responses measured by both measurement systems.The phase response measurements obtained with the *FlexiForce*® sensors are not presented due to very large inter-subject variability. High variability in the phase response measured using the instrumented handle is also observed in Figure 5.4(b), with deviations as high as 40° near 8 Hz. The data obtained with the two measurement systems, however, show comparable trends in the finger impedance magnitude. The results show an increase in the finger impedance magnitude with an increase in the excitation frequency, while the phase response decreased with the same increase in frequency. Similar results were obtained for the 3.0 m/s^2 excitation.

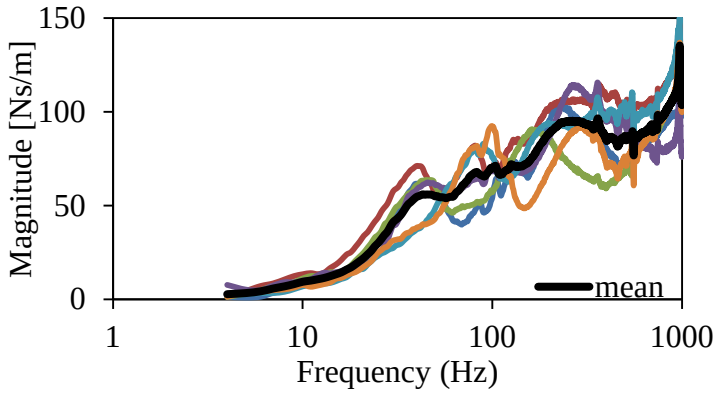

(a)

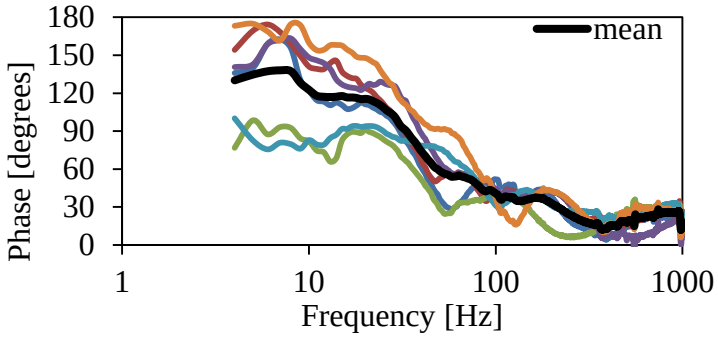

(b)

Figure 5.4 Comparison of finger impedance of 6 subjects as measured with the instrumented handle for a 30 N grip force, a 50 N push force and a 1.5 m/s^2 excitation: (a) magnitude and (b) phase.

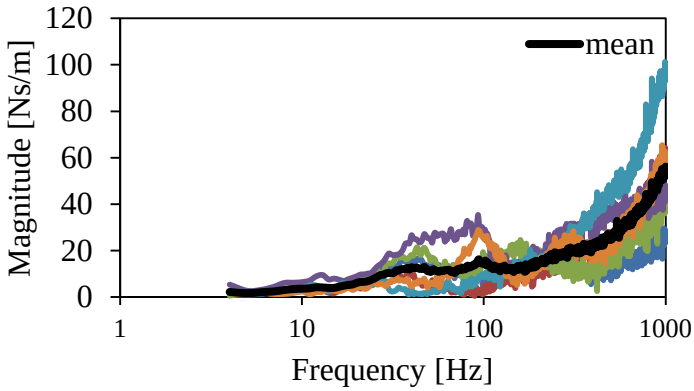

Figure 5.5 Comparison of finger impedance magnitude of 6 subjects as measured with the *FlexiForce*® sensor for a 30 N grip force, a 50 N push force and a 1.5 m/s^2 excitation.

5.2.2 Comparisons of the measured response with the reported data

The palm and finger impedance responses of the human hand-arm exposed to handle vibration have been reported by Dong et al. in a single study [49]. The study reported palm and finger impedance responses under a constant velocity (14 mm/s) sinusoidal excitation at 10 discrete frequencies (16, 25, 40, 63, 100, 160, 250, 400, 630 and 1000 Hz). The frequency weighted acceleration due to this excitation was 1.4 m/s^2 rms, which is comparable with the lower magnitude excitation used in this study. The hand-arm posture used in the reported study was similar to that used, while it employed a 50 N push and 50 N grip force combination. The validity of the measurements was examined through comparisons of the mean palm and finger impedance responses measured using the *FlexiForce*® sensors and the instrumented handle with the reported responses.

The mean palm impedance responses corresponding to two grip/push force combinations (30/50 N and 50/50 N) measured using the *FlexiForce*® sensor and the instrumented handle are compared with the reported responses in Figure 5.6. The comparisons suggest reasonably good agreements between the responses obtained with the instrumented handle and the reported data. Some differences, however, are evident in the 63 to 160 Hz frequency range, where the reported magnitudes are lower than the measured magnitudes. The *FlexiForce*® measurements also exhibit comparable trend, while the impedance magnitude is substantially lower in the entire frequency range. The magnitude is nearly 117 Ns/m lower than that derived from the instrumented handle around the most conspicuous peak near 46 Hz. Better agreement, however, is evident in the palm impedance phase response of the *FlexiForce*® sensor with the reported responses and that obtained from the instrumented handle, although notable differences exist, particularly in the 40 to 100 Hz frequency range.

The finger mean impedance responses obtained from the instrumented handle and the *FlexiForce*® sensor are also compared with the reported data in Figure 5.7. The comparison of finger impedance phase response, however, is limited to that derived from the instrumented handle alone. The measured responses exhibit trends similar to those of the reported responses, while the magnitude and phase values differ notably. The finger impedance magnitude obtained from the instrumented handle compares reasonably well with the reported magnitudes up to 100 Hz, while the measured magnitudes are slightly lower at higher frequencies. Considerable differences in the phase response, however, are evident at lower frequencies up to 100 Hz. The finger impedance magnitudes obtained from the *FlexiForce*® sensor are substantially lower than the reported values in the entire frequency range, as it was observed in the case of the palm impedance magnitude.

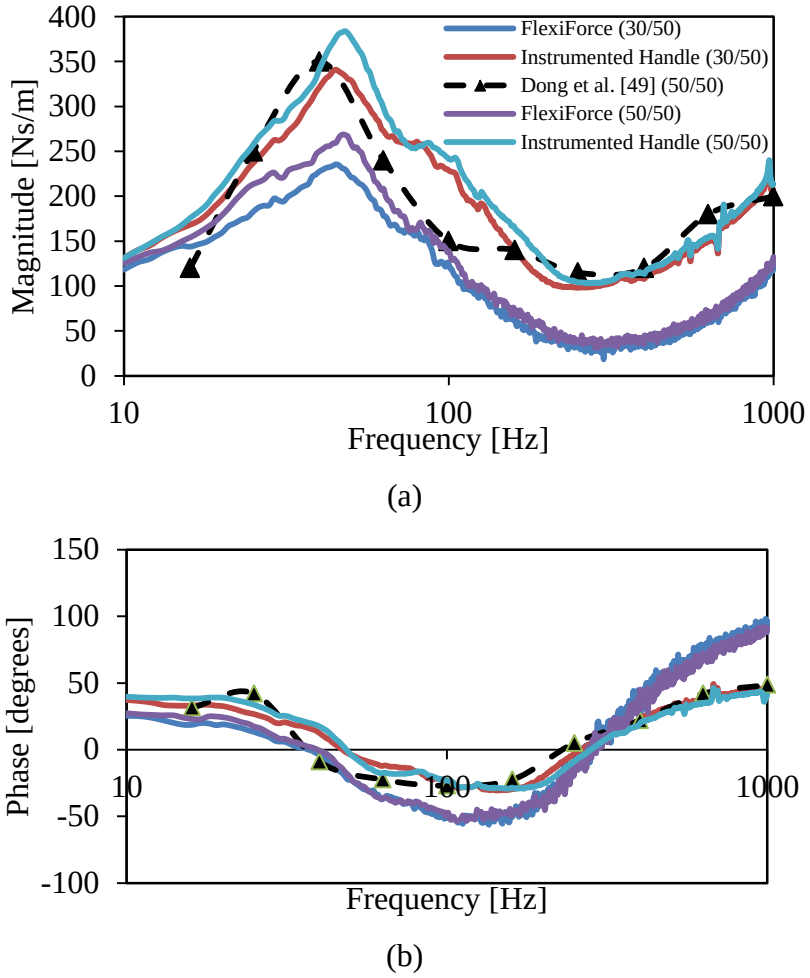

Figure 5.6 Comparisons of the mean palm impedance responses obtained from the instrumented handle and the *FlexiForce*® sensor with the data reported by Dong et al. [49], for a 1.5 m/s^2 excitation: (a) magnitude and (b) phase.

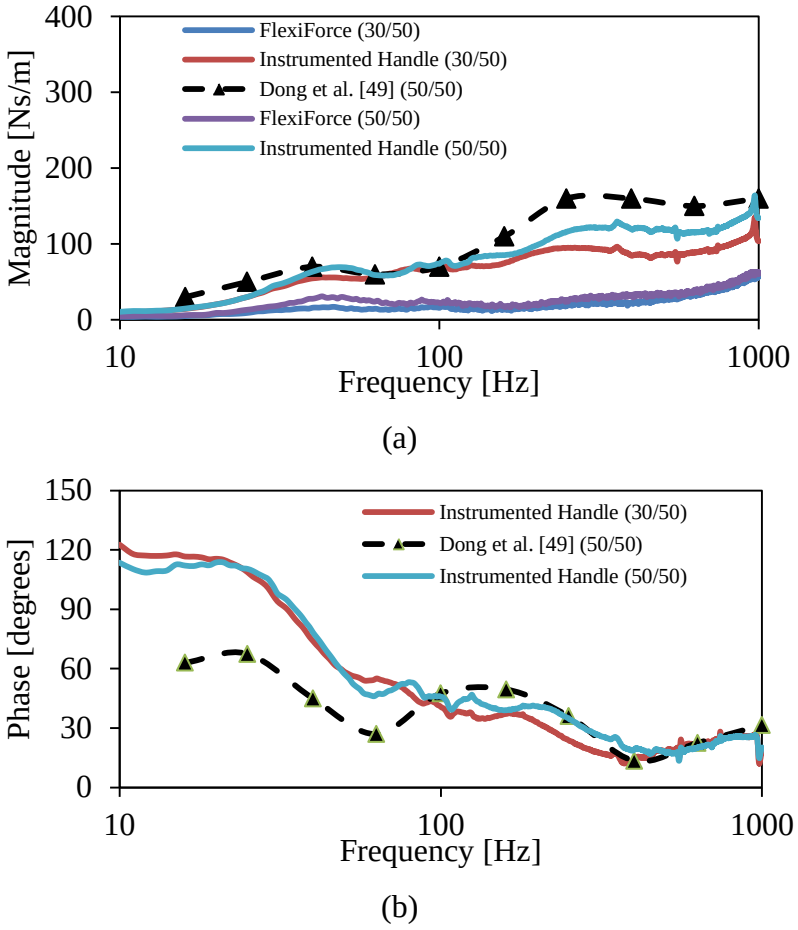

Figure 5.7 Comparisons of the mean finger impedance responses obtained from the instrumented handle and the *FlexiForce*® sensor with the data reported by Dong et al. [49], for a 1.5 m/s^2 excitation: (a) magnitude and (b) phase.

5.2.3 Frequency response characteristics of the FlexiForce® sensor

Lower impedance magnitude responses obtained from the *FlexiForce*® sensors are believed to be caused by the poor frequency response of the resistive sensors. A recent study measured the biodynamic responses of the seated body exposed to whole-body vibration using resistive pressure sensors [51]. The study also reported substantially lower magnitudes of the apparent mass measured by the resistive pressure sensors compared to a force plate, which was attributed to the limited frequency response of the resistive sensors. The study also proposed a methodology to compensate for the limited frequency response using the inverse frequency response of the sensing system. In the current study, the frequency response characteristics of the *FlexiForce*® sensor are evaluated from the measured impedance responses, which could be applied as a correction for obtaining better estimates of the hand-arm system impedance.

The frequency response function (FRF) of the *FlexiForce*® sensor was estimated from the ratio of the complex impedance response measured with the *FlexiForce*® sensor to the reference response from the instrumented handle. The FRFs were obtained for each subject, hand grip and

push force combination, and excitation level. As an example, Figures 5.8 and 5.9 illustrate the FRFs of the palm and finger-side sensors, respectively, corresponding to the 1.5 m/s^2 excitation, and the 50 N push and 30 N grip force combination. The figures show the FRFs obtained from the data acquired for all the six subjects, as well as the mean FRF. It should be noted that the FRF phase response of the sensor is not presented for the finger-side due to extreme variations, as noted in the previous section. The results show comparable trends in the FRFs obtained for different subjects, although considerable scatter is also evident. This data scatter is attributable to the inter-subject variabilities of the measurements, which have been reported to be significant in hand-arm impedance responses [12,19-23,29].

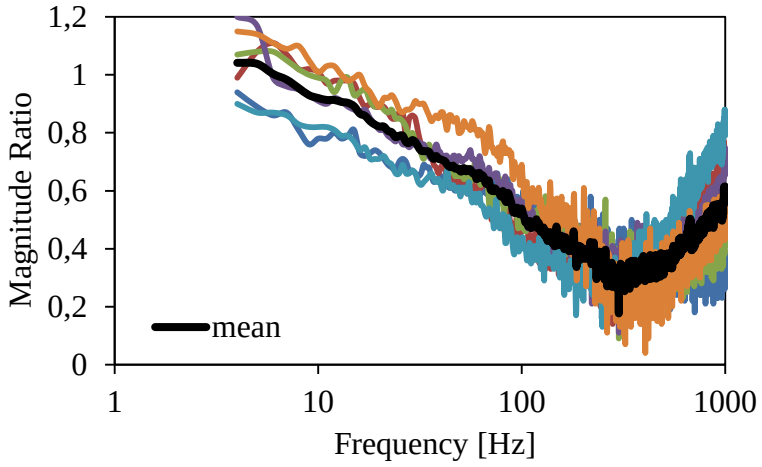

(a)

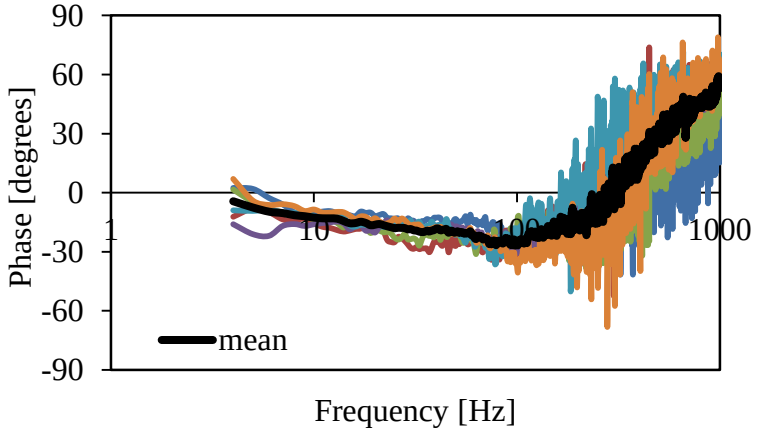

(b)

Figure 5.8 Frequency response characteristics of the *FlexiForce*® sensor obtained from the palm impedance response of all six subjects (colored lines). The mean values are indicated with black lines: (a) magnitude ratio and (b) phase (50 N push force, 30 N grip force and 1.5 m/s^2 excitation).

The results show nearly unity ratio of the palm impedance FRF magnitude at very low frequencies, which decreases to nearly 0.3 near 240 Hz and subsequently increases to about 0.5

at 1000 Hz. The mean ratio of the finger magnitude responses also show similar tendency. The palm sensor FRF phase response is also observed to be very small at low frequency but it decreases slowly to about -25° near 90 Hz and then increases with increase in frequency. The frequency response characteristics of the sensors obtained with different subjects, hand force and excitation level combinations revealed similar trends, while the magnitude ratio and the phase values differed considerably. These were attributed to strong dependence of the sensor output on hand dimensions, contact force and contact area. The influence of vibration level on the frequency response characteristics of the sensor, however, was small compared to the influence of hand force and hand size.

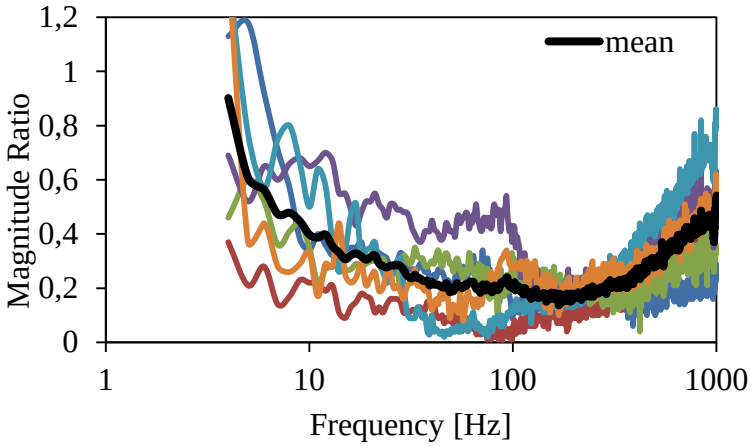

Figure 5.9 Frequency response characteristics of the *FlexiForce*® sensor obtained from the finger impedance magnitude of all six subjects (colored lines). The mean value is indicated with a black line (50 N push force, 30 N grip force and 1.5 m/s^2 excitation).

Figure 5.10, as an example, presents the FRF characteristics of the palm-side sensor, obtained for one of the subjects (#6 in Table 4.1) in terms of the magnitude ratio and phase, corresponding to different hand grip and push force combinations, and the 3 m/s^2 excitation. The magnitude ratio of the finger-side sensor for different hand force combinations are presented in Figure 5.11. The results clearly show highly nonlinear frequency response characteristics of the sensor which strongly depend upon the hand forces. Application of the frequency response as a correction factor would thus necessitate the characterization of the response for each experimental condition (hand force, handle size and vibration level), for each subject.

5.2.4 Application of frequency response function of the FlexiForce® sensor

The inverse of the mean frequency function of the *FlexiForce*® sensors corresponding to each grip and push force combination is applied to the mean response measured from the *FlexiForce*® sensors, as proposed in [51]. This approach permits compensation of the limited frequency response of the sensors. The corrected palm and finger impedance responses are obtained from:

$$Z_{c,palm}(j\omega) = CF_{palm}(\omega)\ \frac{S_{Fpf,v}(j\omega)}{S_{vv}(j\omega)} \tag{5.5}$$

$$Z_{c,finger}(j\omega) = CF_{finger}(\omega)\frac{S_{Fff,v}(j\omega)}{S_{vv}(j\omega)} \quad (5.6)$$

where $Z_{c,palm}(j\omega)$ and $Z_{c,finger}(j\omega)$ are the corrected palm and finger impedance responses, respectively, obtained through application of the inverse of the respective FRFs $CF_{palm}(\omega)$ and $CF_{finger}(\omega)$.

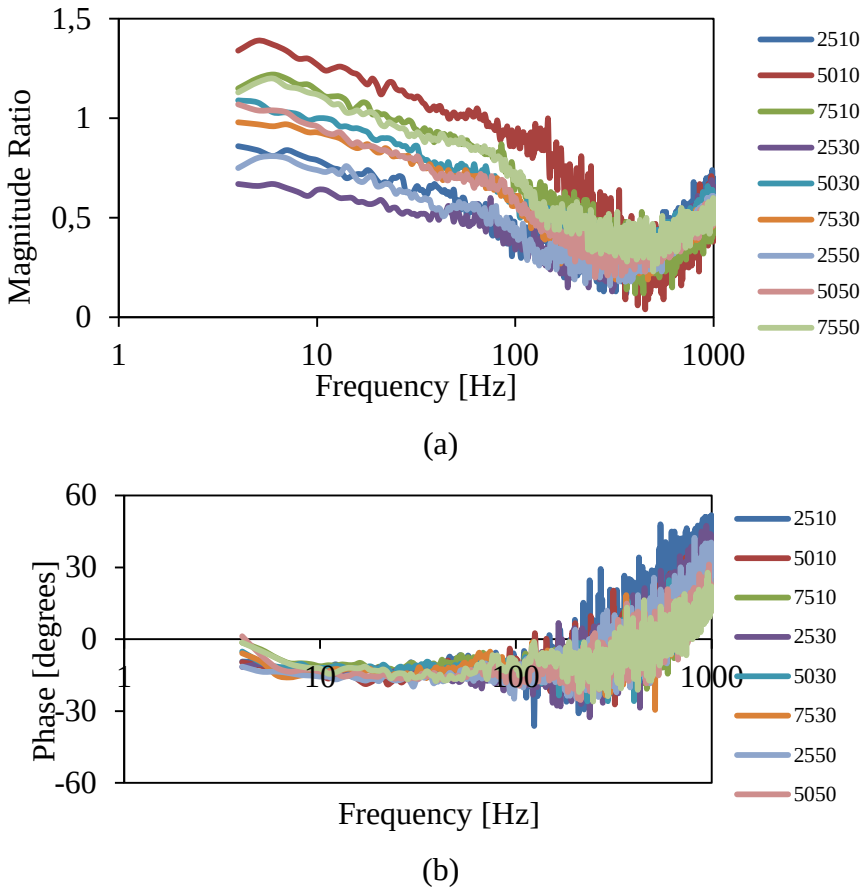

Figure 5.10 Frequency response characteristics of the *FlexiForce*® sensor obtained from the palm impedance responses corresponding to different hand force combinations for subject #6: (a) magnitude ratio and (b) phase. The push and grip forces are indicated on the right hand side of the graphs, where the first two digits refer to the push force followed by the grip force.

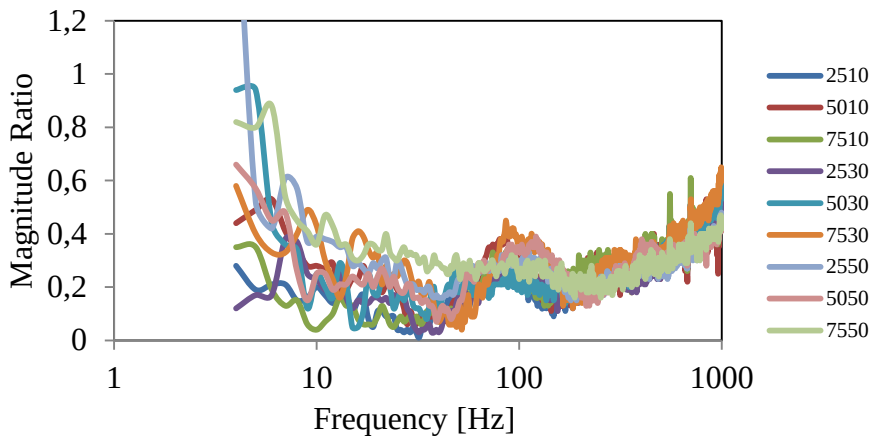

Figure 5.11 Frequency response characteristics of the *FlexiForce*® sensor obtained from the finger impedance magnitude corresponding to different hand force combinations for subject #6. The push and grip forces are indicated on the right hand side of the graphs, where the first two digits refer to the push force followed by the grip force.

Figures 5.12 and 5.13 illustrate the comparison of the corrected palm and finger impedance responses with the reference values corresponding to the selected grip and push force combinations under 1.5 and 3 m/s^2 rms acceleration excitation, respectively. The figures also show the uncorrected responses obtained directly from the *FlexiForce*® sensor signals, while the reference responses are those derived from the instrumented handle. It should be noted that the corrections were performed using the mean frequency response of the sensors obtained for each subject, corresponding to each hand force combination. The comparisons clearly show that the *FlexiForce*® sensors could provide reliable measurements of the palm and finger impedance responses in the entire frequency range, when the frequency response correction is applied. Such sensors could thus be applied for the measurement of biodynamic responses and hand forces on power tool handles in the field. The determination of the frequency response function of the sensors, however, would be quite challenging considering their nonlinear dependence on hand size, hand force and handle size. Further efforts to identify a generalized frequency response function would be worthy in order to facilitate the measurements of biodynamic responses under representative field conditions.

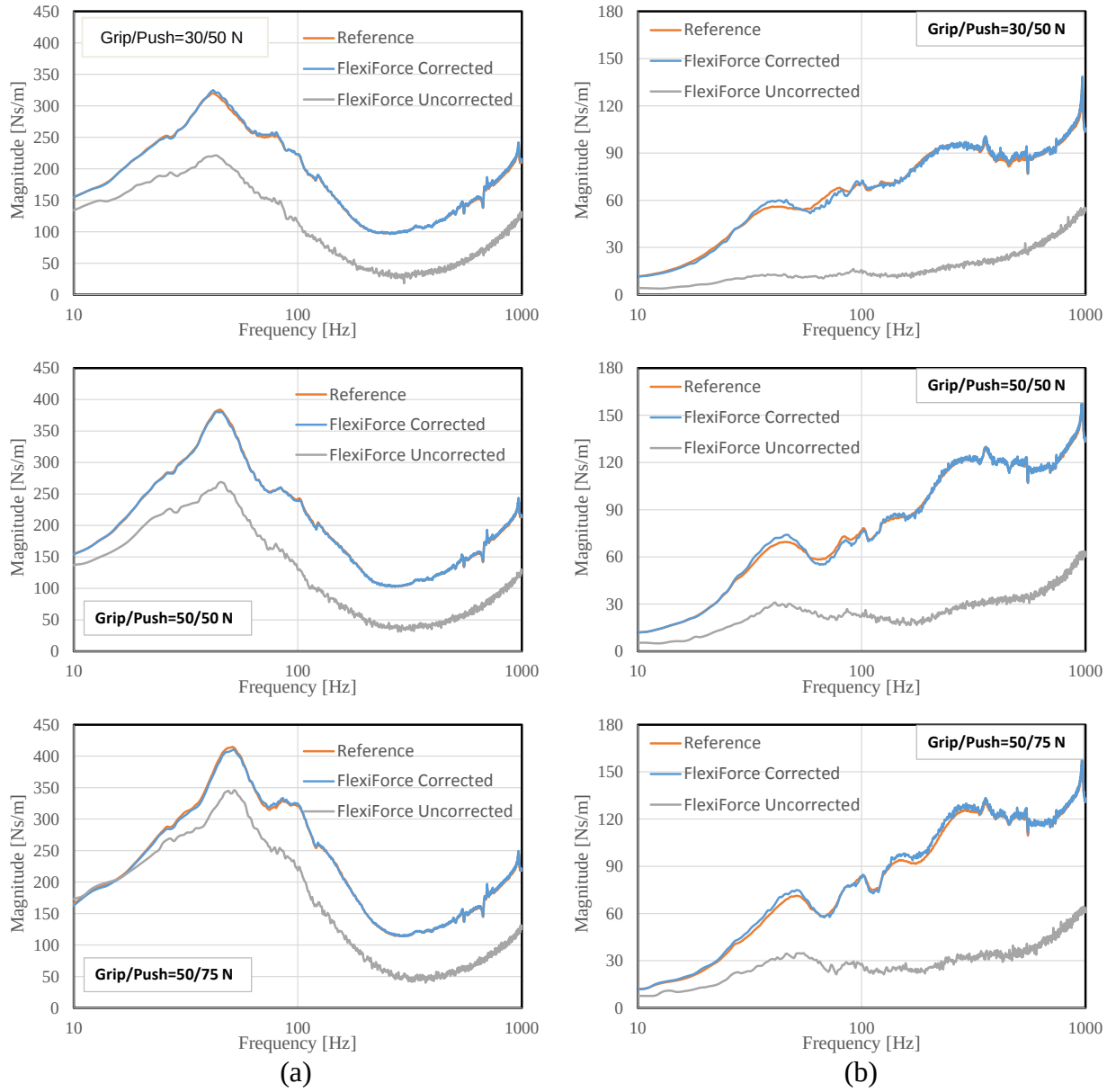

Figure 5.12 Corrected and uncorrected impedance responses obtained from the *FlexiForce*® sensors compared with the reference response obtained from the instrumented handle for a 1.5 m/s^2 excitation: (a) palm impedance and (b) finger impedance.

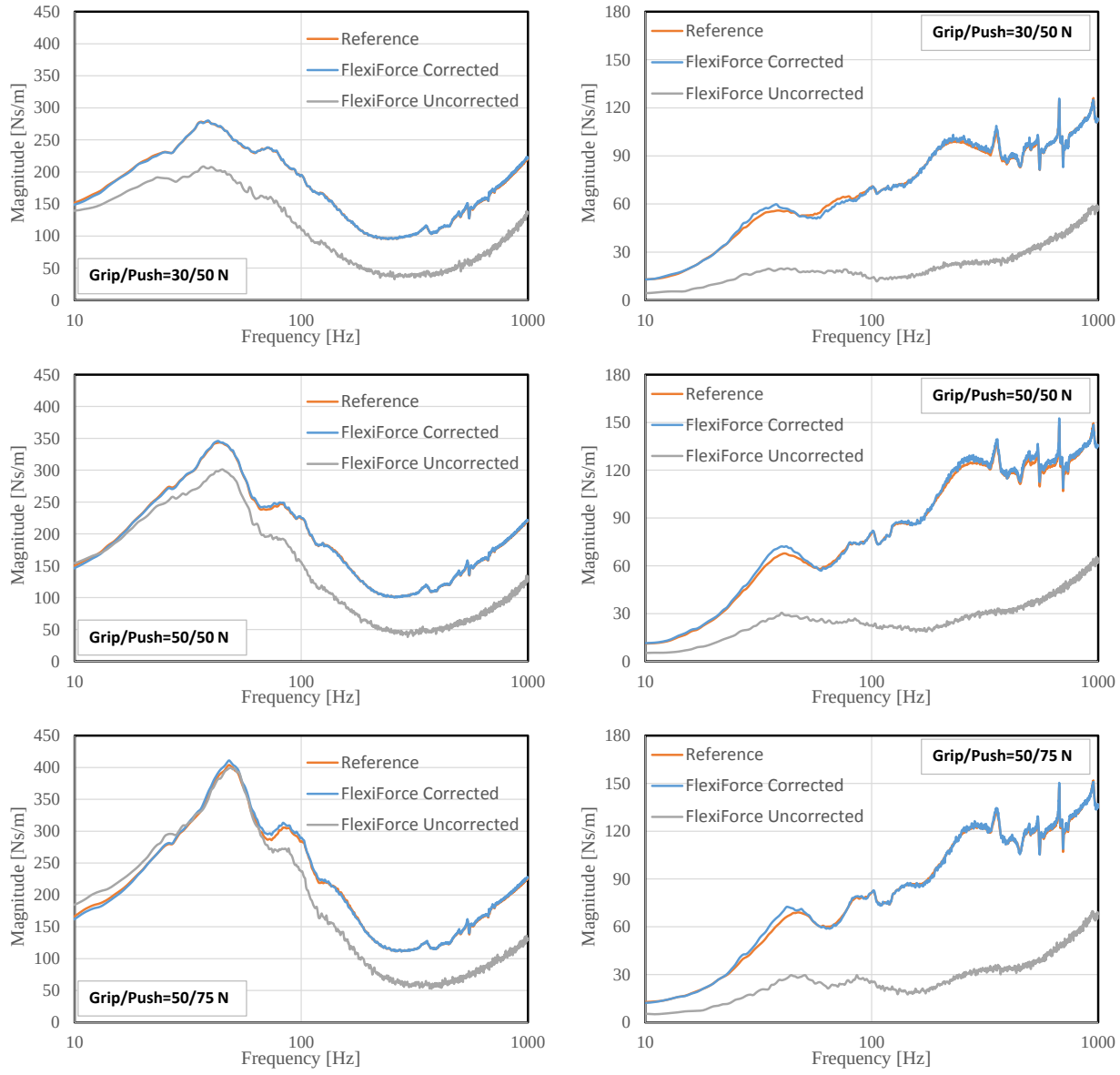

Figure 5.13 Corrected and uncorrected impedance responses obtained from the *FlexiForce*® sensors compared with the reference response obtained from the instrumented handle for a 3 m/s^2 excitation: (a) palm impedance and (b) finger impedance.

6 EVALUATION OF THE *FLEXIFORCE*® SENSORS FOR THEIR USE WITH POWER TOOLS

The primary goal of the study was to explore a low-cost system for the measurement of hand-handle coupling forces on vibrating power tools. It needs to be emphasized that significant effects of hand coupling force on the severity of vibration transmitted to the operator's hand and arm have been widely recognized [7,8]. Consequently, considerable efforts are made to seek practical and reliable methods for measuring the hand-handle coupling forces during tool operations in the field, particularly within the European Community [17,18]. The reported studies have shown the effectiveness of the capacitive pressure measurement system in accurately capturing the hand-handle interface forces with tool handles. The feasibility of the capacitive pressure measurement system for field applications, however, would be of concern due to, not only the high cost of the sensors, but also their sustainability in the field conditions. The *FlexiForce*® resistive sensors offer many distinct advantages compared to the capacitive measurement system, namely, the low cost of the sensors, and the low cost and simplicity of the signal conditioning circuit compared to the capacitive system. From the laboratory explorations, it is evident that such sensors can provide reliable estimates of the palm and finger contact forces with uniform cylindrical and elliptical handle cross sections in static as well as dynamic environments, provided that the sensors are calibrated for specific handle and subject. The resistive sensors offer flexibility similar to the capacitive sensors for applications to tool handles of varying cross section. Moreover, unlike the capacitive sensors, the damages or failures of the *FlexiForce*® sensors in a field setting would not be of concern due to their low cost.

Considering the aforementioned potential merits of the resistive sensors, the feasibility of the low cost *FlexiForce*® sensors for measuring hand grip and push forces with actual hand-held vibrating tools is investigated in the laboratory. The study employed an electric percussion chipping hammer, operating in an energy dissipator that was designed in accordance with ISO 8662 [52].

6.1 Methods

An experiment was designed to evaluate the applicability of the sensors for measuring hand forces when coupled with the chipping hammer (BOSCH 11313 EVS) shown in Figure 6.1. The tool comprised a variable speed electric drive capable of delivering 1300 to 2600 blows per minute (BPM) under no load condition. The speed of the tool could be varied through a six position dial located near the primary tool handle. The operator would normally grasp the tool using its two handles. The primary handle is located on the main tool housing with the motor drive (Figure 6.1), where the operator imparts the grip and push forces. The secondary handle is located near the chuck, which is used for necessary guidance of the tool. The *FlexiForce*® sensors were applied to measure the hand forces applied to the primary handle.

The tool was positioned in an energy dissipator, where the chisel bit was replaced by an anvil, as recommended in ISO 8662-2 [52]. Considering an upright posture of a standing operator, it was decided to place the sensors on the top and bottom surfaces of the primary handle for the measurement of the palm- and finger-side forces (Figure 6.2a). These forces could be subsequently applied to determine the hand grip and push forces using Eqs. (3.1) and (3.2). The

primary handle offered a flat top surface, which facilitated the installation of the palm-side *FlexiForce*® sensor. The bottom part of the handle comprised a curved surface, as seen in Figure 6.1. The sensors were attached to the two handle surfaces using masking tape. Figure 6.2b illustrates the tool handle with the palm- and finger-side sensors.

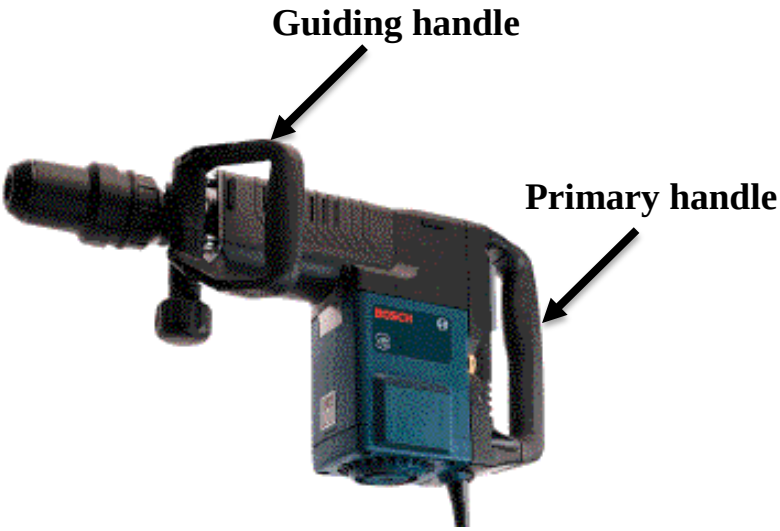

Figure 6.1 A pictorial view of the percussion chisel hammer (BOSCH 11313 EVS).

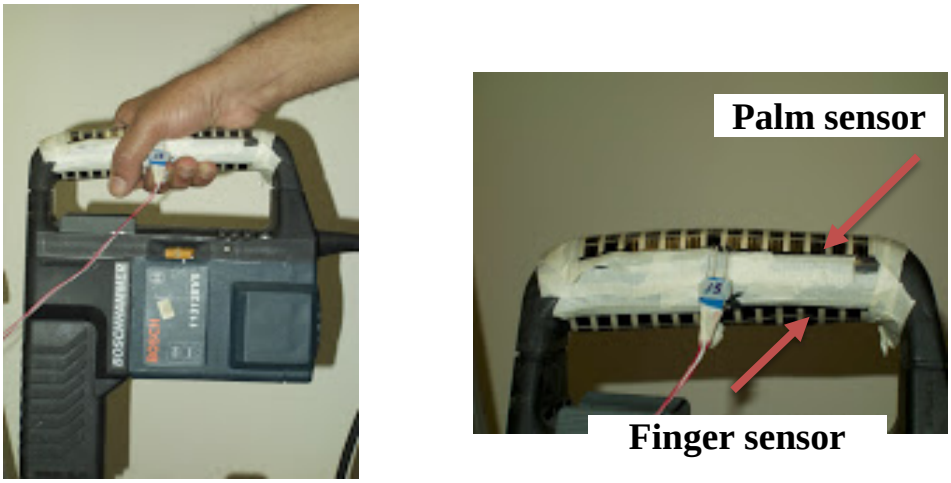

(a) (b)

Figure 6.2 (a) Position of the operator hand on the palm and finger sensors on the primary handle; and (b) palm- and finger-side *FlexiForce*® sensors installed on the handle.

The experiment design involved three sequential stages of measurement conducted with three adult male subjects with hand size ranging from 9 to 10. The first measurement stage involved

the identification of the palm- and finger-side sensor sensitivity. For the second measurement stage, the validity of the sensors was examined for different combinations of grip and push forces imparted by each subject on the stationary tool handle. For the final measurement stage, the measurements were repeated when the subject operated the tool in the energy dissipator. The tool speed was selected arbitrarily by the subject. Each measurement during each stage was repeated three times.

Unlike the testing done with the instrumented handle, the experiments with the tool posed difficult challenges in establishing the reference values of the palm and grip forces. A force plate was used such that the subject could apply a controlled push force. During the first stage of the experiments, the palm-side sensor was initially calibrated for 4 levels of palm force (25, 50, 75 and 100 N) by displaying the force plate signal to the subject. As the subject stood on the force plate in an upright posture, he was asked to hold the handle in a power grip manner and apply the desired push force while ensuring nearly zero grip or finger pressure (Figure 6.3). This permitted a more representative hand position for the tool operation. For this purpose, the finger-side *FlexiForce*® sensor output was also displayed to the subject. All 3 subjects were able to achieve this condition with peak finger-side force below 2 N. The palm-side sensor sensitivity was subsequently computed and entered in the LabView program to display the palm force in Newton.

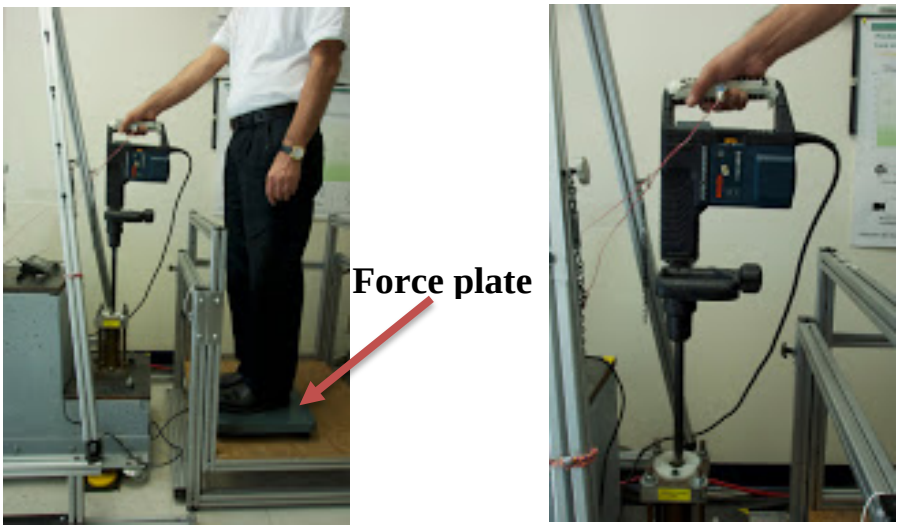

Figure 6.3 Posture of the subject grasping the tool handle.

For the calibration of the finger-side sensor, the subject applied a known palm force using both palm-side sensor and force plate signals displayed on a monitor. The subject was then advised to gradually increase the finger force to fully compensate the push force output of the force plate, while retaining a steady palm force output of the palm-side sensor. The force plate output thus decreased to zero while the *FlexiForce*® palm sensor output remained constant. This approach provided reference values of the grip or finger forces for the calibration of the finger-side sensor. These steps were conducted for 4 different levels of grip force (25, 50, 75 and 100 N). The finger-side sensor sensitivity was subsequently computed and entered in the LabView program to display the finger force in Newton.

In the second stage of the experiments, the validity of the calibrated *FlexiForce*® sensors was examined while the subject grasped the handle under 5 different combinations of grip and push forces (F_{gr}/F_{pu} = 0/30, 30/30, 30/50, 30/75 and 50/75 N) in a power grip manner. The output signals of the force plate (push force) and finger-side *FlexiForce*® sensor (grip force) were displayed on a monitor in order to help the subject control the applied forces. The output of the palm sensor was, however, not displayed to the subject. The order of the grip and push forces was randomized and each measurement was repeated three times. Two different approaches were attempted to examine the validity of both *FlexiForce*® sensors in a static power grip condition. With the first approach, the palm sensor output was directly compared to the sum of the displayed push and grip forces. Secondly, the push force was estimated by subtracting the finger sensor output from that of the palm sensor.

The same methodology was also employed in the final stage of the experiment where the subject operated the tool while grasping the tool handle. Neither the tool speed nor the handle vibration was monitored in this stage, as the goal was to examine the validity of the calibrated *FlexiForce*® sensors with the vibrating tool. All three stages of the measurements were conducted in a sequential manner with each subject while a fresh set of *FlexiForce*® sensors was installed for each subject.

6.2 Results

6.2.1 Static calibration

Figures 6.4 and 6.5 illustrate the static calibration data for three sets of palm and finger sensors, used for the three subjects, respectively. The reference values of the push force were obtained from the force plate, while those of the grip force were obtained from the palm sensor outputs when the subject compensated for the push force. The palm sensor output thus corresponds to the pure push force, while the finger sensor output corresponds to the grip force alone. The results were obtained from 12 measurements involving three repeats at each of 4 levels of force (25, 50, 75 and 100 N). The figures also illustrate the mean sensitivity of each sensor together with the r^2 values. The results show good linearity of all sensors with $r^2 \geq 0.86$. However, the sensitivities of the three sets of sensors used with the three subjects differ, as it was expected. The sensitivity of the palm sensors ranged from 2.991 mV/N for subject #2 to 5.584 mV/N for subject #1, while the sensitivity of the finger sensors ranged from 3.362 mV/N for subject #2 to 4.436 mV/N for subject #1.

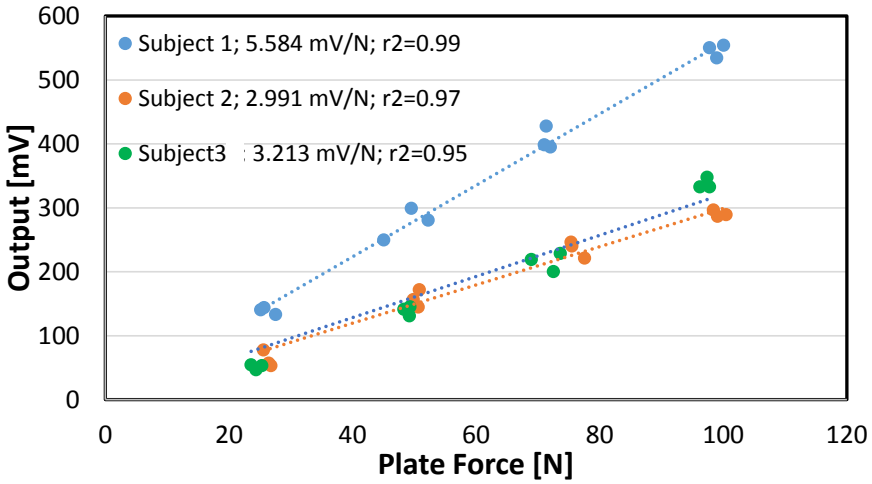

Figure 6.4 Output voltage of 3 palm sensors used for 3 subjects at 4 levels of push force measured from the force plate (3 repeats per level).

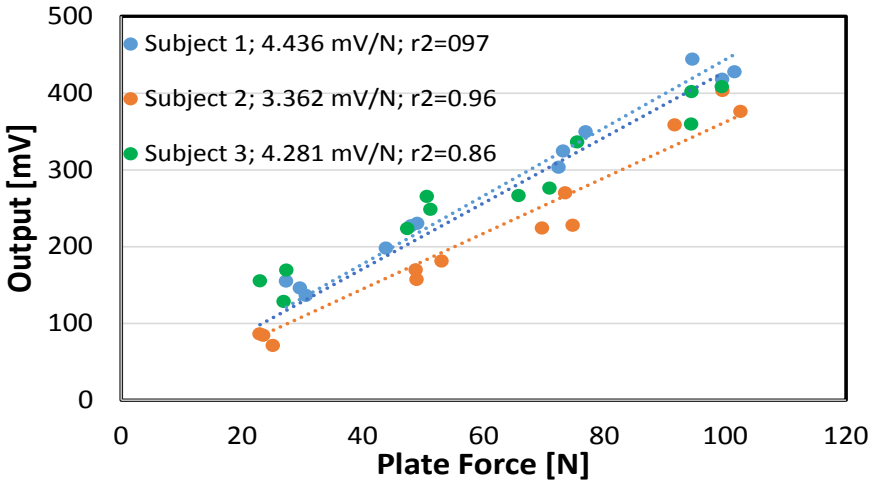

Figure 6.5 Output voltage of 3 finger sensors used for 3 subjects, at 4 levels of grip force measured from the force plate (3 repeats per level).

From these results, it is concluded that the *FlexiForce*® sensor applied to the tool handle yield good repeatability of the measurements and provides linear outputs with the applied force. The sensitivity of each individual sensor was subsequently input into the LabView program for evaluating the feasibility of using these sensors for the measurement of hand-tool interface forces under static as well as dynamic conditions.

6.2.2 Measurement of coupling forces under static conditions

The data obtained for each subject grasping the stationary tool handle with five different combinations of hand grip and push forces were analyzed to assess the feasibility of the proposed low-cost measurement system. The push force was obtained by subtracting the finger-side sensor output from the palm-side sensor output. Figure 6.6 illustrates the correlation of the push force obtained from the *FlexiForce*® measurement system with that obtained from the force plate. The figure shows, for each subject, 15 measurements involving three repeats of five hand force combinations. The results show very good repeatability of the measurements and a reasonably good agreement between the push forces obtained from the two measurement systems, with r^2 values ranging from 0.84 to 0.91 for the three subjects. The ratio of the push force obtained from the *FlexiForce*® measurement system to the force plate signal ranged from 0.90 for subject #2 to 1.06 for subject #1.

The palm sensor measurements are also correlated with the hand-handle coupling force in Figure 6.7 to further examine the validity of the measurement system. The coupling force is obtained from the summation of the force plate and finger sensor outputs. The results suggest better correlations of the palm sensor data with the coupling force, with r^2 values ranging from 0.95 to 0.97 for the three subjects. The ratio of the palm force obtained from the *FlexiForce*® measurement system to the coupling force range from 0.96 for subject #1 to 1.06 for subject #2. The results presented in Figures 6.6 and 6.7 demonstrate the validity of the proposed measurement system in obtaining reasonably good estimates of hand grip, push and coupling forces, when grasping the handle of a stationary tool in a power grip manner.

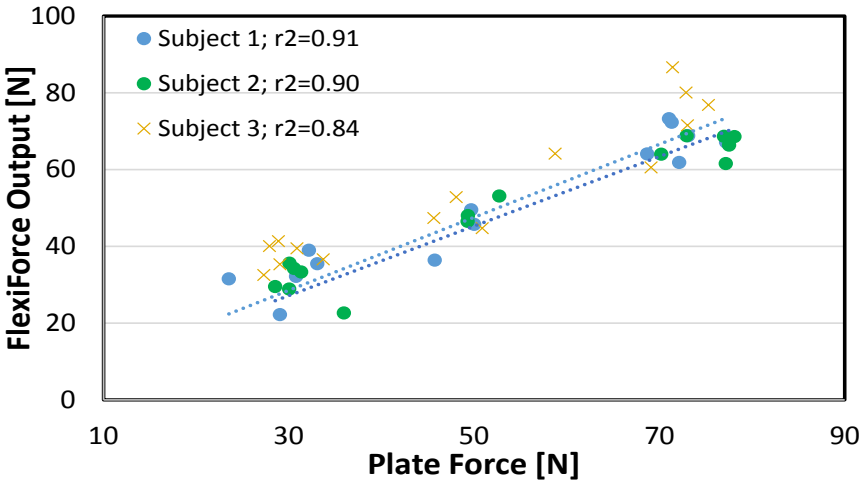

Figure 6.6 Correlation of the push force data obtained from the *FlexiForce*® sensors with the data from the force plate, for each subject grasping the stationary tool handle with 5 different grip and push forces.

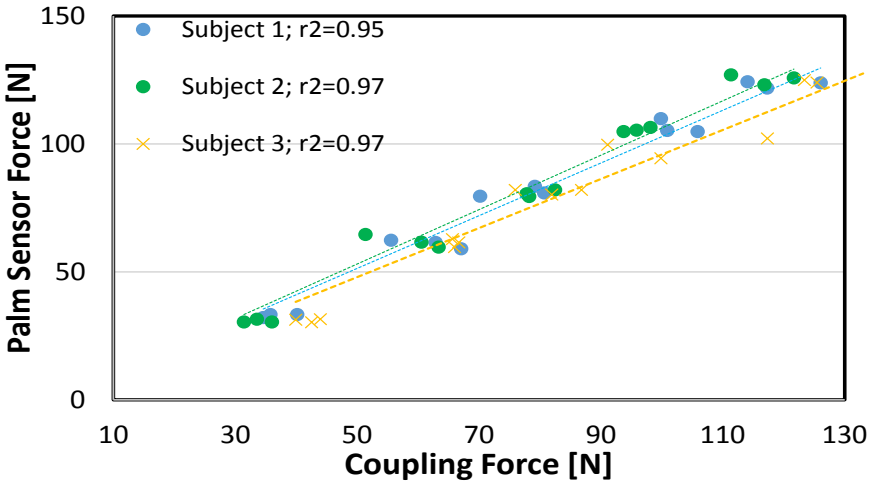

Figure 6.7 Correlation of the palm sensor data with the data from the coupling force for each subject grasping the stationary tool handle with 5 different grip and push forces.

6.2.3 Measurement of coupling forces under dynamic conditions

The measured data acquired with each subject grasping the handle of the tool operating in the energy dissipator for five different combinations of hand grip and push forces were analyzed to evaluate the feasibility of the *FlexiForce*® measurement system under vibrations. The subjects were permitted to select the tool speed arbitrarily. The data were analyzed to derive both the push and coupling forces, as in the case of the static tool. Figure 6.8 illustrates very good correlations of the push force measured by the *FlexiForce*® sensors with the data obtained from the force plate. The r^2 values range from 0.73 to 0.95 for the three subjects. The ratio of the push force obtained from the *FlexiForce*® measurement system to the force plate signal ranges from 0.92 to 1.06 for the three subjects. Figure 6.9 also illustrates very good correlations between the palm sensor measurements with the hand-handle coupling force. The r^2 values range from 0.93 to 0.98 for the three subjects. The ratio of the palm force obtained from the *FlexiForce*® measurement system to the coupling force ranges from 0.96 to 1.05 for the three subjects. A comparison of the measurements obtained with the static and vibrating tool handle suggests that the *FlexiForce*® measurement system yields an equally accurate estimation of the push and coupling forces with the vibrating tool.

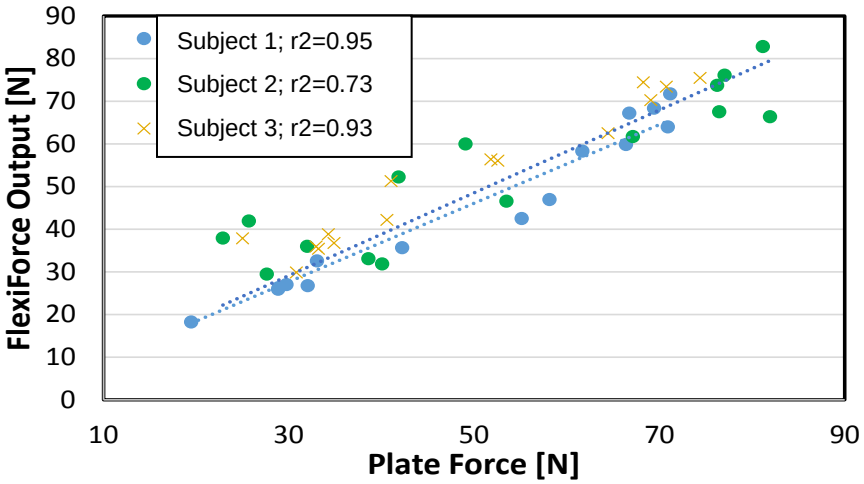

Figure 6.8 Correlation of the push force data obtained from the *FlexiForce*® sensors with the data from the force plate, for each subject grasping the vibrating tool handle with 5 different grip and push forces.

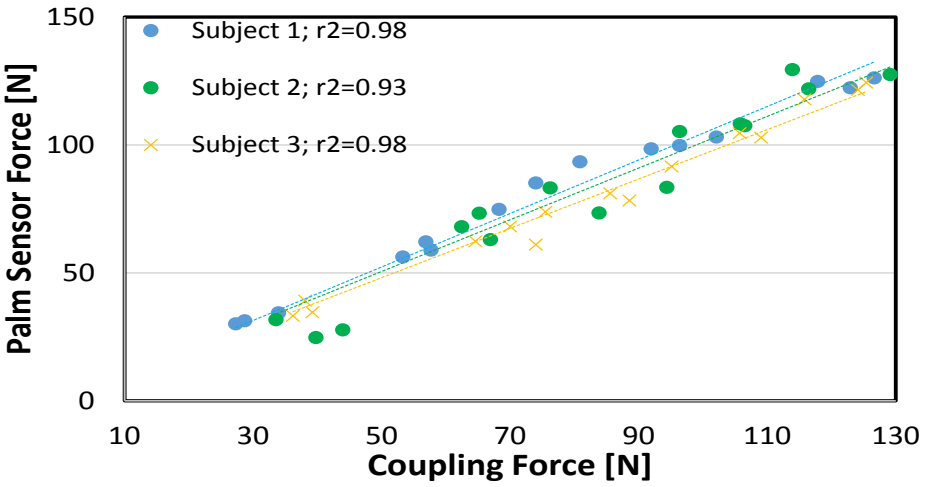

Figure 6.9 Correlation of the palm sensor force with the coupling force, for each subject grasping the vibrating tool handle with 5 different combinations of grip and push forces.

7 CONCLUSION

A low-cost system was developed for the measurement of hand-handle coupling forces, and the feasibility of its use with real tool handles was assessed through systematic laboratory measurements. The measurement system is based upon thin and flexible resistive sensors (*FlexiForce*®) that offer substantial merits for the measurements of hand forces on power tool handles. The most attractive features of the sensors include their low cost, simple signal conditioning requirement and ability to be trimmed to different lengths in order to adapt to the size of different tool handles. Each sensor revealed very good linearity with the applied force, low hysteresis and good repeatability over the desired range of the force (up to 100 N) on flat as well as on curved surfaces under both static and dynamic conditions. The sensor outputs, however, showed nonlinear dependence on the loading area, the load position with respect to the sensor surface, and the sensor length and flexibility of the loading media. However, the output deteriorated with repeated usage and time, and very little consistency in the output was observed across different sensors. But each sensor provided repeatable measurements on both flat and curved surfaces. It was thus concluded that such sensors could be used for measuring hand forces provided that each sensor is carefully calibrated prior to its usage.

The analysis of the hand-handle interface force distribution and hand-handle geometry suggested that dominant palm- and finger-side forces occur nearly symmetrically about the handle axis, in the forearm axis. The *FlexiForce*® sensors applied symmetrically on opposite sides of the handle provided good linearity with the hand grip and push forces imposed on the tool handle, irrespective of the hand and handle size. This was evident over the range of hand grip (up to 50 N) and push (up to 75 N) forces, handle sizes (32, 38 and 43 mm cylindrical handles, and 32 mm x 38 mm and 38 mm x 44 mm elliptical handles) considered under static as well as vibrating conditions. The measurements, however, revealed a strong dependence of the sensor outputs on the hand and handle sizes. It was thus concluded that the sensors could be effectively used for measuring palm and finger forces on vibrating tool handles, provided that each sensor is calibrated for specific subject prior to measurement.

The feasibility of the proposed measurement system in acquiring the biodynamic response of the hand-arm system exposed to vibrations was further investigated in the laboratory. While the palm and finger impedance responses measured with the *FlexiForce*® sensors showed very good trends with the reference values obtained from the instrumented handles, the impedance magnitude was substantially lower compared to the reference values. This was attributed to the poor frequency response characteristics of the sensors, showing a substantial attenuation of the measured force with increasing frequency. The use of a correction function based upon the measured frequency response resulted in a much better agreement of the measured impedance response with the corresponding reference value for different hand grip and push force combinations, and for the different vibration excitations considered in the study. The proposed system offers two significant benefits in view of the biodynamic response measurements: (i) it eliminates the need for inertial correction of the responses measured using instrumented handles, known to be a major source of error; and (ii) it facilitates the measurement of biodynamic responses and vibration power absorption into the hand-arm system under representative work posture and vibration conditions. The determination of the frequency response functions of the sensors, however, would be quite challenging considering its nonlinear dependence on different operating factors. Further efforts for identifying a generalized frequency response function would

be desirable to facilitate the measurements of biodynamic responses and of power absorption under representative field conditions.

The feasibility of the proposed measurement system for its application to a tool handle under static and vibration conditions was evaluated on a chisel hammer. The palm- and finger-side *FlexiForce*® sensors applied symmetrically on opposite sides of the handle around the handle axis (in the forearm axis) of the primary handle of a tool provided very good estimates of the hand push and coupling forces under both stationary as well as tool vibration conditions. The estimation errors were observed to be well below 10% for the entire range of hand grip and push force combinations considered in the study.

Therefore, from this study, it is concluded that the *FlexiForce*® sensors can provide good estimates of the hand forces imparted on a tool handle under simulated field conditions. The *FlexiForce*® sensors can be trimmed to the desired length and easily applied to tool handles of different cross-sections and geometry. The sensors, owing to their very low cost, can be discarded following measurements for a given tool and operating conditions. The primary limitations of the proposed system however lie with the lack of repeatability of the output from different sensors, and the need to calibrate them for each subject and handle. Through a discussion with the manufacturer, it was realized that these sensors were designed only for qualitative tactile sensing and would likely show poor repeatability of objective measurements across a sample of sensors. It would, however, be possible to fabricate such sensors with an enhanced consistency in repeatable objective measurements, although this would involve a setup cost. Considering the very good repeatability and applicability of the sensors when used with proper individual calibration, in addition to their low cost, it is recommended that a batch of sensors be used for further evaluation and development of a reliable hand-handle interface force measurement system. The acquisition of sensors with comparable properties can also help to get a generalized frequency response function for the measurement of the hand-arm biodynamic responses and vibration power absorption for different tools in the field. This may also permit relative injury risk assessment of different tools.

REFERENCES

1. Bovenzi M, Petronio L, DiMarino F (1980) Epidemiological survey of shipyard workers exposed to hand-arm vibration. Int Arch Occup Environ Health, 46, 251 - 266.
2. Malchaire J, Maldague B, Huberlant JM, Crouqet F (1986) Bone and joint changes in the wrists and elbows and their association with hand and arm vibration exposure. Ann Occup Hyg, 30, 461 – 468.
3. Bovenzi M (1998) Exposure-response relationship in the hand–arm vibration syndrome: an overview of current epidemiology research. Int Arch Occup Environ Health, 71(8), 509–19.
4. International Organization for Standardization (2001) Mechanical vibration and shock – Measurement and evaluation of human exposure to mechanical vibration – Part 1: General requirements. International Standard, ISO 5349-1.
5. Bovenzi M (2012) Epidemiological evidence for new frequency weightings of hand-transmitted vibration. Industrial Health, 50, 377-387.
6. Griffin M (2012) Frequency-dependence of psychophysical and physiological responses to hand-transmitted vibration. Industrial Health, 50, 354-369.
7. Hartung E, Dupuis H, Scgeffer M (1993) Effects of grip and push forces on the acute response of the hand-arm system under vibrating conditions. Responses. Int Arch Occup Environ Health, 64, 463-467.
8. Griffin MJ (1990) Handbook of human vibration, Academic Press, London.
9. International Organization for Standardization (2007) Mechanical vibration and shock - Coupling forces at the man--machine interface for hand-transmitted vibration. International Standard, ISO 15230.
10. Radwin RG, Armstrong TJ, Chaffin DB (1987) Power hand tool vibration effects on grip exertions. Ergonomics, 30(5) 833-855.
11. Adewusi S, Rakheja S, Marcotte P, Boutin J (2010**)** Vibration transmissibility characteristics of the human hand-arm system under different postures, hand forces and excitation levels. J Sound and Vibration, 329, 2953 – 2971.
12. Marcotte P, Aldien Y, Boileau P-É, Rakheja S, Boutin J (2005) Effect of handle size and hand-handle contact force on the biodynamic response of the hand-arm system under z_h-axis vibration. J Sound and Vibration, 283, no 3-5, 1071-1091.
13. Gurram R, Rakheja S, Gouw GJ (1995) A study of hand grip pressure distribution and EMG of finger flexor muscles under dynamic loads. Ergonomics, 38(4) 684-699.
14. Kaulbars U (1995) Measurement and evaluation of coupling forces when using hand-held power tools. Proc. 7th Intl Hand-Arm Vibration Conf, Prague.
15. Riedel S (1995) Consideration of grip and push forces for the assessment of vibration exposure. Proc. 7th Intl Hand-Arm Vibration Conf, Prague.
16. Kaulbars U, Raffler N (2011) Study of vibration transmission on a paver's hand hammer. Can Acoustics, 39(2), 52-53.

17. VIBTOOL (2008) Grip force mapping for characterization of hand-held vibrating tools. European Community Competitive and Sustainable Growth Program Report, project No.G6RD-CT-2002-00843.

18. Lemerle P, Klinger A, Cristalli A, Geuder M (2008) Application of pressure mapping techniques to measure push and gripping forces with precision. Ergonomics, 51(2), 168-191.

19. Aldien Y, Marcotte P, Rakheja S, Boileau P-É (2005) Mechanical impedance and absorbed power of hand-arm under x_h-axis vibration and role of hand forces and posture. Industrial Health, 43, 495-508.

20. Aldien Y, Marcotte P, Rakheja S, Boileau P-É (2006) Influence of hand-arm posture on biodynamic response of the human hand-arm exposed to z_h-axis vibration. Int J Industrial Ergonomics, 36, 45-59.

21. Burstrom L (1990) Measurement of the impedance of the hand and arm. Int Arch Occup Environ Health, 62, 431 – 439.

22. Burström L (1997) The influence of biodynamic factors on the mechanical impedance of the hand and arm. Int Arch Occup Environ Health, 69, 437 – 446.

23. Lundström R, Burström L (1989) Mechanical impedance of the human hand–arm system. Int J Industrial Ergonomics, 3, 235 – 242.

24. International Organization for Standardization (1998) Mechanical vibration and shock – Free mechanical impedance of the human hand-arm system at the driving-point. International Standard, ISO 10068.

25. Kattel BP, Fredericks TK, Frenandez JE, Lee DC (1996) The effect of upper extremity posture on maximum grip strength. Int J Industrial Ergonomics, 18, 423-429.

26. Kuzala EA, Vargo MC (1992) The relationship between elbow position and grip strength, American J Occ Therapy, 46, 509-512.

27. Marley RJ, DeBree TS, Wehrman R (1993) Grip strength as a function of forearm and elbow posture on maximum grip strength. Proc. 2nd Ind Engineering Research Conf, Los Angeles, 525-529

28. Cronjäger L, Hesse M (1990) Hand-arm system response to stochastic excitation. Proc. 5th Intl Hand-Arm Vibration Conf, Kanzawa, Japan.

29. Adewusi SA, Rakheja S, Marcotte P, Boileau P-É (2008) On the discrepancies in the reported human hand– arm impedance at higher frequencies. Int J Industrial Ergonomics, 38, 703– 714.

30. Dong RG, Welcome DE, McDowell TW, Wu JZ (2008) Analysis of handle dynamics-induced errors in hand biodynamic measurements. J Sound and Vibration, 318, 1313–1333.

31. Aldien Y, Marcotte P, Rakheja S, Boileau P-É (2006) Influence of hand-arm forces on power absorption of the human hand-arm exposed to z_h-axis vibration. J Sound and Vibration, 290, 1015-1039.

32. German proposal for a revision of “ISO 15230:2007 Mechanical vibration and shock — Coupling forces at the man machine interface for hand-transmitted vibration”, Document ISO/TC 108/SC 4/WG 3 N 203.

33. McGorry RW (2001) A system for the measurement of grip forces and applied moments during hand tool use. Appl Ergonomics, 32(3), 271–279.

34. Chadwick EKJ, Nicol AC (2001) A novel force transducer for the measurement of grip force. J Biomech, 34(1), 125–128.

35. Wimer B, Dong RG, Welcome DE, Warren C, McDowell TW (2009) Development of a new dynamometer for measuring grip strength applied on a cylindrical handle. Medical Engineering & Physics, 31 ,695–704

36. Reynolds DD, Falkenberg RJ (1984) A study of hand vibration on chipping and grinding operators, Part I: Four-degree-of-freedom lumped parameter model of the vibration response of the human hand. J Sound and Vibration, 95, 499–514.

37. Dong RG, Welcome DE, McDowell TW, Wu JZ (2006) Measurement of biodynamic response of human hand–arm system. J Sound and Vibration, 294, 807-827.

38. International Organization for Standardization (2012) Mechanical vibration and shock — Hand-arm vibration —Method for the measurement and evaluation of the vibration transmissibility of gloves at the palm of the hand. International Standard, ISO 10819.

39. Van der Kamp M, Conway BA, Nicol AC (2001) A novel instrumented ring for the measurement of gripforce adjustments during precision grip tasks. I Mech E, Part H: J. Engineering in Medicine, 215(H2), 421–427.

40. Yun MH, Kotani K, Ellis D (1992) Using force sensitive resistors to evaluate hand tool grip design. Proc 36th Ann Meet of the Human Factors Society, Santa Monica, CA, 806–810.

41. Welcome D, Rakheja S, Dong R, Wu JZ, Schopper AW (2004) An investigation on the relationship between grip, push and contact forces applied to a tool handle. Int J Industrial Ergonomics, 34, 507–518

42. Aldien Y, Welcome D, Rakheja S, Dong R, Boileau P-É (2005) Contact pressure distribution at hand-handle interface: role of hand forces and handle size. Int. J. of Industrial Ergonomics, 35(3): 267-286.

43. Young JG, Sackllah ME, Armstrong TJ (2010) Force distribution at the hand/handle interface for the grip and pull tasks, Proc 54th Ann Meet of the Human Factors and Ergonomics Society.

44. Deboli R, Calv A (2009) The use of capacitive sensor matrix to determine grip forces applied to olive hand held harvesters, Agricultural Engineering Int, The CIGR e-Journal Manuscript MES 1144 ,Vol XI.

45. Komi ER, Roberts JR, Rothberg SJ (2007) Evaluation of thin flexible sensors for time resolved grip force measurement. Proc. I MechE, Part C: J Mechanical Engineering Science, 221.

46. Rossi J, Berton J, Grélot L, Barla C, Vigouroux L (2012) Characterisation of forces exerted by the entire hand during the power grip: effect of the handle diameter. Ergonomics, 55(6), 682-692

47. Marcotte P, Adewusi S, Rakheja S (2011) Development of a low-cost system to evaluate coupling forces on real power tool handles. Can Acoustics, 39(2), 36-37.

48. British Standard (1994) General requirements for gloves. BS EN 420.

49. Dong RG, Wu JZ, McDowell TW, Welcome DE, Schopper AW (2005) Distribution of mechanical impedance at the fingers and palm of the human hand. J Biomechanics, 38, 1165-1175.

50. Dong R, Rakheja S, Schoppwer AW, Han B, Smutz WP (2001) Hand-transmitted vibration and biodynamic response of the human hand-arm: A critical review. Critical Reviews in Biomed Engineering, 29(4), 391-441.

51. Rakheja S, Dewangan K, Marcotte P, Shahmir A, Patra S (2015) An exploratory study for characterizing seated body apparent mass coupled with elastic seats under vertical vibration. Research Report # R-884, IRSST.

52. International Organization for Standardization (1992) Hand-held portable power tools – measurement of vibrations at the handle – part 2: Chipping hammers and riveting hammers. International Standard, ISO 8662-2.